

Entanglement entropy of local gravitational quenches

Justin R. David, Jyotirmoy Mukherjee

*Centre for High Energy Physics,
Indian Institute of Science,
C. V. Raman Avenue, Bangalore 560012, India.*

E-mail: justin@iisc.ac.in, jyotirmoy@iisc.ac.in

ABSTRACT: We study the time dependence of Rényi/entanglement entropies of locally excited states created by fields with integer spins $s \leq 2$ in 4 dimensions. For spins 0, 1 these states are characterised by localised energy densities of a given width which travel as a spherical wave at the speed of light. For the spin 2 case, in the absence of a local gauge invariant stress tensor, we probe these states with the Kretschmann scalar and show they represent localised curvature densities which travel at the speed of light. We consider the reduced density matrix of the half space with these excitations and develop methods which include a convenient gauge choice to evaluate the time dependence of Rényi/entanglement entropies as these quenches enter the half region. In all cases, the entanglement entropy grows in time and saturates at $\log 2$. In the limit, the width of these excitations tends to zero, the growth is determined by order $2s + 1$ polynomials in the ratio of the distance from the co-dimension-2 entangling surface and time. The polynomials corresponding to quenches created by the fields can be organised in terms of their representations under the $SO(2)_T \times SO(2)_L$ symmetry preserved by the presence of the co-dimension 2 entangling surface. For fields transforming as scalars under this symmetry, the order $2s + 1$ polynomial is completely determined by the spin.

Contents

1	Introduction	1
2	Scalar and vector quenches	4
2.1	Time evolution of the scalar quench	5
2.2	Time evolution of the vector quench	13
3	Local gravitational quenches	22
3.1	Gauge fixing and the graviton propagator	23
3.2	Two-point function of Riemann curvatures	25
3.3	Growth of entanglement after curvature quenches	31
4	Conclusions	38
A	BCFT interpretation of scalar 2-point function on Σ_2.	40
B	Details for curvature correlators	42
C	Expectation value of the Kretschmann scalar	50
D	Relations due to isotropy	52

1 Introduction

The study of systems driven out of equilibrium and its subsequent evolution is important to understand the phenomenon of thermalization in quantum systems. Holography relates thermalization in theories which admit gravitational duals to the formation of black holes in the bulk which is another important question in quantum gravity, see [1] for a review on the holographic aspects of systems away from equilibrium. A simple way to kick a system out of equilibrium is to change the Hamiltonian of the theory at a given time and then study the dynamics as the system evolves unitarily with the new Hamiltonian [2, 3]. These quenches can be of 2 types, one in which the parameters of the Hamiltonian is changed uniformly in space which is called the ‘global quench’. The other in which the quench is generated by a localized change in the initial quantum state or the density matrix so that the system is excited and departs from the ground state only locally at a specific instance of time. Then one studies the evolution of various observables subsequently, such quenches are termed ‘local quenches’ [4-8].

One specific protocol to set up local quenches is to insert a local operator at some point, which then creates a local change in the ground state density matrix. The time evolution of observables after local such quenches have been extensively studied in CFT and even

in non-conformal field theories [9]. In CFT's that admit a gravity dual, such quenches are dual to an in-falling particle in the bulk. Most of these detailed studies have been confined to 2 dimensions [10–23]. The quantum corrections to the entanglement entropy of local quenches have also been studied both in CFT and holography [24]. But there have been only a few studies in higher dimensions, particularly in 4d for quenches created by free fields and restricted to spins ≤ 1 [12, 14, 25, 26]. In this paper, we revisit the study of these quenches and develop methods so that we can study quenches created by the linearized graviton. The observables that we wish to study after the quench are the Rényi entropies and entanglement entropy. In this context it is important to point out that the entanglement properties of the linearized graviton have only been recently studied. The coefficient of the logarithmic term for the entanglement entropy of a spherical region in a theory of linearized gravitons has been evaluated in [27, 28]. The contribution to the entropy from gravitational edge modes has been understood in [29]. The graviton after all is a fundamental particle of nature, and therefore it is useful and important to study its information theoretic properties.

Let us briefly describe the set up for the local quenches we will consider in this paper. We excite the ground state by an operator \mathcal{O} , then the density matrix at time t is given by

$$\rho = \mathcal{N} e^{-iHt} e^{-\epsilon H} \mathcal{O}(y) |0\rangle \langle 0| \mathcal{O}^\dagger(y) e^{-\epsilon H} e^{iHt}. \quad (1.1)$$

Here the excitation is created by the operator \mathcal{O} inserted at coordinates $y = (0, 0, y_0, 0)$, the density matrix is then evolved by time $t - i\epsilon$. \mathcal{N} is the factor used to normalise the state. The small imaginary part added to the time evolution, gives a width to the excitation. An example for \mathcal{O} is the conformal scalar field ϕ . On probing this state by the stress tensor we find that the excitation creates a spherical pulse of energy which travels as a spherical wave at the speed of light as shown in figure 2.1. Consider the reduced density matrix ρ_A obtained by tracing out the region $y < 0$, the entangling surface is a plane of co-dimension 2. We study the evolution of both the Rényi and entanglement entropies of this local quench. These entropies are defined by

$$S_A^{(n)} = \frac{\log \text{Tr}(\rho_A^n)}{1 - n}. \quad (1.2)$$

As an example consider the excitation corresponding to the scalar, the difference in entanglement entropy from that of the ground state is shown in the figure 6. As the pulse enters the entangling region, the entanglement increases and saturates to $\log(2)$.

In this paper we study the growth of entanglement for excitations for operators with spins ≤ 2 . For local quenches in $2d$, the entanglement growth saturates to the logarithm of the quantum dimension of the corresponding operator [15]. When width ϵ approaches zero, the growth of entanglement follows a step function ¹ However in $d > 2$, even in the zero width limit, the entanglement growth depends on a non-trivial function and then saturates at $\log(2)$ for free fields. In this paper we obtain this function for quenches created by all

¹The leading behaviour of entanglement growth in $2d$ local quenches at finite width ϵ has been shown to be universal [19].

curvature components of the Riemann tensor. The saturation at $\log(2)$ has been interpreted in terms of entanglement pairs [12].

We first revisit the study of the quenches due to a scalar and $U(1)$ field strengths and then extend the study to all the components of the curvature tensor of the linearised graviton. Note that for theories with local gauge invariance, the natural local gauge invariant operators are field strengths. Therefore we use components of the Riemann as operators to create the quench. Furthermore, since a local stress tensor does not exist for the graviton, we demonstrate the state that we consider behaves as a local quench by probing it with the Kretschmann scalar. The behaviour of the Kretschmann scalar for a graviton quench is shown in figure 5. Thus the quench created by Riemann tensors, represents a curvature density travelling at the speed of light. The study of Rényi/entanglement entropies involve evaluating $2n$ point functions of the operators creating the quench on the replica surface. For the spin-1 and the graviton quenches, we need to choose a convenient gauge for the propagator of the gauge potential and the metric on the replica surface. We develop the gauge used in [28, 30] for this purpose. The presence of the co-dimension 2 entangling surface reduces the symmetry of the system to $SO(2)_T \times SO(2)_L$, where the subscripts T, L refers to transverse and longitudinal directions to the entangling surface. The gauge choice is compatible with this symmetry.

Since we are dealing with free fields, the $2n$ point function on the Replica surface which captures the Rényi entropies of the operators creating the quench can be evaluated using Wick contractions. In the limit of zero width of the quench, we can isolate the leading Wick contractions and obtain the time dependence of the growth of Rényi entropies when the quench enters the region $y > 0$. In all cases, including the quenches created by Riemann tensor components the entanglement grows and saturates at $\log(2)$. We observe that the time dependence of Rényi/entanglement entropies for quenches created by the spin s field is determined by order $2s + 1$ polynomials in $r = \frac{y_0}{t}$, where y_0 is the perpendicular distance at which the quench was released and t is the time elapsed. We find the structure of the polynomials can be organised in terms of the $SO(2)_T \times SO(2)_L$ representation of the operator creating the quench. These polynomials can be read from the tables 1, 3, 5 for scalars, vectors and symmetric tensors of $SO(2)_T \times SO(2)_L$ respectively. The growth of the entanglement entropy for the corresponding quenches are given in figures 6, 7, 8. The polynomial which determines the growth of Rényi entropies for fields transforming as scalar under $SO(2)_T \times SO(2)_L$ is completely determined by the spin. The constraints on the polynomial also show that the long time behaviour of Rényi entropies can always be written as

$$\lim_{t \rightarrow \infty} \Delta S^{(n)}(t) = \log 2 - \frac{n}{2} \frac{y_0^2}{t^2} a_\infty^2 + \dots \quad (1.3)$$

where a_∞ is a rational number and can be read out from tables 1, 3, 5.

One of our main motivations for this work is to explore the information theoretic properties of the graviton. As we mentioned earlier, some of these properties of the graviton have only been recently investigated. It has been argued that in a theory of quantum gravity that the wave function exterior to a given sub-region determines the wave function interior to it [31, 32]. Therefore the ‘split property’ of quantum local field theories does not hold

in the theory of quantum gravity. From this paper as well as the earlier work [27–29], we see that the theory of linearised gravitons behaves just as a local quantum field theory with gauge symmetry. It will be interesting to see explicitly how this behaviour departs from that of a local quantum field theory once the theory becomes interacting. The methods developed in this paper, especially the construction of the graviton propagator on the replica surface will be useful to study this question.

The organization of the paper is as follows. In section 2 we discuss the set up for the quench in detail and revisit the study of quenches created by the scalar and the $U(1)$ field strengths. Here we introduce the gauge which is consistent with the $SO(2)_T \times SO(2)_L$ symmetry of the problem. We also develop simple methods to obtain the leading contributions of the $2n$ point function which determines the Rényi entropies. These methods make it convenient to study the graviton quenches. Then in section 3 we study all the independent quenches due to components of the curvature tensor. Our results are summarised in the tables and figures of this section. Section 4 contains our conclusions. The appendices B, C D contain details of the calculations to arrive at our results. Appendix A shows how the scalar correlator on the replica surface can be interpreted as a 2 point function in a BCFT.

2 Scalar and vector quenches

In this section we first describe the set up for local quenches. The correlator which evaluated the change in Rényi entropy/entanglement entropy as the quench enters the entangling region is the $2n$ point correlator on the replica geometry [12]. We re-examine local quench represented by the state (1.1) where $\mathcal{O} = \phi(y)$ the free scalar field in $4d$. We will see that to obtain the growth of entanglement when the width $\epsilon \rightarrow 0$ it is sufficient to study the 2 point function of the scalar field in the replica geometry. We cast it as a correlator in a boundary conformal field theory, this allows us to isolate the singularities of the correlator which are responsible for the growth of the entanglement entropy as the pulse or the local quench enters the entangling region. We carry this observation ahead for the Maxwell theory. For the Maxwell theory, the quenches we consider are where $\mathcal{O} = F_{\mu\nu}(y)$, the field strength, which is a local gauge invariant operator. One consistency check we perform for both the scalar and Maxwell theory relates to the leading correction to the shape of the growth of entanglement due to the width ϵ before the pulse enters the entangling region. This correction is determined by the expectation value of the composite bilinear $:\mathcal{O}^2:$ in the replica geometry.

As we have stated in the introduction we wish to consider the quench represented by the state

$$\begin{aligned} \rho &= e^{\tau_e H} \mathcal{O}(0, -y_0) |0\rangle \langle 0| \mathcal{O}(0, -y_0) e^{-\tau_l H}, \\ &= \mathcal{O}(\tau_e, -y_0,) |0\rangle \langle 0| \mathcal{O}(\tau_l, -y_0), \end{aligned} \tag{2.1}$$

where $\tau_e = -\epsilon - it$, $\tau_l = \epsilon - it$ and we have assumed \mathcal{O} is Hermitian. Let ρ_A be the reduced density matrix obtained by tracing over the region $y < 0$, therefore the x, z plane divides space into two parts. To obtain $S_A^{(n)}$ we can appeal to the path integral and write it as a

path integral over replicas. The reduced density matrix ρ_A^n can be written as the following partition function

$$\text{Tr}(\rho_A^n) = \frac{Z_n}{(Z_1)^n}. \quad (2.2)$$

Here Z_n is the path integral over the surface Σ_n which is a n -branched cover over $y > 0$. On each sheet of the cover there is a pair of operators inserted at points $r_e e^{i\theta_e^{(k)}}$, $r_l e^{i\theta_l^{(k)}}$ where (k) labels the sheet. These locations are specified by setting

$$\begin{aligned} r_e e^{i\theta_e} &= -y_0 + i\tau_e, & r_l e^{i\theta_l} &= -y_0 + i\tau_l, \\ \theta_e^{(k)} &= \theta_e + 2\pi(k-1), & \theta_l^{(k)} &= \theta_l + 2\pi(k-1), \quad k = 1, \dots, n. \end{aligned} \quad (2.3)$$

The angle θ takes values from 0 to $2\pi n$ on the branched cover Σ_n . The partition function Z_1 is just the normalization needed to ensure $\text{Tr}\rho = 1$ and therefore it is 2 point function of $\langle \mathcal{O}(\tau_e, -y_0) \mathcal{O}(\tau_l, -y_0) \rangle_{\Sigma_1}$ in $4d$ flat Euclidean space. Similarly, when there is no insertions of operators, that is when we consider the vacuum we have the partition functions Z_{0n} and Z_{01} . The former is the path integral of the theory on the n -branched replica surface and the latter is the path integral on $4d$ flat Euclidean space. The reduced density matrix of the vacuum is given by

$$\text{Tr}\rho_{0A}^n = \frac{Z_{0n}}{(Z_{01})^n}, \quad (2.4)$$

where the subscript ‘0’ refers to the vacuum. Using these partition functions we can write the difference of the Rényi/entanglement entropy of the quench compared to the vacuum

$$\begin{aligned} \Delta S_A^{(n)} &= \frac{1}{1-n} (\log \text{Tr}\rho_A^n - \log \text{Tr}\rho_{0A}^n), \\ &= \frac{1}{1-n} \left(\log \frac{Z_n}{Z_{0n}} - n \log \frac{Z_1}{Z_{01}} \right), \\ &= \frac{1}{1-n} \left(\log \left\langle \prod_{k=1}^n \mathcal{O}(r_l, \theta_l^{(k)}) \mathcal{O}(r_e, \theta_e^{(k)}) \right\rangle_{\Sigma_n} - n \log \langle \mathcal{O}(r_l, \theta_l) \mathcal{O}(r_e, \theta_e) \rangle_{\Sigma_1} \right). \end{aligned} \quad (2.5)$$

The study of the time evolution of the local quench due to an operator reduces to the evaluation of its $2n$ point function on the replica surface. For free fields, this $2n$ point function can be obtained using Wick contractions of the 2 point function.

2.1 Time evolution of the scalar quench

Let us consider the case when the quench is due to the free scalar ϕ given by

$$\rho(t, -y_0) = \phi(\tau_e, -y_0,)|0\rangle\langle 0|\phi(\tau_l, -y_0). \quad (2.6)$$

To show that this state corresponds to a pulse with width ϵ moving at the speed of light, we can evaluate the expectation value of the stress tensor on this state. The stress tensor

for the conformal scalar is given by

$$\begin{aligned} T_{00} &= \partial_0 \phi \partial_0 \phi - \frac{1}{12} (2\partial_0^2 - \square) \phi^2, \\ &= \frac{1}{2} \partial_0 \phi \partial_0 \phi - \frac{1}{2} \phi \partial_0^2 \phi + \frac{1}{6} \partial_y \phi \partial_y \phi + \frac{1}{6} \phi \partial_y^2 \phi + \frac{1}{6} (\partial_x \phi \partial_x \phi + \partial_z \phi \partial_z \phi) + \frac{1}{6} (\phi \partial_x^2 \phi + \phi \partial_z^2 \phi). \end{aligned} \quad (2.7)$$

The expectation value of the stress tensor placed at the origin reduces to the evaluation of the following 3pt function

$$\begin{aligned} \text{Tr}[T_{00}(0, 0)\rho(t, -y_0)] &= \text{Tr}[T_{00}(0, y_0)\rho(t, 0)], \\ &= \frac{\langle \phi(-\epsilon - it, 0) T_{00}(0, y_0) \phi(\epsilon - it, 0) \rangle}{\langle \phi(-\epsilon - it, 0) \phi(\epsilon - it, 0) \rangle}. \end{aligned} \quad (2.8)$$

Here we have specified only the temporal and the y coordinate, it is understood that the fields are placed at $x_1 = x_2, z_1 = z_2$. In the first line of the above equation we have used translation invariance. All the correlators are evaluated in $4d$ Euclidean space, the two-point function of the scalar is given by

$$\langle \phi(x) \phi(y) \rangle_{\Sigma_1} = \frac{1}{4\pi^2 |x - y|^2}. \quad (2.9)$$

Evaluating both the 3 point function and 2 point in (2.8) using Wick's rule we obtain

$$\text{Tr}[T_{00}(0, y_0)\rho(t, 0)] = \frac{8\epsilon^4 \left(3t^4 + 2t^2 (5y_0^2 + 3\epsilon^2) + 3(y_0^2 + \epsilon^2)^2 \right)}{3\pi^2 \left(t^4 + 2t^2 (\epsilon^2 - y_0^2) + (y_0^2 + \epsilon^2)^2 \right)^3}. \quad (2.10)$$

We have verified that this correlator agrees with the general expression for the 3 point function of the stress tensor with 2 scalar operators obtained in [33] using the Ward identity. We interpret this result as the expectation value of the stress tensor placed at y_0 after the quench placed at the origin has evolved for a time t . The behaviour of the stress tensor is shown in figure (1). Since there is spherical symmetry in the set up, the quench is a spherical pulse of energy of width ϵ travelling at the speed of light. Note that the amplitude of the pulse decreases in time as the energy spreads over a sphere of increasing radius.

The two-point function on Σ_n and its singularities

As discussed in the paragraph leading to (2.5), to evaluate the change in Rényi/entanglement entropy when the quench enters the region $y > 0$, we need the two-point function of the scalar field on replica surface which is a cone in which the angle θ is identified with $\theta + 2\pi n$. The Greens function is obtained by solving the differential equation

$$\left(\partial_r^2 + \frac{1}{r} \partial_{r_1} + \frac{1}{r_1^2} \partial_{\theta_1}^2 + \partial_{\mathbf{x}_1}^2 \right) G(r_1, r_2, \theta_1, \theta_2, \mathbf{x}_1, \mathbf{x}_2) = -\frac{1}{r_1} \delta(r_1 - r_2) \delta(\mathbf{x}_1 - \mathbf{x}_2), \quad (2.11)$$

with the boundary condition $G(r_1, r_2, \theta_1, \theta_2, \mathbf{x}_1, \mathbf{x}_2) = G(r_1, r_2, \theta_1 + 2\pi n, \mathbf{x}_1, \mathbf{x}_2)$. The label \mathbf{x} refers to the cartesian x, z directions. The solution of the Greens function is well known

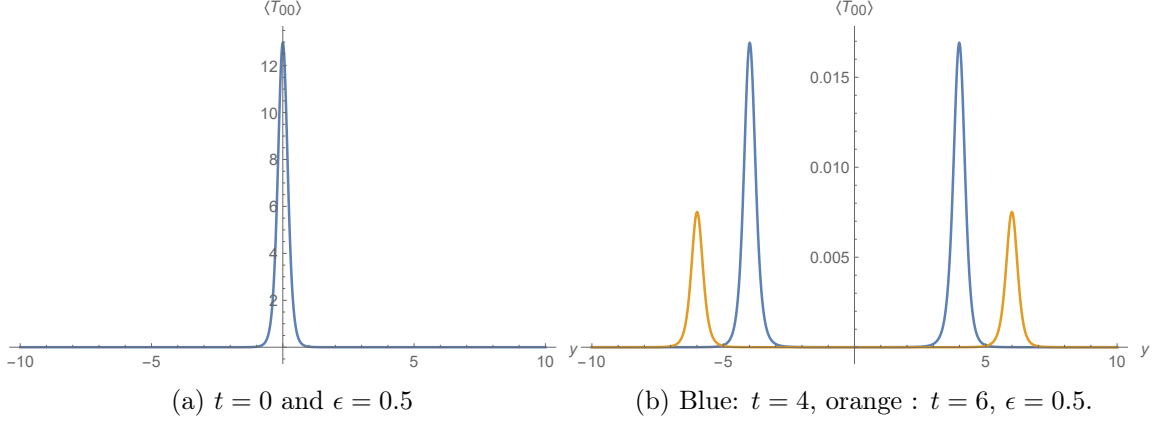


Figure 1: Energy density profile in the y direction for the excitation created by a quench due to the scalar ϕ placed at the origin at times $t = 0, 4, 6$. The width $\epsilon = 0.5$. The energy density is spherically symmetric and travels at the speed of light. Unlike in $d = 2$, the amplitude decreases in time as the density spreads over a sphere of increasing radius.

and has been studied in various contexts before, see [12] for a recent discussion.

$$\begin{aligned} \langle \phi(r_1, \theta_1, \mathbf{x}_1) \phi(r_2, \theta_2, \mathbf{x}_2) \rangle_{\Sigma_n} &= G(r_1, r_2, \theta_1, \theta_2, \mathbf{x}_1, \mathbf{x}_2), \\ &= \frac{\sinh \frac{\eta}{n}}{8\pi^2 n r_1 r_2 \sinh \eta (\cosh \frac{\eta}{n} - \cos \frac{\theta_1 - \theta_2}{n})}, \end{aligned} \quad (2.12)$$

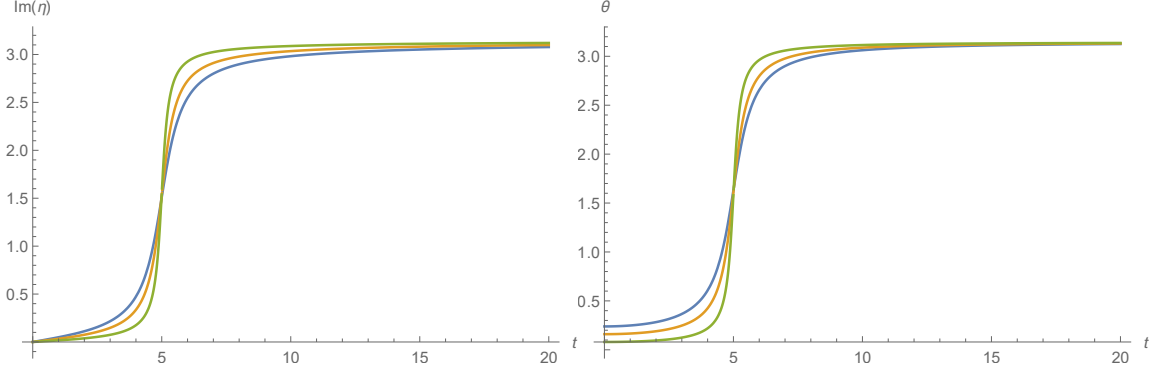
with

$$\begin{aligned} \cosh \eta &= \frac{r_1^2 + r_2^2 + (x_1 - x_2)^2 + (z_1 - z_2)^2}{2r_1 r_2}, & \cos(\theta_1 - \theta_2) &= \frac{y_1 y_2 + \tau_1 \tau_2}{r_1 r_2}, \\ r_1 &= y_1^2 + \tau_1^2, & r_2 &= y_2^2 + \tau_2^2. \end{aligned}$$

The expression of the Greens function suggests that the correlator is that of 2 conformal scalars of unit dimensions in a BCFT with a co-dimension 2 surface in $d = 4$. This can be seen from comparing the expressions in [34]. The behaviour correlator is determined by the cross ratios η and $\theta = \theta_1 - \theta_2$. Let us study their behaviour as the quench starting from $y = -y_0 < 0$ and enters the region $y > 0$. This is easily seen in the plots shown in figure 2. To obtain these plots we have chosen $x_1 = x_2 = z_1 = z_2 = 0, y_0 = -5$ and three different values of ϵ . Note that the angle η is purely imaginary and it begins with $\eta = 0$ and for $t > y_0$ it reaches $\eta = -i\pi$, similarly θ begins with $\theta = 0$ and asymptotically tends to the value of $\theta = \pi$. The transition is sharper as the width of the pulse becomes narrower.

As seen from the plots, the cross ratios would have different expansions for $t < y_0$ and for $t > y_0$. Let us first expand the parameters in small ϵ for $t < y_0$ case,

$$\begin{aligned} \eta_b &= i \tan^{-1} \left(\frac{\epsilon}{y_0 - t} \right) - i \tan^{-1} \left(\frac{\epsilon}{y_0 + t} \right), \\ \theta_b &= \tan^{-1} \left(\frac{\epsilon}{y_0 - t} \right) + \tan^{-1} \left(\frac{\epsilon}{y_0 + t} \right). \end{aligned} \quad (2.13)$$



(a) Imaginary part of η as a function of real-time. (b) θ as a function of real-time.

Figure 2: We plot imaginary part of η and θ as a function of real-time by varying ϵ . Blue line corresponds to $\epsilon = 0.6$, orange line corresponds to $\epsilon = 0.4$, and green line corresponds to $\epsilon = 0.2$. We keep $y_0 = -5$ in all cases.

These expressions should be understood as a power series expansion in ϵ . Similarly the expansions of the cross ratios for $t > y_0$ are given by

$$\begin{aligned}\eta_a &= i\pi - i \tan^{-1} \left(\frac{\epsilon}{t - y_0} \right) - i \tan^{-1} \left(\frac{\epsilon}{t + y_0} \right), \\ \theta_a &= \pi - \tan^{-1} \left(\frac{\epsilon}{t - y_0} \right) + \tan^{-1} \left(\frac{\epsilon}{t + y_0} \right).\end{aligned}\tag{2.14}$$

We now examine the leading divergence of the correlator (2.12) for $t < y_0$ in the $\epsilon \rightarrow 0$ limit. This will be useful to isolate the leading behaviour of the $2n$ point function in (2.5) for $t < y_0$ and obtain the Rényi entropy. Note that in this regime both the cross ratios are proportional to ϵ and tend to zero. Examining the correlator it is clear that the divergence arises due to the term $(\cosh \frac{\eta}{n} - \cos \frac{\theta}{n})$ in the denominator which is proportional to ϵ^2 .

$$\begin{aligned}\lim_{\epsilon \rightarrow 0} G(r_1, r_2, \theta_1, \theta_2)_{(t < y_0)} &= \frac{1}{4\pi^2(y_0^2 - t^2)(\eta^2 + \theta^2)} + O(\epsilon^0), \\ &= \frac{1}{16\pi^2\epsilon^2} + O(\epsilon^0).\end{aligned}\tag{2.15}$$

In the second line we have substituted the leading term in the expansions of the cross ratios from (2.13). Thus this correlator in the small ϵ limit reduces to the correlator on R^4 . Essentially the 2 operators separated in Euclidean time on the same sheet approach each other closely, so the fact that they are on the replica surface does not matter. Note that we have suppressed the dependence of the correlator on the x, z coordinates since the Green's function is independent of these coordinates. It is useful to keep track of the $O(\epsilon^0)$ which is given by

$$\lim_{\epsilon \rightarrow 0} G(r_1, r_2, \theta_1, \theta_2)_{(t < y_0)} = \frac{1}{16\pi^2\epsilon^2} \left(1 + \epsilon^2 \frac{1 - n^2}{3n^2(y_0^2 - t^2)} + \dots \right).\tag{2.16}$$

The Green's function with point r_1, θ_1 on the k_1 -sheet and r_2, θ_2 on the k_2 -sheet is obtained by shifting $\theta = \theta_1 - \theta_2$ to $\theta \rightarrow 2\pi(k_1 - k_2)$. From the expression of the Green's function in (2.12) and the cross ratios for $t < y_0$ in (2.13), we see that there are no other singularities for $k_1 - k_2 \neq 0$. Therefore, the leading contribution to the Green's function in this regime arises when the operators are present on the same sheet.

Let us also understand the singularities of correlator in the $t > y_0$ regime. From (2.14) we see that the cross ratios η, θ take values $i\pi, \pi$ respectively. We re-write the correlator as

$$G(r_1, r_2, \theta_1, \theta_2) = -\frac{\sin \frac{i\eta}{n}}{16\pi^2 n r_1 r_2 \sin i\eta \left(\sin \frac{i\eta+\theta}{2n} \sin \frac{i\eta-\theta}{2n} \right)}. \quad (2.17)$$

From (2.14) we see that in this regime the $\sin(i\eta)$ goes to zero as ϵ , and $\sin\left(\frac{i\eta+\theta}{2n}\right)$ goes to zero as ϵ . The expression $\sin\left(\frac{i\eta-\theta}{2n}\right)$ remains finite and tends to $-\sin\frac{\pi}{n}$. Therefore the correlator again diverges as ϵ^{-2} . Taking this limit we obtain

$$\lim_{\epsilon \rightarrow 0} G(r_1, r_2, \theta_1, \theta_2)_{(t > y_0)} = \frac{t + y_0}{32\pi^2 t \epsilon^2} + O(\epsilon^0). \quad (2.18)$$

This is the leading behaviour of the correlator when the operators are placed on the same sheet. Consider the situation when the operators are placed at r_1, θ_1 on the k_1 -sheet and r_2, θ_2 on the k_2 -sheet. For this we need to substitute $\theta \rightarrow \theta + 2\pi(k_1 - k_2)$ in (2.17) to obtain

$$G(r_1, r_2, \theta_1^{(k_1)}, \theta_2^{(k_2)}) = -\frac{\sin \frac{i\eta}{n}}{16\pi^2 n r_1 r_2 \sin i\eta \left(\sin \frac{i\eta+\theta+2\pi(k_1-k_2)}{2n} \sin \frac{i\eta-\theta-2\pi(k_1-k_2)}{2n} \right)}. \quad (2.19)$$

On using the expansions for the cross ratios in (2.19) we see that the most singular behaviour of this correlator arises when $k_1 - k_2 = -1$. In this case $\sin i\eta$ goes to zero as ϵ and $\sin\left(\frac{i\eta-\theta-2\pi(k_1-k_2)}{2n}\right)$ goes to zero as ϵ , while $\sin\left(\frac{i\eta+\theta+2\pi(k_1-k_2)}{2n}\right)$ remains finite. Again the correlator diverges as ϵ^{-2} ,

$$\lim_{\epsilon \rightarrow 0} G(r_1, r_2, \theta_1^{(k_1)}, \theta_2^{(k_2)})_{(t > y_0, k_1 - k_2 = -1)} = \frac{t - y_0}{32\pi^2 t \epsilon^2} + O(\epsilon^0). \quad (2.20)$$

Here the operators are placed so that they are on adjacent sheets and the 2nd operator is on a sheet above the 1st operator. It is important to note that the 2 singular behaviours for $t > y_0$ in (2.18) and (2.20) are related by $y_0 \rightarrow -y_0$. This arises because the contribution to the singularity arises from different factors in the product $\sin\left(\frac{i\eta-\theta}{2n}\right) \sin\left(\frac{i\eta+\theta}{2n}\right)$ present in the correlator (2.17). There is one more observation regarding the singular behaviour of the correlators in (2.18) and (2.20). We see that apart from the factor of $1/\epsilon^2$, which sets the dimensions, the function of y_0, t is only a function of the ratio $\frac{y_0}{t}$. Note that there are no other singular contributions. One particular case worth mentioning is when one examines the same point say $r_1 = r_2, \theta = 0$, but they are on different sheets, that is $k_1 - k_2 \neq 0$. Then from (2.19) we see that the correlator is finite and not divergent.

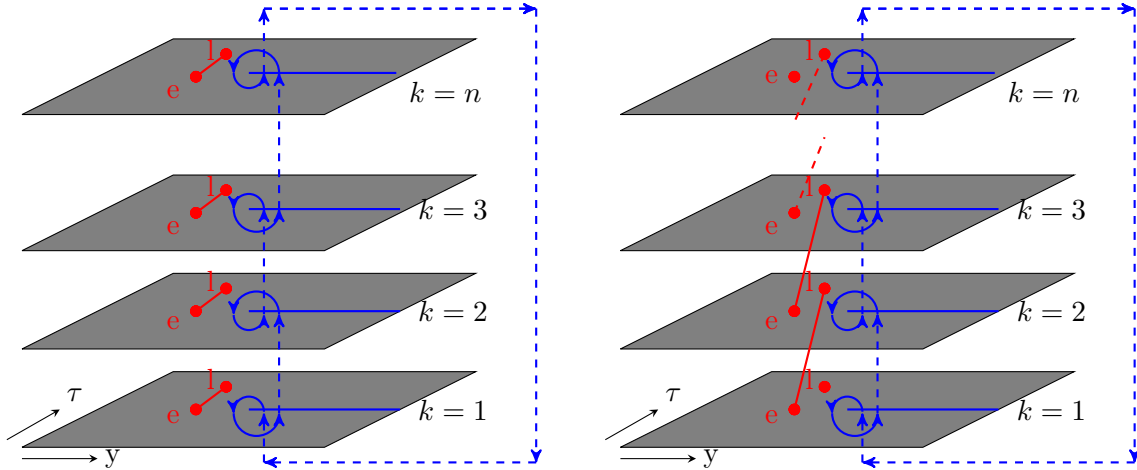


Figure 3: The leading Wick contractions in the $2n$ point function on Σ_n . For $t < y_0$, only the Wick contractions on the same sheet as shown in the figure on the left contributes. For $t > y_0$, both the Wick contractions, that is the one on the same sheet as well as the cyclic Wick contractions along adjacent sheet contributes equally. In the figure on the right, the operator at ‘ e ’ on the last sheet is contracted with the operator at ‘ l ’

Evaluation of $\Delta S_A^{(n)}$

With the information of the leading behaviour of the two-point function on the replica surface, we can proceed to evaluate the leading contributions to the Rényi entropies. For free fields the correlator in (2.5) can be evaluated using Wick contraction. For $t < y_0$ we see that the leading contribution comes from the contraction in which the two operators are on the same sheet. This is shown in the diagram on the left of figure 3. From (2.16) we see that this contribution is given by

$$\lim_{\epsilon \rightarrow 0, t < y_0} \left\langle \prod_{k=1}^n \mathcal{O}(r_l, \theta_l^{(k)}) \mathcal{O}(r_e, \theta_e^{(k)}) \right\rangle_{\Sigma_n} \Big|_{\text{same sheet contraction}} = \left[\frac{1}{16\pi^2 \epsilon^2} \left(1 + \epsilon^2 \frac{1 - n^2}{3n^2(y_0^2 - t^2)} + \dots \right) \right]^n. \quad (2.21)$$

As discussed below (2.16), the contractions of operators located on 2 different sheets are not singular they are $O(\epsilon^0)$. The next leading contraction will be from $n - 2$ pairs of operators on the same sheet and 2 pairs of operators contracted across sheets. This contribution is $O(\epsilon^{-2(n-2)})$. Therefore the leading and the next sub-leading contribution comes from the contractions on the same sheet given in (2.21). Substituting this in (2.5) and using the

expression for the correlator on Σ_1 from (2.9) we obtain

$$\begin{aligned}\Delta S_{t < y_0}^{(n)} &= \frac{1}{1-n} \log \left(1 + \epsilon^2 \frac{1-n^2}{3n^2(y_0^2 - t^2)} + \dots \right)^n \\ &= \frac{n}{1-n} \frac{(1-n^2)\epsilon^2}{3n^2(y_0^2 - t^2)} + \mathcal{O}(\epsilon^4)\end{aligned}\tag{2.22}$$

$$= \frac{n+1}{3n} \frac{\epsilon^2}{y_0^2 - t^2} + \mathcal{O}(\epsilon^4).\tag{2.23}$$

The entanglement vanishes as ϵ^2 before the pulse enters the entangling region. The coefficient of the ϵ^2 term has an interesting explanation. This is due to the fact that the leading contribution to the OPE of the operators on the same sheet is identical to the OPE of 2 scalars on R^4

$$\phi(x_1)\phi(x_2) \sim \frac{1}{4\pi^2|x_1 - x_2|^2} \left(1 + C_{\phi\phi:\phi^2} |x_1 - x_2|^2 : \phi^2(x_2) : + \dots \right).\tag{2.24}$$

The constant then in (2.22) should be proportional to the expectation value of the $: \phi^2 :$ on the replica surface. This can be obtained from the Green's function using the point split method.

$$\langle : \phi^2 : \rangle_{\Sigma_n} = \lim_{\substack{r_1 \rightarrow r_2 \\ \theta_1 \rightarrow \theta_2}} \left(G(r_1, r_2, \theta_1, \theta_2) - \frac{1}{4\pi^2 (r_1^2 + r_2^2 - 2r_1 r_2 \cos(\theta_1 - \theta_2))} \right).\tag{2.25}$$

We have set the parallel directions x, y of the both points to be the same. Now we can take the limit $r_1 \rightarrow r_2 = \sqrt{y^2 + \tau^2}$, from (2.13) we see that $\eta \rightarrow 0$, therefore we obtain

$$\begin{aligned}\langle : \phi^2 : \rangle_{\Sigma_n} &= \lim_{\theta \rightarrow 0} \frac{1}{4\pi^2} \left(\frac{1}{2n^2(y^2 + \tau^2) (1 - \cos(\frac{\theta}{n}))} - \frac{1}{2(y^2 + \tau^2)(1 - \cos(\theta))} \right), \\ &= \frac{1}{16\pi^2} \frac{1-n^2}{3n^2(y^2 + \tau^2)}.\end{aligned}\tag{2.26}$$

Comparing (2.22) and (2.26), we see that indeed that the ϵ^2 coefficient is proportional to the expectation value of the bilinear $: \phi^2 :$. We will see that as expected a similar feature persists in all the cases we study in this paper. This will serve as a simple consistency check of our calculations.

In the domain $t > y_0$, from the discussion of the singularities of the 2 point function we see that there are 2 set of contractions that contribute. The contractions of pairs of operators on the same sheet as shown in the left diagram of figure 3. Using (2.18) we obtain

the following contribution

$$\lim_{\epsilon \rightarrow 0, t > y_0} \left\langle \prod_{k=1}^n \mathcal{O}(r_l, \theta_l^{(k)}) \mathcal{O}(r_e, \theta_e^{(k)}) \right\rangle_{\Sigma_n} \Big|_{\text{same sheet contraction}} = \left(\frac{t - y_0}{32\pi^2 t \epsilon^2} \right)^n + O(\epsilon^{-(2n-1)}) \dots \quad (2.27)$$

The contractions shown in the right diagram of figure 3, also leads to the same order of divergence in the $2n$ point function. These contractions are due to contractions across nearest neighbour sheets cyclically. From (2.20) we obtain

$$\lim_{\epsilon \rightarrow 0, t > y_0} \left\langle \prod_{k=1}^n \mathcal{O}(r_l, \theta_l^{(k)}) \mathcal{O}(r_e, \theta_e^{(k)}) \right\rangle_{\Sigma_n} \Big|_{\text{cyclic contraction}} = \left(\frac{t - y_0}{32\pi^2 t \epsilon^2} \right)^n + O(\epsilon^{-(2n-1)}) \dots \quad (2.28)$$

All other contractions are sub-leading since they involve at least one contraction which is not nearest neighbour contraction or they involve contractions of the same point say r_e, θ_e but across 2 different sheets. Combining the contributions (2.27) and (2.28) we see that we obtain the following contribution to the change in entanglement entropy for $t > y_0$

$$\lim_{\epsilon \rightarrow 0, t > y_0} \Delta S_A^{(n)} = \frac{1}{1-n} \log \left[\frac{\left(\frac{t+y_0}{32\pi^2 t} \right)^n + \left(\frac{t-y_0}{32\pi^2 t} \right)^n}{\left(\frac{1}{16\pi^2} \right)^n} \right]. \quad (2.29)$$

At this point, it is useful to observe that the term in the square bracket is the leading contribution of the ratio of the $2n$ point function on the surface Σ_n to n products of the 2 point function on Σ_1 . By definition this ratio should be one at $n = 1$, which is indeed true as can be seen in (2.29). Also observe that the expression is a function of a linear polynomial in the ratio of y_0/t . We can take the $n \rightarrow 1$ limit to obtain the entanglement entropy

$$\begin{aligned} \Delta S_A &= \lim_{n \rightarrow 1} \Delta S_A^{(n)}, \\ &= \log(2) + \frac{y_0}{2t} \log \left[\frac{1 - \frac{y_0}{t}}{1 + \frac{y_0}{t}} \right] - \frac{1}{2} \log \left[1 - \left(\frac{y_0}{t} \right)^2 \right]. \end{aligned} \quad (2.30)$$

Another important behaviour to observe is the long time behaviour of the growth of Rényi/entanglement entropies, we see that it is given by

$$\lim_{t \rightarrow \infty} \Delta S_A^{(n)} = \log 2 - \frac{ny_0^2}{2t^2} + O\left(\frac{y_0^4}{t^4}\right) + \dots \quad (2.31)$$

We have seen that the growth profile of the entanglement as the quench enters the interval is entirely determined from the singular behaviour of 2 point function on the replica surface (2.12). This correlator is of the form of 2 conformal primaries of weight 1 in a BCFT

with a defect of co-dimension 2. Therefore it is interesting to cast the behaviour at the singularities to that seen for the case of quenches in 2 dimensions earlier in [19]. In the appendix we cast the correlator for $n = 2$ in terms of cross ratios similar to that in 2 dimensions and we will show that the growth of entanglement entropy is due to a similar phenomenon seen in 2 dimensions, that is the holomorphic cross ratio crosses a branch cut, while the anti-holomorphic does not.

2.2 Time evolution of the vector quench

In this section we study local quantum quenches in free Maxwell field theory in $d = 4$ dimension. The theory is free and conformal in four dimension. We study quenches obtained by exciting the ground state by field strengths. Therefore we would need the two-point function of the gauge field on the replica surface to evaluate the change in entanglement entropy. This two-point function can be constructed from the two-point function of the scalar given in (2.12) by taking suitable derivatives. Just as in the case of a co-dimension 2 defect correlator in (2.12) preserves $SO(2)_T \times SO(2)_L$ symmetry of R^4 . It is convenient to fix a gauge which gauge which is compatible with this symmetry. The $U(1)$ theory is gauge invariant under the transformation

$$A_\mu \rightarrow A_\mu + \partial_\mu \epsilon, \quad (2.32)$$

where ϵ is the gauge parameter. We use this gauge symmetry to first fix the gauge

$$\partial^\mu A_\mu = 0. \quad (2.33)$$

The equations of motion in the covariant gauge reduces to

$$\nabla^2 A_\mu = 0. \quad (2.34)$$

Now there are still allowed gauge transformations which preserve the covariant gauge, these are of the form

$$A'_\mu = A_\mu + \partial_\mu \epsilon, \quad \text{with} \quad \square \epsilon = 0. \quad (2.35)$$

Given a gauge potential which satisfies (2.33) and (2.34) we make a further gauge transformation so that the gauge potential satisfies

$$\partial^a A'_a = 0, \quad \partial^i A'_i = 0 \quad a \in \{t, y\}, i \in \{x, z\}. \quad (2.36)$$

The gauge potential satisfies the transversality condition independently in the directions perpendicular to the defect as well as the directions parallel to the defect. These conditions can be satisfied by choosing the gauge transformation to be

$$\epsilon = -\frac{\partial^i A_i}{\nabla^2}, \quad \nabla^2 = \partial_x^2 + \partial_z^2. \quad (2.37)$$

To show (2.36) is satisfied, we need to use (2.34) and (2.33). The gauge transformation also satisfies $\square \epsilon = 0$, which ensures that it is a valid choice of gauge. Such a gauge was

first used to construct the vector propagator for a conical defect in [30] and evaluate the expectation value of the stress tensor. We can follow the same construction for the replica surface Σ_n , which leads to [28],

$$\begin{aligned} G_{\mu\nu'}(x, x') &\equiv \langle A_\mu(x) A_{\nu'}(x') \rangle, \\ G_{ab'}(x, x') &= \frac{P_a P_{b'}}{\nabla^2} G(x, x'), \quad G_{ij'}(x, x') = \left[\delta_{ij} - \frac{\partial_i \partial_j}{\nabla^2} \right] \tilde{G}(x, x'), \\ G_{ai'}(x, x') &= G_{ia'}(x, x') = 0. \end{aligned} \tag{2.38}$$

where $G(x, x')$ is the scalar propagator on the cone which is given in (2.12). Note that by construction, the two-point function satisfies the condition

$$\partial^\mu G_{\mu\nu'}(x, x') = 0. \tag{2.39}$$

Here we label the 2 points as x and x' , and P_a are defined as

$$P_a = \epsilon_{ab} g^{bc} \nabla_c, \quad \epsilon_{ty} = -\epsilon_{yt} = 1, \quad \epsilon_{tt} = \epsilon_{yy} = 0. \tag{2.40}$$

One useful fact of writing the correlator in this way is that it is easy to write the components $G_{ab'}$ in polar coordinates if necessary. We just need to write the covariant form of P_a and $P_{b'}$. Earlier work on quenches for the $U(1)$ field used the Feynman gauge. We will see, the result for the entanglement jump in the $\epsilon \rightarrow 0$ limit is the same as that obtained in [26] using the gauge used here.

Two-point function of field strengths

There are 6 components of the field strengths and in principle one would have thought one needs to evaluate the 6 correlators of these field strengths to study their respective quenches. However due to the rotational symmetry in x and z directions and electro-magnetic duality, there are only 2 independent quenches. We will show this by explicit evaluation of the correlators, the fact that due to duality the entanglement growth of quenches of electric fields is the same as magnetic fields was first observed in [26]. Here we will see that the correlator on the replica surface, Σ_n of electric fields is same as that of magnetic fields.

First consider the two-point function of F_{ty} .

$$\begin{aligned} &\langle F_{ty}(x) F_{ty}(x') \rangle_{\Sigma_n} \\ &= \partial_{t_1} \partial_{t_2} \langle A_y(x) A_y(x') \rangle + \partial_{y_1} \partial_{y_2} \langle A_t(x) A_t(x') \rangle - \partial_{t_1} \partial_{y_2} \langle A_y(x) A_t(x') \rangle - \partial_{t_2} \partial_{y_1} \langle A_t(x) A_y(x') \rangle, \\ &= \left[\partial_{t_1} \partial_{t_2} \left(\frac{\partial_{t_1} \partial_{t_2}}{\nabla^2} \right) + \partial_{y_1} \partial_{y_2} \left(\frac{\partial_{y_1} \partial_{y_2}}{\nabla^2} \right) - \partial_{t_1} \partial_{y_2} \left(\frac{-\partial_{t_1} \partial_{y_2}}{\nabla^2} \right) - \partial_{t_2} \partial_{y_1} \left(\frac{-\partial_{t_2} \partial_{y_1}}{\nabla^2} \right) \right] G(x, x'), \\ &= -(\partial_{t_1}^2 + \partial_{y_1}^2) G(x, x'), \\ &= -\frac{(\coth(\eta) + 1) \left(\cosh\left(\frac{\eta}{n}\right) \cos\left(\frac{\theta}{n}\right) + n \coth(\eta) \sinh\left(\frac{\eta}{n}\right) \left(\cosh\left(\frac{\eta}{n}\right) - \cos\left(\frac{\theta}{n}\right) \right) - 1 \right)}{4\pi^2 n^2 r_1^3 r_2 \sinh \eta \left(\cos\left(\frac{\theta}{n}\right) - \cosh\left(\frac{\eta}{n}\right) \right)^2}. \end{aligned} \tag{2.41}$$

In this and subsequent equations, it is understood that x, x' refers to the first and the second coordinate. To derive the last line, we use the on-shell condition on the Green's function for separated points

$$(\partial_{t_2}^2 + \partial_{y_2}^2 + \partial_{x_2}^2 + \partial_{z_2}^2)G(x, x') = 0. \quad (2.42)$$

We then used the fact there is translation invariance in the x, z , which results in the following relations

$$\begin{aligned} \partial_{x_1} G(x, x') &= -\partial_{x_2} G(x, x'), \\ \partial_{z_1} G(x, x') &= -\partial_{z_2} G(x, x'). \end{aligned} \quad (2.43)$$

Note that the final result is (pseudo) scalar in the t, y directions, this is expected since we are working with the field strength F_{ty} .

To evaluate the time dependence of the entanglement entropy after the quench we need the singular behaviour of the correlator for $t < y_0$ and $t > y_0$. This can be obtained by examining (2.41) just as in the case of the scalar correlator. Again the leading singularity for $t < y_0$ occurs when the 2 points of the correlator are on the same sheet,

$$\lim_{\epsilon \rightarrow 0} \langle F_{ty}(r_1, \theta_1^k) F_{ty}(r_2, \theta_2^{(k)}) \rangle_{t < y_0} = -\frac{1}{16\pi^2\epsilon^4} - \frac{-11n^4 + 10n^2 + 1}{720\pi^2 n^4 (t^2 - y_0^2)^2} + O(\epsilon^2). \quad (2.44)$$

As expected, the leading singularity is the same as that of the correlator on Σ_1 . The correlator is not singular when the 2 points lie on different sheets. The leading correction at order $O(\epsilon^0)$ in (2.44) can be understood using the same reasoning as in the case for the scalar correlator. It is due to the expectation value of the composite F_{ty}^2 on Σ_n . We will demonstrate this in the next sub-section. Let us now obtain the leading behaviour in the $\epsilon \rightarrow 0$ limit for $t > y_0$. For this we can again examine (2.41) when θ, η is around π and $i\pi$ as discussed for the scalar case. When the operators are on the same sheet $k_1 = k_2 = k$, we obtain

$$\lim_{\epsilon \rightarrow 0} \langle F_{ty}(r_1, \theta_1^{(k)}) F_{ty}(r_2, \theta_2^{(k)}) \rangle_{t > y_0} = -\frac{(2t - y_0)(t + y_0)^2}{64\pi^2 t^3 \epsilon^4} + \mathcal{O}\left(\frac{1}{\epsilon^3}\right) + \dots \quad (2.45)$$

Similarly when the operators are placed on adjacent sheets we obtain

$$\langle F_{ty}(r_1, \theta_1^{(k_1)}) F_{ty}(r_2, \theta_2^{(k_2)}) \rangle_{t > y_0, k_1 - k_2 = -1} = -\frac{(t - y_0)^2 (2t + y_0)}{64\pi^2 t^3 \epsilon^4} + \mathcal{O}\left(\frac{1}{\epsilon^3}\right) + \dots \quad (2.46)$$

As we discussed in detail for the scalar, the reason the correlators in (2.45), (2.46) are related by $y \rightarrow y_0$ is due to the fact in one case $\sin\left(\frac{i\eta + \theta}{2n}\right)$ tends to zero and in the other $\sin\left(\frac{i\eta - \theta - 2\pi(k_1 - k_2)}{2n}\right)$ tends to zero. Further more, the power of ϵ^{-4} is determined by the dimension of the operator F_{ty} . The time dependence of the leading term is determined by a cubic polynomial through the ratio y_0/t . The order of the polynomial is one less the power of the ϵ . The leading behaviours of these correlators in (2.44), (2.45) and (2.46) obtained using the gauge in this paper agree with that obtain in [26] using the Feynman gauge.

Let us proceed and evaluate the two-point function of F_{xz} .

$$\begin{aligned}
& \langle F_{xz}(x)F_{xz}(x') \rangle_{\Sigma_n} \\
&= \partial_{x_1}\partial_{x_2}\langle A_z(x)A_z(x') \rangle + \partial_{z_1}\partial_{z_2}\langle A_x(x)A_x(x') \rangle - \partial_{x_1}\partial_{z_2}\langle A_z(x)A_x(x') \rangle - \partial_{x_2}\partial_{z_1}\langle A_x(x)A_z(x') \rangle \\
&= \left(\partial_{x_1}\partial_{x_2}\frac{\partial_{x_1}^2}{\nabla^2} + \partial_{z_1}\partial_{z_2}\frac{\partial_{z_1}^2}{\nabla^2} - \partial_{x_1}\partial_{z_2}\left(\frac{-\partial_{x_1}\partial_{z_1}}{\nabla^2}\right) - \partial_{x_2}\partial_{z_1}\left(\frac{-\partial_{x_1}\partial_{z_1}}{\nabla^2}\right) \right) G(x, x'), \\
&= -(\partial_{x_1}^2 + \partial_{z_1}^2)G(x, x') = (\partial_{t_1}^2 + \partial_{y_1}^2)G(x, x'). \tag{2.47}
\end{aligned}$$

To arrive at the last line, we have again used translation invariance (2.43) and the on shell condition (2.42). Comparing (2.41) and (2.47), we see that they are identical up to a sign. This is because the source free Maxwell theory is self dual under electro-magnetic duality and in Euclidean space the equations relating the dual components is given by

$$\tilde{F}_{ty} = -i\epsilon_{tyxz}F_{xz}. \tag{2.48}$$

Let us now evaluate the two-point function of F_{tx}

$$\begin{aligned}
& \langle F_{tx}(x)F_{tx}(x') \rangle_{\Sigma_n} = \\
& \partial_{t_1}\partial_{t_2}\langle A_x(x)A_x(x') \rangle + \partial_{x_1}\partial_{x_2}\langle A_t(x)A_t(x') \rangle - \partial_{t_1}\partial_{x_2}\langle A_x(x)A_t(x') \rangle - \partial_{t_2}\partial_{x_1}\langle A_t(x)A_x(x') \rangle, \\
&= \partial_{t_1}\partial_{t_2}\langle A_x(x)A_x(x') \rangle + \partial_{x_1}\partial_{x_2}\langle A_t(x)A_t(x') \rangle = \left(\partial_{t_1}\partial_{t_2}\frac{\partial_{y_1}^2}{\nabla^2} - \partial_{x_1}^2\frac{\partial_{y_1}\partial_{y_2}}{\nabla^2} \right) G(x, x'), \\
&= \frac{1}{2}(\partial_{t_1}\partial_{t_2} - \partial_{y_1}\partial_{y_2})G(x, x'). \tag{2.49}
\end{aligned}$$

In the last but one line we have used translation invariance (2.43) and then we have used the following isotropy property of the Greens function

$$\begin{aligned}
\partial_{x_1}^2 G(x, x') \Big|_{x_1 \rightarrow x_2, z_1 \rightarrow z_2} &= \frac{1}{2} \nabla^2 G(x, x') \Big|_{x_1 \rightarrow x_2, z_1 \rightarrow z_2}, \\
\partial_{z_1}^2 G(x, x') \Big|_{x_1 \rightarrow x_2, z_1 \rightarrow z_2} &= \frac{1}{2} \nabla^2 G(x, x') \Big|_{x_1 \rightarrow x_2, z_1 \rightarrow z_2}.
\end{aligned} \tag{2.50}$$

We can take the coincident limit in the x, z directions, since all the operators involved in the quench are placed at $x = z = 0$. In appendix D, we have derived these and similar relations which helps to simplify the computation of the correlators. Repeating the steps involved in the evaluation of the F_{tx} in (2.49), it is easy to see the two-point function of F_{tz} would be identical.

$$\langle F_{tz}(x)F_{tz}(x') \rangle_{\Sigma_n} \Big|_{x_1 \rightarrow x_2, z_1 \rightarrow z_2} = \langle F_{tx}(x)F_{tx}(x') \rangle_{\Sigma_n} \Big|_{x_1 \rightarrow x_2, z_1 \rightarrow z_2}. \tag{2.51}$$

Finally we have the two-point function of F_{yx}

$$\begin{aligned}
& \langle F_{yx}(x)F_{yx}(x') \rangle_{\Sigma_n}, \\
&= \partial_{y_1}\partial_{y_2}\langle A_x(x)A_x(x') \rangle + \partial_{x_1}\partial_{x_2}\langle A_y(x)A_y(x') \rangle - \partial_{y_1}\partial_{x_2}\langle A_x(x)A_y(x') \rangle - \partial_{y_2}\partial_{x_1}\langle A_x(x)A_y(x') \rangle, \\
&= \partial_{y_1}\partial_{y_2}\langle A_x(x)A_x(x') \rangle + \partial_{x_1}\partial_{x_2}\langle A_y(x)A_y(x') \rangle, \\
&= \left(\partial_{y_1}\partial_{y_2}\left(\frac{\partial_{z_1}^2}{\nabla^2}\right) + \partial_{x_1}\partial_{x_2}\left(\frac{\partial_{t_1}\partial_{t_2}}{\nabla^2}\right) \right) G(x, x'), \\
&= \frac{1}{2}(-\partial_{t_1}\partial_{t_2} + \partial_{y_1}\partial_{y_2}) G(x, x'). \tag{2.52}
\end{aligned}$$

To arrive at the last line we have used translation invariance (2.43) as well as (2.50). It is again clear from this calculation that if we repeat the same steps for we have the relation

$$\langle F_{yx}(x)F_{yx}(x') \rangle_{\Sigma_n} \Big|_{x_1 \rightarrow x_2, z_1 \rightarrow z_2} = \langle F_{yz}(x)F_{yz}(x') \rangle_{\Sigma_n} \Big|_{x_1 \rightarrow x_2, z_1 \rightarrow z_2}. \tag{2.53}$$

Comparing (2.49) and (2.52) we see that as expected they are identical up to a sign due to the electro magnetic duality of the Maxwell theory. In conclusion due to isotropy and duality we have only one independent quench among those created by field strengths $F_{tx}, F_{tz}, F_{yx}, F_{yz}$. The explicit form of two-point function of say F_{tx} on Σ_n is quite long and cumbersome. But for our purpose we just need the singular behaviour in the $\epsilon \rightarrow 0$ limit for $t < y_0$ and $t > y_0$. A simple method to evaluate this is to first convert the derivatives in t_1, t_2, y_1, y_2 in terms of θ, η, r_1, r_2 using the chain rule of differentiation, substitute the singular behaviour of the scalar correlator and the coefficients occurring from the chain rule and isolate the leading singularity². For $t < y_0$, the leading behaviour again is when the operators are placed on the same sheet and is given by

$$\lim_{\epsilon \rightarrow 0} \langle F_{tx}(r_1, \theta_1^k) F_{tx}(r_2, \theta_2^{(k)}) \rangle_{(t < y_0)} = -\frac{1}{16\pi^2\epsilon^4} + O(\epsilon^0). \tag{2.54}$$

For operators placed on different sheets, the correlator is finite. Again, for $t > y_0$, the leading singular behaviour for operators on the same sheet is

$$\lim_{\epsilon \rightarrow 0} \langle F_{tx}(r_1, \theta_1^k) F_{tx}(r_2, \theta_2^{(k)}) \rangle_{(t > y_0)} = -\frac{(t + y_0)(4t^2 - ty_0 + y_0^2)}{128\pi^2 t^3 \epsilon^4} + \dots. \tag{2.55}$$

Then there is an equally singular contribution from operators located on adjacent sheets which is given by

$$\langle F_{tx}(r_1, \theta_1^{(k_1)}) F_{tx}(r_2, \theta_2^{(k_2)}) \rangle_{(t > y_0, k_1 - k_2 = -1)} = -\frac{(t - y_0)(4t^2 + ty_0 + y_0^2)}{128\pi^2 t^3 \epsilon^4} + \dots. \tag{2.56}$$

Observe, as discussed in detail for the scalar case the correlator in (2.55) with operators on the same sheet is related to (2.56) that with operators on adjacent sheets by $y_0 \rightarrow -y_0$. Also note that power of ϵ is determined by the dimension of the field strength, so it is ϵ^4 and the dependence in time is through a polynomial of order 3 in the ratio y_0/t . Again, the

²This has been done using Mathematica.

singular behaviour of the correlators in (2.54), (2.55) and (2.56) agree with that obtained in [26] using the Feynman gauge.

Evaluation of $\Delta S_A^{(n)}$

Let us consider the state in which the ground state is excited by the operator F_{ty} given by

$$\rho(t, -y_0) = F_{ty}(\tau_e, -y_0)|0\rangle\langle 0|F_{ty}(\tau_l, -y_0). \quad (2.57)$$

Just as in the scalar case we wish to probe this state by the stress tensor and show that it corresponds to a spherical pulse moving at the speed of light. We evaluate the expectation value of then energy density

$$\begin{aligned} \text{Tr}[T_{00}(0, 0)\rho(t, -y_0)] &= \text{Tr}[T_{00}(0, y_0)\rho(t, 0)], \\ &= \frac{\langle F_{ty}(-\epsilon - it, 0)T_{tt}(0, y_0)F_{ty}(\epsilon - it, 0) \rangle}{\langle F_{ty}(-\epsilon - it, 0)F_{ty}(\epsilon - it, 0) \rangle}. \end{aligned} \quad (2.58)$$

The energy density of the Maxwell field is given by

$$T_{00} = F_{0\lambda}F_0^\lambda - \frac{1}{4}F_{\alpha\beta}F^{\alpha\beta}. \quad (2.59)$$

The Wick contractions in (2.58) are on flat R^4 or Σ_1 , therefore we use the same 2 point functions given in (2.38) with $n = 1$. Expanding the terms in the stress tensor, one encounters Wick contractions of the following type

$$\begin{aligned} \lim_{\substack{x_1 \rightarrow x_2 \\ z_1 \rightarrow z_2}} \langle F_{ty}(r_1, \theta_1, x_1, z_1)F_{ti}(r_2, \theta_2, x_2, z_2) \rangle &= 0, \\ \lim_{\substack{x_1 \rightarrow x_2 \\ z_1 \rightarrow z_2}} \langle F_{ty}(r_1, \theta_1, x, z)F_{yi}(r_2, \theta_2, x_2, z_2) \rangle &= 0, \\ \lim_{\substack{x_1 \rightarrow x_2 \\ z_1 \rightarrow z_2}} \langle F_{ty}(r_1, \theta_1, x, z)F_{ij}(r_2, \theta_2, x_2, z_2) \rangle &= 0, \quad \{i, j\} \in \{x, z\}. \end{aligned} \quad (2.60)$$

Using these simplifications, we find the evaluation of the expectation value of the energy density of the excited state (2.57) involves only product of two-point functions of F_{ty} . Evaluating this product at the coordinates in (2.58) we obtain

$$\text{Tr}[T_{00}(0, 0)\rho(t, -y_0)] = \frac{64\epsilon^4}{\left(t^4 + 2t^2(\epsilon^2 - y^2) + (y^2 + \epsilon^2)^2\right)^2}. \quad (2.61)$$

We can also interpret this expectation value can also be thought of as the value of the energy density at time t at position y . Figure 4 shows the profile of energy density at times $t = 0, 4, 6$ for quenches created by F_{ty} . Again the profile indicates a spherical wave of energy density which travels at the speed of light.

Let us evaluate the time dependence of the entanglement due to the excitation in (2.57). The analysis proceeds just as in the case of the scalar excitation. We need to evaluate the

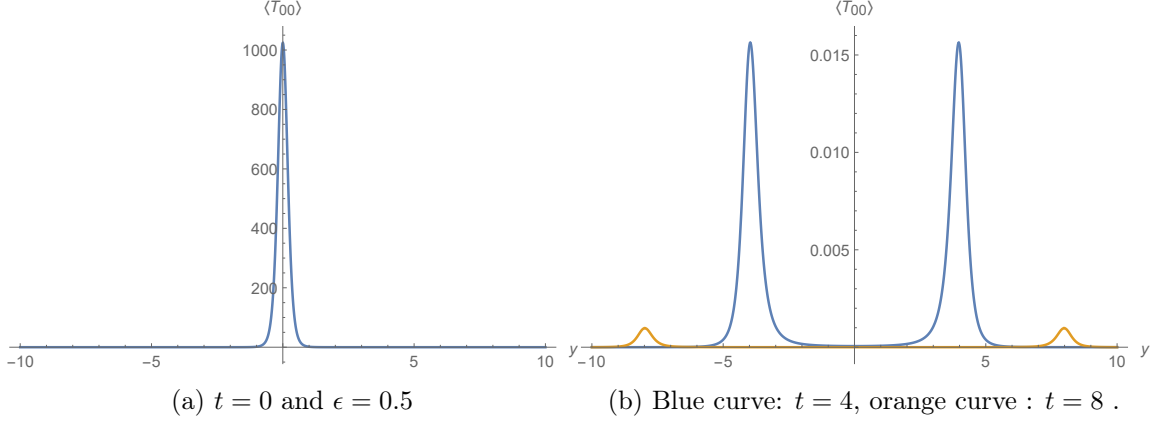


Figure 4: Energy density profile for the local quench created by field strength F_{ty} at times $t = 0, 4, 8$ with width $\epsilon = 0.5$.

$2n$ -point function in (2.5) with $\mathcal{O} = F_{ty}$. For $t < y_0$ the leading contribution comes from Wick contractions on the same sheet given in (2.44). Substituting this in (2.5) we obtain

$$\begin{aligned} \Delta S_{t < y}^{(n)}[F_{ty}] &= \frac{1}{1-n} \log \left(1 + \frac{(-11n^4 + 10n^2 + 1) \epsilon^4}{45n^4 (-t^2 + y_0^2)^2} + \dots \right)^n, \\ &= \frac{n}{1-n} \frac{(-11n^4 + 10n^2 + 1) \epsilon^4}{45n^4 (t^2 - y_0^2)^2} + \mathcal{O}(\epsilon^4). \end{aligned} \quad (2.62)$$

To evaluate the denominator in (2.5) we have used the two-point function of F_{ty} on Σ_1 which is given by

$$\langle F_{ty}(\tau_1, y_1) F_{ty}(\tau_2, y_2) \rangle_{\Sigma_1} = -\frac{1}{\pi^2 [(\tau_1 - \tau_2)^2 + (y_1 - y_2)^2]^2}. \quad (2.63)$$

Therefore for $t < y_0$, the change in Rényi entropy vanishes as ϵ^4 . This term is due to the presence of the composite operator $:F_{ty}^2:$ in the OPE of the two excitations on the same sheet which implies that the coefficient of the ϵ^4 term should be proportional to the expectation value of the composite operator on Σ_n . This expectation value can be obtained by the point split method

$$\begin{aligned} \langle :F_{ty}^2: \rangle_{\Sigma_n} &= -\lim_{\substack{r_2 \rightarrow r_1 \\ \theta_1 \rightarrow \theta_2}} \tilde{\nabla}^2 \left(G(r_1, r_2, \theta_1, \theta_2, \mathbf{x}, \mathbf{x}) - \frac{1}{4\pi^2 (r_1^2 + r_2^2 - 2r_1 r_2 \cos(\theta_1 - \theta_2))} \right), \\ &= -\lim_{\theta \rightarrow 0} \left(\frac{\csc^2\left(\frac{\theta}{2n}\right) (2n^2 + 3 \csc^2\left(\frac{\theta}{2n}\right) - 2)}{48\pi^2 n^4 r_1^4} - \frac{1}{4\pi^2 r_1^4 (\cos(\theta) - 1)^2} \right), \\ &= -\frac{(-11n^4 + 10n^2 + 1)}{720\pi^2 n^4 (\tau^2 + y^2)^2}. \end{aligned} \quad (2.64)$$

Here $\tilde{\nabla}^2 = (\partial_{r_1}^2 + \frac{1}{r_1} \partial_{r_1} + \frac{1}{r_1^2} \partial_{\theta_1}^2)$ is the Laplacian in $r - \theta$ plane. Therefore the ϵ^4 term in

(2.62) is due to the presence of the composite operator : F_{ty}^2 :

In the regime $t > y_0$, the leading contributions in the $\epsilon \rightarrow 0$ limit arises from the Wick contractions on the same sheet given in (2.45) as well as cyclic contractions on adjacent sheets given in (2.45). Substituting these contributions in (2.5) and normalising with the correlator on Σ_1 we obtain

$$\lim_{\epsilon \rightarrow 0} \Delta S_A^{(n)}[F_{ty}] = \frac{1}{1-n} \log \left[\frac{\left(\frac{(2t-y_0)(t+y_0)^2}{64\pi^2 t^3 \epsilon^4} \right)^n + \left(\frac{(t-y_0)^2(2t+y_0)}{64\pi^2 t^3 \epsilon^4} \right)^n}{\left(\frac{1}{16\pi^2 \epsilon^4} \right)^n} \right]. \quad (2.65)$$

At the leading order in ϵ , $\Delta S_A^{(n)}$ is independent of ϵ . The asymptotic behaviour at large times is given by

$$\lim_{t \rightarrow \infty} \Delta S_A^{(n)}[F_{ty}] = \log(2) - \frac{9ny_0^2}{8t^2} + O\left(\frac{y_0^4}{t^4}\right) + \dots \quad (2.66)$$

The coefficient of y_0^2/t^2 is important, in fact we will see that the knowledge of this coefficient is sufficient to determine the entire time dependent profile given in (2.65).

Taking the $n \rightarrow 1$ limit we obtain the change in the entanglement entropy

$$\begin{aligned} \lim_{n \rightarrow 1} \Delta S^{(n)}[F_{ty}] &= \Delta S_{\text{EE}}[F_{ty}], \\ &= \log 2 - \frac{1}{2} \log \left(1 - \frac{y_0^2}{t^2} \right) - \frac{y_0}{t} \tanh^{-1} \left(\frac{y_0}{t} \right). \end{aligned} \quad (2.67)$$

We repeat the same exercise for the excitation created by the field strength F_{tx} . In the $\epsilon \rightarrow 0$ limit, the change in entanglement entropy vanishes for $t < y_0$. For this case we are not keeping track of the ϵ^4 contribution. The growth in the Rényi entropy for $t > y_0$ in the zero width limit is given by

$$\lim_{\epsilon \rightarrow 0} \Delta S_A^{(n)}[F_{tx}] = \frac{1}{1-n} \log \left[\frac{\left(\frac{(t+y_0)(4t^2 - ty_0 + y_0^2)}{128\pi^2 t^3 \epsilon^4} \right)^n + \left(\frac{(t-y_0)(4t^2 + ty_0 + y_0^2)}{128\pi^2 t^3 \epsilon^4} \right)^n}{\left(\frac{1}{16\pi^2 \epsilon^4} \right)^n} \right]. \quad (2.68)$$

The asymptotic behaviour of the Rényi entropy at large times is given by

$$\lim_{t \rightarrow \infty} \Delta S_A^{(n)}[F_{tx}] = \log(2) - \frac{9ny_0^2}{32t^2} + O\left(\frac{y_0^3}{t^3}\right) + \dots \quad (2.69)$$

Finally the entanglement entropy is given by

$$\begin{aligned} \lim_{n \rightarrow 1} \Delta S^{(n)}[F_{tx}] &= \Delta S_{\text{EE}}[F_{tx}], \\ &= \frac{1}{8} \left[8 \log 8 - \left(\frac{y_0^3}{t^3} + \frac{3y_0}{t} + 4 \right) \log \left(\frac{y_0^3}{t^3} + \frac{3y_0}{t} + 4 \right) \right. \\ &\quad \left. - \left(4 - \frac{y_0^3}{t^3} - \frac{3y_0}{t} \right) \log \left(4 - \frac{y_0}{t} \left(\frac{y_0^2}{t^2} + 3 \right) \right) \right]. \end{aligned} \quad (2.70)$$

We make some observations regarding the Rényi/entanglement entropy growth after $t > y_0$ for the quenches created by the field strengths F_{ty} in (2.65) and F_{tx} in (2.68).

1. The 2 leading Wick contractions, those on the same sheet and that on adjacent sheets are related by $y_0 \rightarrow -y_0$.
2. The time dependence of the leading Wick contractions is a polynomial in the ratio y_0/t of order 3, which is equal to $2s + 1$ for $s = 1$. For example, the F_{tx} , the leading contribution to the F_{tx} correlator can be written as

$$\lim_{\epsilon \rightarrow 0} \langle F_{tx}(r_1, \theta_1^k) F_{tx}(r_2, \theta_2^{(k)}) \rangle_{(t > y_0)} = -\frac{(1+r)(4-r+r^2)}{128\pi^2\epsilon^4} + \dots, \quad r = \frac{y_0}{t}. \quad (2.71)$$

The scaling dimension is set by the power of ϵ in the denominator which is 4. The polynomial is of the order 3. The correlator of the operator on the adjacent sheets is obtained by $r \rightarrow -r$.

3. The ratio of the $2n$ point function on Σ_n to the n -th power of the 2-point function on Σ_1 at $n = 1$, by definition is unity. This, together with the fact that two leading contributions for the $2n$ point function are related by $r \rightarrow -r$ implies that at $n = 1$, the polynomials that occur in the logarithm of the Rényi entropy must satisfy

$$P(r) + P(-r) = 1. \quad (2.72)$$

Note that due to this condition the polynomial should be of the form

$$P(r) = \frac{1}{2}(1 + a_1 r + a_3 r^2). \quad (2.73)$$

Note that the even power r^2 is missing in the polynomial. By examining (2.65) and (2.68) we see that both the contributions in the argument of the logarithm is in this form.

4. The leading contribution to the F_{ty} correlator on the same sheet has a factor of $(1+r)^2$, while the corresponding contribution from the F_{tx} correlator has a factor $(1+r)$. F_{ty} is transforms as a (pseudo)scalar under $SO(2)_T$ and a scalar under $SO(2)_L$. F_{tx} transforms as vector under $SO(2)_T$ as well as $SO(2)_L$. The pseudo-scalar has higher power of the factor $(1+r)^2$ which is equal to $s + 1$.
5. The polynomial corresponding to the scalar of $SO(2)_T \times SO(2)_L$, F_{ty} is completely determined by the above conditions. It should be of the form

$$P_{F_{ty}}(r) = \frac{1}{2}(1+r)^2(1+a_1 r) = \frac{1}{2}[1 + (a_1 + 2)r + (2a_1 + 1)r^2 + a_1 r^3]. \quad (2.74)$$

This implies we must have $a_1 = -1/2$, therefore we have

$$P_{F_{ty}}(r) = \frac{1}{2}(1+r)^2(1 - \frac{1}{2}r) \quad (2.75)$$

This reasoning agrees with the result in (2.45).

6. The polynomial corresponding to the vector of $SO(2)_T \times SO(2)_L$ is determined to a single number. It is of the form

$$\begin{aligned} P_{F_{ty}}(r) &= \frac{1}{2}(1+r)(1+a_1r+a_2r^2), \\ &= \frac{1}{2}(1+(a_1+1)r+(a_1+a_2)r^2+a_2r^3). \end{aligned} \tag{2.76}$$

Since we have only odd terms in r we must have $a_2 = -a_1$. There the polynomial is of the form

$$P_{F_{ty}}(r) = \frac{1}{2}(1+r)(1+a_1r-a_1r^2) \tag{2.77}$$

Comparison with (2.55) we see that indeed the polynomial is of this form with $a_1 = -1/4$.

7. Finally if the polynomial is given by

$$P(r) = \frac{1}{2}(1+a_1r+a_2r^3). \tag{2.78}$$

The leading terms in the Rényi entropy is given by

$$\begin{aligned} S_A^{(n)}(P) &= \frac{1}{(1-n)} \log \left[\left(\frac{1}{2} \right)^n \left(1 + na_1r + \frac{n(n-1)}{2} a_1^2 r^2 + \dots \right) + (r \rightarrow -r) \right], \\ &= \log(2) - \frac{n}{2} a_1^2 r^2 + \dots \end{aligned} \tag{2.79}$$

The reason the sub-leading correction to the long time behaviour of the Rényi entropies starts at r^2 is clearly due to the fact that there are no even powers of r in the polynomial corresponding to the 2-point function. The coefficient which determines the asymptotic behaviour at large times is entirely determined by the linear term a_1 of the polynomial corresponding to the correlator. Thus the polynomial of the field strengths in the vector representation of $SO(2)_T \times SO(2)_L$ is completely determined by the asymptotic behaviour of the Rényi entropies.

It is easy to see the linear polynomial $P_\phi = \frac{1}{2}(1+r)$ obtained for the scalar $s = 0$, quench is consistent with these observations. In this next section we will see that these observations generalise to quenches induced by the curvature of the linearised graviton.

3 Local gravitational quenches

In this section we apply the methods developed in previous section to quenches created by the Riemann curvature tensor in the theory of linearised gravity in $d = 4$. As we have mentioned in the introduction, the information theoretic properties of the graviton has only been recently studied. Quenches with the spin-2 field have not been studied earlier. In [31, 32] it has been argued that the absence of the ‘split’ property of local quantum theories

in gravity implies that sub-regions in gravity are ill defined. We will see in this section, that the methods of the previous section can be extended to the theory of linearised gravity and the results for the entanglement of quenches is qualitatively similar to that obtained for the vector and scalar quenches.

The Lagrangian for the theory of linearised gravity is given by

$$\mathcal{L} = -\partial_\mu h^{\mu\nu} \partial_\alpha h_\nu^\alpha + \frac{1}{2} \partial^\alpha h_{\mu\nu} \partial_\alpha h^{\mu\nu} + \partial_\mu h^{\mu\nu} \partial_\nu h_\alpha^\alpha - \frac{1}{2} \partial_\alpha h_\mu^\mu \partial^\alpha h_\nu^\nu. \quad (3.1)$$

It admits the following gauge symmetry

$$\delta h_{\mu\nu} = \partial_\mu \xi_\nu + \partial_\nu \xi_\mu. \quad (3.2)$$

We need to consider operators which are gauge invariant to create the quenches. In the theory of linearised gravity, it is easy to see that the Riemann curvature is gauge invariant. It is defined by

$$R_{\mu\nu\rho\sigma} = \frac{1}{2} (\partial_\nu \partial_\rho h_{\mu\sigma} - \partial_\mu \partial_\rho h_{\nu\sigma} + \partial_\mu \partial_\sigma h_{\nu\rho} - \partial_\nu \partial_\sigma h_{\mu\rho}). \quad (3.3)$$

We will study quenches created by all the components of the Riemann tensor. By explicit computation we will show that there are only 7 distinct quenches created by the 20 independent components of the Riemann tensor.

3.1 Gauge fixing and the graviton propagator

Just as in the case of the $U(1)$ theory, we need to obtain the 2 point function of the graviton on the replica surface Σ_n . For this it is convenient to fix the gauge which preserves the $SO(2)_T \times SO(2)_L$ symmetry of the defect geometry. Using the gauge invariance in (3.2), we can ensure that the graviton is transverse and traceless

$$\partial^\mu h_{\mu\nu} = 0, \quad h_\mu^\mu = 0. \quad (3.4)$$

The Einstein's equations then implies that the graviton satisfies the equations

$$\square h_{\mu\nu} = 0. \quad (3.5)$$

There is still a residual gauge invariance which preserves the transverse, traceless conditions, these transformations are of the form

$$h'_{\mu\nu} = h_{\mu\nu} + \partial_\mu \epsilon_\nu + \partial_\nu \epsilon_\mu, \quad (3.6)$$

where the gauge parameter satisfies the conditions

$$\square \epsilon_\mu = 0, \quad \partial^\mu \epsilon_\mu = 0. \quad (3.7)$$

We can use this degree of freedom to ensure that the graviton satisfies the transverse conditions both perpendicular and parallel to the defect. That is obtain a gauge parameter,

so that we have

$$\partial^a h'_{a\mu} = 0, \quad \partial^i h'_{i\mu} = 0, \quad a \in \{t, y\}, i \in \{x, z\}, \quad h'^{\mu}{}_{\mu} = 0. \quad (3.8)$$

The gauge parameter which does this job is given by

$$\begin{aligned} \epsilon_a &= -\frac{1}{\nabla^2} \left(\partial^i h_{ia} - \frac{\partial_a \partial^i \partial^j h_{ij}}{2\nabla^2} \right), \\ \epsilon_i &= -\frac{1}{\nabla^2} \left(\partial^j h_{ij} - \frac{\partial_i \partial^j \partial^k h_{jk}}{2\nabla^2} \right), \\ \nabla^2 &= \partial^i \partial_i. \end{aligned} \quad (3.9)$$

On substituting this gauge parameter in (3.6) it is easy to see that the conditions (3.8) is satisfied. To show this we need the transverse condition in (3.4) and the equations of motion (3.5). It is also useful to realise that the choice in (3.9) satisfies

$$\partial^a \epsilon_a = -\partial^i \epsilon_i = +\frac{\partial^i \partial^j}{2\nabla^2} h_{ij}, \quad (3.10)$$

To arrive at these relations we have again used the gauge condition $\partial^i h_{i\mu} = 0$ and the on shell condition $\square h_{\mu\nu} = 0$. Therefore the gauge transformation in (3.9) satisfies the transverse condition in (3.7). It is also easy to see that the gauge parameter satisfies the condition $\square \epsilon_\mu = 0$ using the on shell condition of $h_{\mu\nu}$.

Graviton Propagator

Since it is possible to choose the gauge conditions in (3.8), we can construct a propagator that is consistent with these conditions. This propagator is given by

$$\begin{aligned} \langle h_{ab}(x) h_{cd}(x') \rangle &= \left(\frac{P_a P'_c P_b P'_d}{\nabla^4} + \frac{P_a P'_d P_b P'_c}{\nabla^4} \right) G(x, x'), \\ \langle h_{ij}(x) h_{kl}(x') \rangle &= \left[\left(\delta_{ik} - \frac{\partial_i \partial_k}{\nabla^2} \right) \left(\delta_{jl} - \frac{\partial_j \partial_l}{\nabla^2} \right) + \left(\delta_{il} - \frac{\partial_i \partial_l}{\nabla^2} \right) \left(\delta_{jk} - \frac{\partial_j \partial_k}{\nabla^2} \right) \right] G(x, x'), \\ \langle h_{ai}(x) h_{bj}(x') \rangle &= \frac{P_a P'_b}{\nabla^2} \left(\delta_{ij} - \frac{\partial_i \partial_j}{\nabla^2} \right) G(x, x'), \\ \langle h_{ab}(x) h_{ij}(x') \rangle &= 2 \frac{P_a P_b}{\nabla^2} \left(\delta_{ij} - \frac{\partial_i \partial_j}{\nabla^2} \right) G(x, x'), \\ \langle h_{ij}(x) h_{ab}(x') \rangle &= 2 \frac{P'_a P'_b}{\nabla^2} \left(\delta_{ij} - \frac{\partial_i \partial_j}{\nabla^2} \right) G(x, x'). \\ \langle h_{ai}(x) h_{ij}(x') \rangle &= \langle h_{ai}(x) h_{cd}(x') \rangle = 0, \end{aligned} \quad (3.11)$$

Here $G(x, x')$ is the scalar propagator on the replica surface given in (2.12). It can be easily verified that the propagator satisfies the conditions

$$\begin{aligned}\nabla_x^a \langle h_{a\mu}(x) h_{\rho\sigma}(x') \rangle &= 0, & \partial^i \langle h_{i\mu}(x) h_{jk}(x') \rangle &= 0, \\ \langle h_{\mu}^{\mu}(x) h_{\rho\sigma}(x') \rangle &= 0, & \square_x \langle h_{\mu\nu}(x) h_{\rho\sigma}(x') \rangle &= 0.\end{aligned}\tag{3.12}$$

A similar set of equations in which the derivatives acts on x' and the trace is taken over $h_{\rho\sigma}(x')$ also holds.

3.2 Two-point function of Riemann curvatures

In this section we evaluate the 2-point functions of all the 20 components of the Riemann curvatures. We will see by explicit calculation that among the 20 correlators we can use to create the quenches, there are only 7 independent quenches. In each case we evaluate the behaviour of the correlator before and after it reaches the entangling surface in the small width limit.

Class 1: $\{R_{tyty}, R_{xzxz}, R_{tyxz}\}$

We begin by evaluating two-point functions of R_{tyty} on replica surface. From (3.3), R_{tyty} is given by

$$\begin{aligned}R_{tyty} &= \frac{1}{2} \left[\partial_y \partial_t h_{ty} - \partial_t^2 h_{yy} + \partial_t \partial_y h_{yt} - \partial_y^2 h_{tt} \right], \\ &= \frac{1}{2} \left[2\partial_y \partial_t h_{ty} - \partial_t^2 h_{yy} - \partial_y^2 h_{tt} \right].\end{aligned}\tag{3.13}$$

We now use the graviton corellator on the replica surface (3.11) to evaluate the two-point function of R_{tyty}

$$\begin{aligned}\langle R_{tyty}(x) R_{tyty}(x') \rangle &= \frac{1}{4} \left[4\partial_{y_1} \partial_{y_2} \partial_{t_1} \partial_{t_2} \langle h_{ty} h_{ty} \rangle - 2\partial_{y_1} \partial_{t_1} \partial_{t_2}^2 \langle h_{ty} h_{yy} \rangle - 2\partial_{y_1} \partial_{t_1} \partial_{y_2}^2 \langle h_{ty} h_{tt} \rangle \right. \\ &\quad - 2\partial_{t_1}^2 \partial_{y_2} \partial_{t_2} \langle h_{yy} h_{ty} \rangle + \partial_{t_1}^2 \partial_{t_2}^2 \langle h_{yy} h_{yy} \rangle + \partial_{t_1}^2 \partial_{y_2}^2 \langle h_{yy} h_{tt} \rangle \\ &\quad \left. - 2\partial_{y_1}^2 \partial_{y_2} \partial_{t_2} \langle h_{tt} h_{ty} \rangle + \partial_{y_1}^2 \partial_{t_2}^2 \langle h_{tt} h_{yy} \rangle + \partial_{y_1}^2 \partial_{y_2}^2 \langle h_{tt} h_{tt} \rangle \right], \\ &= \frac{1}{2} \frac{(\partial_{t_1}^2 + \partial_{y_1}^2)^2 (\partial_{t_2}^2 + \partial_{y_2}^2)^2}{\nabla^4} G(x, x'), \\ &= \frac{1}{2} (\partial_{t_1}^2 + \partial_{y_1}^2)^2 G(x, x').\end{aligned}\tag{3.14}$$

To derive the last line we use the on-shell condition of the scalar Green's function in the second coordinate x' given in (2.42) and translation invariance in x, z direction (2.43), to convert the derivatives to the first coordinate.

Similarly, we evaluate $\langle R_{xzxz} R_{xzxz} \rangle$. The expression of R_{xzxz} is given by (3.3)

$$R_{xzxz} = \frac{1}{2} \left[2\partial_x \partial_z h_{xz} - \partial_x^2 h_{zz} - \partial_z^2 h_{xx} \right].\tag{3.15}$$

Using the correlators from (3.11), we get

$$\begin{aligned}
\langle R_{xzxz}(x)R_{xzxz}(x') \rangle &= \frac{1}{4} \left[4\partial_{x_1}\partial_{x_2}\partial_{z_1}\partial_{z_2}\langle h_{xz}h_{xz} \rangle - 2\partial_{x_1}\partial_{z_1}\partial_{x_2}^2\langle h_{xz}h_{zz} \rangle - 2\partial_{x_1}\partial_{z_1}\partial_{z_2}^2\langle h_{xz}h_{xx} \rangle \right. \\
&\quad - 2\partial_{x_1}^2\partial_{z_2}\partial_{x_2}\langle h_{zz}h_{xz} \rangle + \partial_{x_1}^2\partial_{x_2}^2\langle h_{zz}h_{zz} \rangle + \partial_{x_1}^2\partial_{z_2}^2\langle h_{zz}h_{xx} \rangle \\
&\quad \left. - 2\partial_{z_1}^2\partial_{z_2}\partial_{x_2}\langle h_{xx}h_{xz} \rangle + \partial_{z_1}^2\partial_{x_2}^2\langle h_{xx}h_{zz} \rangle + \partial_{z_1}^2\partial_{z_2}^2\langle h_{xx}h_{xx} \rangle \right], \\
&= \frac{(\partial_{x_1}^2 + \partial_{z_1}^2)^4}{2\nabla^4} G(x, x'), \\
&= \frac{1}{2}(\nabla^2)^2 G(x, x') = \frac{1}{2}(\partial_{t_1}^2 + \partial_{t_2}^2)^2 G(x, x'). \tag{3.16}
\end{aligned}$$

In the last line we have used the on-shell condition satisfied by $G(x, x')$. Therefore this correlator is identical to $\langle R_{tyty}(x)R_{tyty}(x') \rangle$ given in (3.14). This implies quenches created by inserting the component R_{tyty} would behave identically to the component R_{xzxz} .

Consider the correlator $\langle R_{tyty}(x)R_{tyty}(x') \rangle$, the expression of R_{tyxz} is given by

$$R_{tyxz} = \frac{1}{2} \left[\partial_y \partial_x h_{tz} - \partial_t \partial_x h_{yz} + \partial_t \partial_z h_{yx} - \partial_y \partial_z h_{tx} \right], \tag{3.17}$$

There are 16 contractions using the graviton correlator in (3.11), which on adding results in

$$\begin{aligned}
\langle R_{tyxz}(x)R_{tyxz}(x') \rangle &= -\frac{1}{4}(\partial_{t_1}^2 + \partial_{y_1}^2)(\partial_{t_2}^2 + \partial_{z_2}^2)G(x, x'), \\
&= -\frac{1}{4}(\partial_{t_1}^2 + \partial_{y_1}^2)^2 G(x, x'). \tag{3.18}
\end{aligned}$$

Comparing with (3.14), (3.16), we see that the two-point function of R_{tyxz} differs from the from two correlators by a factor of 2. The overall factor of 2 does not affect the calculation of The Rényi/entanglement entropy corresponding to quenches just depends on the ratio of the correlators as can be seen from (2.5). Therefore the time dependence of the entanglement entropy of quenches created by all components $R_{tyty}, R_{xzxz}, R_{tyxz}$ will be the same. For these quenches we will take the excited state by R_{tyty} to be the representative quench.

The explicit expression of the R_{tyty} correlator on Σ_n is given in (B.1). But, all we need is the leading singular behaviour of the 2-points functions to obtain the time dependence of the entanglement entropy in the $\epsilon \rightarrow 0$ limit. For $t < y_0$, the leading singularity arises when the operators are on the same sheet and is given by

$$\begin{aligned}
\lim_{\epsilon \rightarrow 0} \langle R_{tyty}(r_1, \theta_1^{(k)}) R_{tyty}(r_2, \theta_2^{(k)}) \rangle_{t < y_0} & \tag{3.19} \\
&= \frac{1}{2} \left(\frac{1}{4\pi^2 \epsilon^6} + \frac{(n-1)(n+1)(191n^4 + 23n^2 + 2)}{3780\pi^2 n^6 (t^2 - y_0^2)^3} + \dots \right).
\end{aligned}$$

The leading singularity is same as that when the 2 points are on R^4 or Σ_1 . The leading correction at $O(\epsilon^0)$ is due to expectation value of the composite : R_{tyty}^2 : on Σ_n . Correlators with points on different sheets are not singular in this regime.

In $t > y_0$ regime, there are 2 leading singular contributions. When the operators are placed on the same sheet we obtain

$$\lim_{\epsilon \rightarrow 0} \langle R_{tyty}(r_1, \theta_1^{(k)}) R_{tyty}(r_2, \theta_2^{(k)}) \rangle_{t > y_0} = \frac{1}{2} \left(\frac{(t + y_0)^3 (8t^2 - 9ty_0 + 3y_0^2)}{64\pi^2 t^5 \epsilon^6} + \mathcal{O}\left(\frac{1}{\epsilon^5}\right) + \dots \right). \quad (3.20)$$

The other leading singular contribution occurs when operators are placed on adjacent sheet and is given by

$$\begin{aligned} \lim_{\epsilon \rightarrow 0} \langle R_{tyty}(r_1, \theta_1^{(k_1)}) R_{tyty}(r_2, \theta_2^{(k_2)}) \rangle_{t > y_0, k_1 - k_2 = -1} \\ = \frac{1}{2} \left(\frac{(t - y_0)^3 (8t^2 + 9ty_0 + 3y_0^2)}{64\pi^2 t^5 \epsilon^6} + \mathcal{O}\left(\frac{1}{\epsilon^5}\right) + \dots \right). \end{aligned} \quad (3.21)$$

Observe that the power of ϵ in the denominator is determined by the dimension of the field and the singular behaviours in this regime on the same sheet and on adjacent sheets are related by $y_0 \rightarrow -y_0$. The time dependence is through the ratio y_0/t which is a polynomial of order $5 = 2s + 1$, $s = 2$. Finally the correlator on Σ_1 is given by

$$\langle R_{tyty}(\tau_1, y_1) R_{tyty}(\tau_2, y_2) \rangle_{n=1} = \frac{8}{\pi^2 [(\tau_1 - \tau_2)^2 + (y_1 - y_2)^2]^3}. \quad (3.22)$$

Class 2: $\{R_{tytx}, R_{tytz}, R_{yzxz}, R_{yxzx}\}$

In equations (B.3), (B.6), (B.8), (B.10) of the appendix we show that the curvature components $\{R_{tytx}, R_{tytz}, R_{yzxz}, R_{yxzx}\}$ have identical 2 point functions when one takes the coincident limit in the directions parallel to the defect, that is $x_1 = x_2, z_1 = z_2$.

$$\langle R_{tytx}(x) R_{tytx}(x') \rangle = \partial_{x_1}^2 (-2\partial_{y_1} \partial_{y_2} + \partial_{t_1} \partial_{t_2}) G(x, x') \Big|_{x_1=x_2, z_1=z_2}. \quad (3.23)$$

After taking the derivative with respect to x_1 coordinate, we evaluate the two-point function in the limit $x_1 \rightarrow x_2$ and $z_1 \rightarrow z_2$. Using this expression the leading singularity of the correlator when the two-points are on the same sheet in the regime $t > y_0$ is given by

$$\lim_{\epsilon \rightarrow 0} \langle R_{tytx}(r_1, \theta_1^{(k)}) R_{tytx}(r_2, \theta_2^{(k)}) \rangle_{t > y_0} = \frac{(t + y_0)^2 (14t^3 - 13t^2 y_0 + 12t y_0^2 - 6y_0^3)}{512\pi^2 t^5 \epsilon^6} + \dots \quad (3.24)$$

In this regime, the other leading singularity arises from correlators with points on adjacent sheets which is given by

$$\langle R_{tytx}(r_2, \theta_2^{(k_1)}) R_{tytx}(r_2, \theta_2^{(k_2)}) \rangle_{t > y_0, k_1 - k_2 = -1} = \frac{(t - y_0)^2 (14t^3 + 13t^2 y_0 + 12t y_0^2 + 6y_0^3)}{512\pi^2 t^5 \epsilon^6} + \dots \quad (3.25)$$

Finally the two-point function on Σ_1 is given by

$$\langle R_{tytx}(\tau + \epsilon)R_{tytx}(\tau - \epsilon) \rangle_{\Sigma_1} = \frac{7}{128\pi^2\epsilon^6}. \quad (3.26)$$

Here it is understood, all other coordinates are taken to be coincident. As expected, the above result is also the leading singularity when points are on the same sheet in the regime $t < y_0$.

Class 3: $\{R_{txxz}$ or R_{tzxz} or R_{tyyx} or $R_{tyyz}\}$

All the curvature components in this class have the same two-point function in the limit the points along the defect are coincident. The details of demonstrating this is given in equations (B.13), (B.15), (B.16), (B.17) of the appendix. Let us take R_{txxz} as the representative in this class, the correlator is given by

$$\langle R_{txxz}(x)R_{txxz}(x') \rangle = \partial_{x_1}^2 (\partial_{y_1} \partial_{y_2} - 2\partial_{t_1} \partial_{t_2}) G(x, x') \Big|_{x_1=x_2, z_1=z_2}. \quad (3.27)$$

In the regime $t > y_0$, the leading singularity in the $\epsilon \rightarrow 0$ limit from the correlators on the same sheet are given by

$$\lim_{\epsilon \rightarrow 0} \langle R_{txxz}(r_1, \theta_1^{(k)}) R_{txxz}(r_2, \theta_2^{(k)}) \rangle_{t > y_0} = -\frac{(t + y_0)^2 (22t^3 - 14t^2 y_0 + 6ty_0^2 - 3y_0^3)}{512\pi^2 t^5 \epsilon^6} + \dots \quad (3.28)$$

Similarly the leading singularity form operators on adjacent sheets is given by

$$\lim_{\epsilon \rightarrow 0} \langle R_{txxz}(r_1, \theta_1^{(k_1)}) R_{txxz}(r_2, \theta_2^{(k_2)}) \rangle_{t > y_0, k_1 - k_2 = -1} = -\frac{(t - y_0)^2 (22t^3 + 14t^2 y_0 + 6ty_0^2 + 3y_0^3)}{512\pi^2 t^5 \epsilon^6} + \dots \quad (3.29)$$

For $t < y_0$ as well as the correlator on the Σ_1 , we obtain the following behaviour

$$\langle R_{txxz}(\tau + \epsilon)R_{txxz}(\tau - \epsilon) \rangle_{\Sigma_1} = -\frac{11}{128\pi^2\epsilon^6}. \quad (3.30)$$

where all the other coordinates are understood to be coincident for the two operators.

Class 4: $\{R_{txtx}, R_{yzyz}, R_{tztz}, R_{yxyx}\}$

All the curvature components in this class have the same two-point function in the limit the points along the defect are coincident. The details of this is given in equations (B.20), (B.25), (B.23) Let us take R_{txtx} as the representative in this class, the correlator is given by

$$\langle R_{txtx}(x)R_{txtx}(x') \rangle = \left[\frac{3}{16} (\partial_{t_1}^2 \partial_{t_2}^2 + \partial_{y_1}^2 \partial_{y_2}^2) + \frac{1}{16} (\partial_{t_1} \partial_{y_2} - \partial_{y_1} \partial_{t_2})^2 \right] G(x, x') \Big|_{x_1=x_2, z_1=z_2}. \quad (3.31)$$

In the regime $t > y_0$, the leading singularity in the $\epsilon \rightarrow 0$ limit from the correlators on the same sheet are given by

$$\lim_{\epsilon \rightarrow 0} \langle R_{txtx}(r_1, \theta_1^{(k)}) R_{txtx}(r_2, \theta_2^{(k)}) \rangle_{t > y_0} = \frac{9(t + y_0) (6t^4 - t^3 y_0 + t^2 y_0^2 - t y_0^3 + y_0^4)}{1024 \pi^2 t^5 \epsilon^6} + \dots \quad (3.32)$$

Similarly the leading singularity form operators on adjacent sheet is given by

$$\lim_{\epsilon \rightarrow 0} \langle R_{txtx}(r_1, \theta_1^{(k_1)}) R_{txtx}(r_2, \theta_2^{(k_2)}) \rangle_{t > y_0, k_1 - k_2 = -1} = \frac{9(t - y_0) (6t^4 + t^3 y_0 + t^2 y_0^2 + t y_0^3 + y_0^4)}{256 \pi^2 t^5 \epsilon^6} + \dots \quad (3.33)$$

For $t < y_0$ as well as the correlator on the Σ_1 , we obtain the following behaviour

$$\lim_{\epsilon \rightarrow 0} \langle R_{txxz}(\tau + \epsilon) R_{txxz}(\tau - \epsilon) \rangle_{\Sigma_1} = \frac{27}{64 \pi^2 \epsilon^6} + \dots \quad (3.34)$$

where all the other coordinates are understood to be coincident for the two operators.

Class 5: $\{R_{txtz}, R_{yxyz}\}$

All the curvature components in this class have the same two-point function in the limit the points along the defect are coincident as shown in equations (B.29), (B.31). Let us take R_{txtz} as the representative in this class, the correlator is given by

$$\begin{aligned} \langle R_{txtz}(x) R_{txtz}(x') \rangle = & \quad (3.35) \\ \left[\frac{1}{8} \partial_{y_1} \partial_{y_2} \partial_{t_1} \partial_{t_2} + \frac{1}{16} (\partial_{t_1} \partial_{t_2} - \partial_{y_1} \partial_{y_2})^2 - \frac{1}{16} (\partial_{t_1} \partial_{y_2} - \partial_{y_1} \partial_{t_2})^2 \right] G(x, x')|_{x_1=x_2, z_1=z_2}. \end{aligned}$$

In the regime $t > y_0$, the leading singularity in the $\epsilon \rightarrow 0$ limit from the correlators on the same sheet are given by

$$\begin{aligned} \lim_{\epsilon \rightarrow 0} \langle R_{txtz}(r_1, \theta_1^{(k)}) R_{txtz}(r_2, \theta_2^{(k)}) \rangle_{t > y_0} & \quad (3.36) \\ = \frac{(t + y_0) (38t^4 - 23t^3 y_0 + 23t^2 y_0^2 - 3t y_0^3 + 3y_0^4)}{1024 \pi^2 t^5 \epsilon^6} + \dots \end{aligned}$$

Similarly the leading singularity form operators on adjacent sheets is given by

$$\begin{aligned} \lim_{\epsilon \rightarrow 0} \langle R_{txtz}(r_1, \theta_1^{(k_1)}) R_{txtz}(r_2, \theta_2^{(k_2)}) \rangle_{t > y_0, k_1 - k_2 = -1} & \quad (3.37) \\ = \frac{(t - y_0) (38t^4 + 23t^3 y_0 + 23t^2 y_0^2 + 3t y_0^3 + 3y_0^4)}{1024 \pi^2 t^5 \epsilon^6} + \dots \end{aligned}$$

For $t < y_0$ as well as the correlator on the Σ_1 , we obtain the following behaviour

$$\lim_{\epsilon \rightarrow 0} \langle R_{txtz}(\tau + \epsilon) R_{txtz}(\tau - \epsilon) \rangle_{\Sigma_1} = \frac{19}{256 \pi^2 \epsilon^6} + \dots \quad (3.38)$$

Class 6: $\{R_{txyx}, R_{tzyz}\}$

The two curvature components in this class have identical two-point functions in the limit the points along the defect coincide as shown in equation (B.34), (B.35). Let us take R_{txyx} as the representative in this class, the correlator is given by

$$\langle R_{txyx}(x)R_{txyx}(x') \rangle = \left[\frac{1}{32} (\partial_{t_1} \partial_{y_2} + \partial_{y_1} \partial_{t_2})^2 - \frac{1}{32} (\partial_{t_1} \partial_{t_2} - \partial_{y_1} \partial_{y_2})^2 \right] G(x, x')|_{x_1=x_2, z_1=z_2}. \quad (3.39)$$

In the regime $t > y_0$, the leading singularity in the $\epsilon \rightarrow 0$ limit from the correlators on the same sheet are given by

$$\lim_{\epsilon \rightarrow 0} \langle R_{txyx}(r_1, \theta_1^{(k)}) R_{txyx}(r_2, \theta_2^{(k)}) \rangle_{t > y_0} = - \frac{3(t + y_0) (16t^4 - 11t^3 y_0 + 11t^2 y_0^2 - t y_0^3 + y_0^4)}{2048 \pi^2 t^5 \epsilon^6} + \dots \quad (3.40)$$

Similarly the leading singularity from operators on adjacent sheet is given by

$$\begin{aligned} \lim_{\epsilon \rightarrow 0} \langle R_{txyx}(r_1, \theta_1^{(k_1)}) R_{txyx}(r_2, \theta_2^{(k_2)}) \rangle_{t > y_0, k_1 - k_2 = -1} & \quad (3.41) \\ & = - \frac{3(t - y_0) (16t^4 + 11t^3 y_0 + 11t^2 y_0^2 + t y_0^3 + y_0^4)}{2048 \pi^2 t^5 \epsilon^6} + \dots \end{aligned}$$

For $t < y_0$ as well as the correlator on the Σ_1 , we obtain the following behaviour

$$\lim_{\epsilon \rightarrow 0} \langle R_{txyx}(\tau + \epsilon) R_{txyx}(\tau - \epsilon) \rangle_{\Sigma_1} = - \frac{3}{16 \pi^2 \epsilon^6} + \dots \quad (3.42)$$

Class 7: $\{R_{txyz}\}$

We are now left with one curvature component R_{txyz} . The correlator is given by (B.37)

$$\langle R_{txyz}(x)R_{txyz}(x') \rangle = - \left[\frac{3}{32} (\partial_{t_1} \partial_{t_2} - \partial_{y_1} \partial_{y_2})^2 + \frac{1}{32} (\partial_{y_1} \partial_{t_2} - \partial_{t_1} \partial_{y_2})^2 \right] G(x, x')|_{x_1=x_2, z_1=z_2}. \quad (3.43)$$

In the regime $t > y_0$, the leading singularity in the $\epsilon \rightarrow 0$ limit from the correlators on the same sheet are given by

$$\lim_{\epsilon \rightarrow 0} \langle R_{txyx}(r_1, \theta_1^{(k)}) R_{txyx}(r_2, \theta_2^{(k)}) \rangle_{t > y_0} = - \frac{3(t + y) (28t^4 - 13t^3 y_0 + 13t^2 y_0^2 - 3t y_0^3 + 3y_0^4)}{2048 \pi^2 t^5 \epsilon^6} + \dots \quad (3.44)$$

Similarly the leading singularity from operators on adjacent sheet is given by

$$\begin{aligned} \lim_{\epsilon \rightarrow 0} \langle R_{txyz}(r_1, \theta_1^{(k_1)}) R_{txyz}(r_2, \theta_2^{(k_2)}) \rangle_{t > y_0, k_1 - k_2 = -1} & \quad (3.45) \\ & = - \frac{3(t - y_0) (28t^4 + 13t^3 y_0 + 13t^2 y_0^2 + 3t y_0^3 + 3y_0^4)}{2048 \pi^2 t^5 \epsilon^6} + \dots \end{aligned}$$

For $t < y_0$ as well as the correlator on the Σ_1 , we obtain the following behaviour

$$\lim_{\epsilon \rightarrow 0} \langle R_{txyz}(\tau + \epsilon) R_{txyz}(\tau - \epsilon) \rangle_{\Sigma_1} = - \frac{21}{256 \pi^2 \epsilon^6} + \dots \quad (3.46)$$

3.3 Growth of entanglement after curvature quenches

In this section we will use the leading singularities of the two-point functions evaluated in section 3.2 to obtain the time dependence of the growth of entanglement after the quench enters the region $y > 0$. We will discuss in detail the evaluation for curvature tensors belonging to class 1 and present the results for the other classes in the tables and figures at the end of this section. We see that, the time dependent polynomials which determine the growth of Rényi/entanglement have similar features when one organises the curvature components in terms of the representations of $SO(2)_T \times SO(2)_L$.

Scalars under $SO(2)_T \times SO(2)_L$, Class 1: $\{R_{tyty}, R_{xzxz}, R_{tyxz}\}$

The time dependence of quenches for components in this class behave identically. The components in this class are either scalars or pseudo-scalars under both $SO(2)_T$ and $SO(2)_L$. To represent this class we consider the state

$$\rho(t, -y_0) = R_{tyty}(\tau_e, -y_0)|0\rangle\langle 0|R_{tyty}(\tau_l, -y_0). \quad (3.47)$$

Since there is no local gauge invariant stress tensor for the theory of gravitons, we use the Kretschmann scalar as a probe of the quench. The expectation value of the Kretschmann scalar in the above state will show that it is a state which corresponds to a spherical pulse with non-zero value of the Kretschmann scalar density travelling at the speed of light. The expectation value of the Kretschmann scalar in the state (3.47) is given by

$$\begin{aligned} \text{Tr}[K(0, 0)\rho(t, -y_0)] &= \text{Tr}[K(0, y_0)\rho(t, 0)], \\ &= \frac{\langle R_{tyty}(-\epsilon - it, 0)K(0, y_0)R_{tyty}(\epsilon - it, 0) \rangle}{\langle R_{tyty}(-\epsilon - it, 0)R_{tyty}(\epsilon - it, 0) \rangle}. \end{aligned} \quad (3.48)$$

where

$$K = R_{\mu\nu\rho\sigma}R^{\mu\nu\rho\sigma}. \quad (3.49)$$

The appendix C, contains the details of evaluating this correlator. This involves the use of the graviton propagator given in (3.11) systematically. The result is given by (C.12)

$$\text{Tr}[K(0, y_0)\rho(t, 0)] = \frac{6144\epsilon^6}{\left(t^4 + 2t^2(\epsilon^2 - y_0^2) + (y_0^2 + \epsilon^2)^2\right)^3}. \quad (3.50)$$

Figure 5 plots the profile of the Kretschmann scalar as a function of the y_0 at $t = 0, 4, 6$ for width $\epsilon = 0.5$. The figure clearly shows that the curvature density due to quench travels as a spherical wave at the speed of light.

Now let us proceed to obtain the change in the Rényi/entanglement in the regime $t < y_0$ before the pulse hits the entangling surface $y_0 = 0$. In this regime and in the $\epsilon \rightarrow 0$ limit, it is only Wick contractions on the same sheet that contribute in the $2n$ point function (2.5). From (3.19), we see that this contribution goes as $\epsilon^{-6(n)}$ and the leading correction to this Wick contraction is proportional to $\epsilon^{-6(n-1)}$. Just as in the case for the scalar, the next leading Wick contraction arises from $n - 2$ operators located on the same sheet and 2 pairs

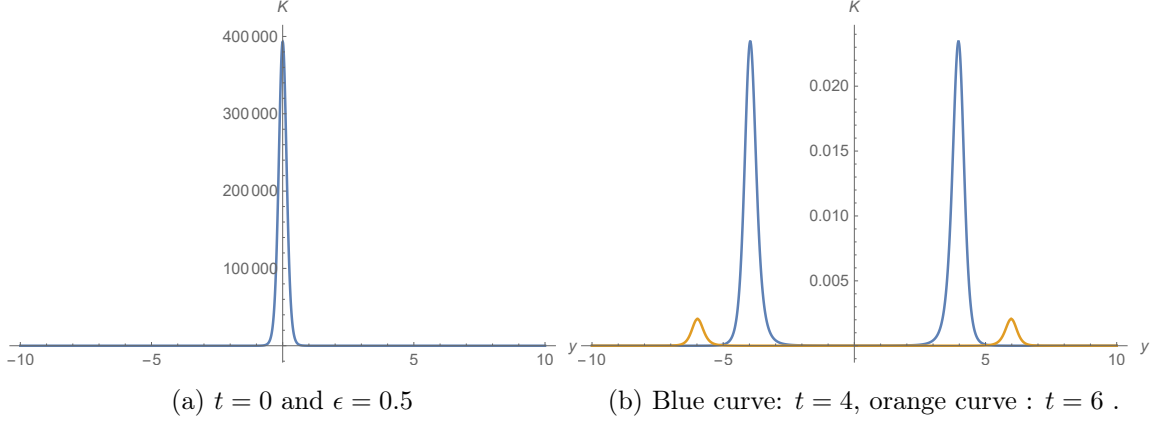


Figure 5: Kretschmann curvature density for the quench created by Riemann curvature R_{tyty} placed at the origin at times $t = 0, t = 4$ and $t = 6$. We choose $\epsilon = 0.5$. The Kretschmann curvature density travels at the speed of light as spherical wave.

of operators contracted across the sheets, this contribution is proportional to $\epsilon^{-6(n-2)}$. So, we conclude that the leading correction to the entanglement in the regime $t < y_0$ arises from the correction in the two-point function on the same sheet. Using (3.19) we get

$$\begin{aligned} \Delta S_{t < y_0}^{(n)} &= \frac{1}{1-n} \log \left(1 + \epsilon^6 \frac{(n-1)(n+1)(191n^4 + 23n^2 + 2)}{945n^6(t^2 - y_0^2)^3} + \dots \right)^n, \\ &= \frac{n}{1-n} \frac{(n-1)(n+1)(191n^4 + 23n^2 + 2)}{945n^6(t^2 - y_0^2)^3} \epsilon^6 + \mathcal{O}(\epsilon^8). \end{aligned} \quad (3.51)$$

The denominator in the ratio (2.5) is evaluated using the two-point function of R_{tyty} on Σ_1 , which is given in (3.22). Using the same arguments as in the case of the scalar and the $U(1)$ field the leading term proportional to ϵ^6 should arise from expectation value of the composite $:R_{tyty}^2:$ on the replica surface. Let us evaluate this expectation value directly for a simple cross check.

$$\begin{aligned} \langle :R_{tyty}R_{tyty}: \rangle_{\Sigma_n} &= - \lim_{\substack{r_1 \rightarrow r_2 \\ \theta_1 \rightarrow \theta_2}} \tilde{\nabla}^4 \left(G(r_1, r_2, \theta_1, \theta_2, \mathbf{x}, \mathbf{x}) - \frac{1}{4\pi^2(r_1^2 + r_2^2 - 2r_1r_2 \cos(\theta_1 - \theta_2))} \right), \\ &= \lim_{\theta \rightarrow 0} \left[\frac{15(n^2 - 1) \csc^4\left(\frac{\theta}{2n}\right) + 2(4n^4 - 5n^2 + 1) \csc^2\left(\frac{\theta}{2n}\right) + 15 \csc^6\left(\frac{\theta}{2n}\right)}{60\pi^2 n^6 r_1^6} \right. \\ &\quad \left. + \frac{2}{\pi^2 r_1^6 (\cos(\theta) - 1)^3} \right], \\ &= \frac{(n-1)(n+1)(191n^4 + 23n^2 + 2)}{3780\pi^2 n^6 (y^2 - t^2)^3}. \end{aligned} \quad (3.52)$$

Here $\tilde{\nabla}^2 = (\partial_{r_1}^2 + \frac{1}{r_1} \partial_{r_1} + \frac{1}{r_1^2} \partial_{\theta_1}^2)$ is the Laplacian in $r-\theta$ plane. Comparing (3.51) and (3.52), we see that indeed the the leading contribution in the $\epsilon \rightarrow 0$ limit to the entanglement is due to the expectation value of the composite of the curvature field. One curious observation

is that the n dependence in the expectation value in (3.52) coincides with the expectation value of the stress tensor for the conformal 2 form in $d = 6$ on Σ_n , which was evaluated in [28]³.

The growth in entanglement in the regime $t > y_0$ in the $\epsilon \rightarrow 0$ limit is evaluated using the leading Wick contractions given in (3.20) and (3.21). This results in

$$\begin{aligned} \lim_{\epsilon \rightarrow 0} \Delta S_A^{(n)}[R_{tyty}] &= \frac{1}{1-n} \log \frac{\left(\frac{(t+y_0)^3(8t^2-9ty_0+3y_0^2)}{32\pi^2 t^5 \epsilon^6}\right)^n + \left(\frac{(t-y_0)^3(8t^2+9ty_0+3y_0^2)}{32\pi^2 t^5 \epsilon^6}\right)^n}{\left(\frac{1}{2\pi^2 \epsilon^6}\right)^n}, \\ &= \frac{1}{1-n} \log \left[\left(\frac{(t+y)^3(8t^2-9ty_0+3y_0^2)}{16t^5}\right)^n + \left(\frac{(t-y_0)^3(8t^2+9ty_0+3y_0^2)}{16t^5}\right)^n \right]. \end{aligned} \quad (3.53)$$

As discussed earlier, the two Wick contractions are related to each other by $y_0 \rightarrow -y_0$. Observe that the time dependence of the growth of Rényi entropy is through a polynomial of order $5 = 2s + 1$, $s = 2$ through the ratio y_0/t . We will see that all time dependences for the curvature quenches are determined by order 5 polynomials. The asymptotic behaviour of the Rényi entropy in the large time limit is given by

$$\lim_{t \rightarrow \infty} \Delta S_A^{(n)}[R_{tyty}] = \log(2) - \frac{n}{2} \left(\frac{15}{8}\right)^2 \frac{y^2}{t^2} + \mathcal{O}\left(\frac{y^4}{t^4}\right) + \dots \quad (3.54)$$

Finally the entanglement entropy can also be written as a function of y_0/t and is given by

$$\begin{aligned} \lim_{n \rightarrow 1} \Delta S_A^{(n)}[R_{tyty}] &= \Delta S_{EE}[R_{tyty}], \\ &= \frac{1}{16} \left[64 \log 2 - (r+1)^3(3(r-3)r+8) \log((r+1)^3(3(r-3)r+8)) \right. \\ &\quad \left. + (r-1)^3(3r(r+3)+8) \log(-(r-1)^3(3r(r+3)+8)) \right], \\ &\quad r = \frac{y_0}{t} \end{aligned} \quad (3.55)$$

Before we conclude the analysis of this class of curvature components, let us generalise the observations of the seen for the $U(1)$ quench. For this class of curvature components the polynomial which determines the growth of Rényi entropy can be completely determined. The components in this class of curvatures are scalars under both $SO(2)_T$ and $SO(2)_L$, they are in fact pseudo-scalars. Therefore from the earlier observations, we expect the polynomial to be

$$P_{R_{tyty}}(r) = \frac{1}{2}(1+r)^3(1+a_1r+a_2r^2), \quad (3.56)$$

where order of the factor $(1+r)$ is $3 = s + 1$, $s = 2$. The coefficients a_1, a_2 should be such that

$$P_{R_{tyty}}(r) + P_{R_{tyty}}(-r) = 1. \quad (3.57)$$

³See equation 3.58 of [28]

This is because the argument of the logarithm in (3.53) is the ratio of $2n$ point function to the n powers of the two-point function and at $n = 1$, this ratio is unity. This implies that the even powers r^2, r^4 of the polynomial in (3.56) must vanish. The condition in (3.57) is enough to determine the coefficients a_1, a_2 uniquely, they are given by

$$a_1 = -\frac{9}{8}, \quad a_2 = \frac{3}{8}. \quad (3.58)$$

The polynomial is therefore

$$P_{R_{tyty}}(r) = \frac{1}{2}(1 + \frac{15}{8}r - \frac{5}{4}r^3 + \frac{3}{8}r^8). \quad (3.59)$$

Comparing this with the polynomial in (3.53) we see that they agree. The Rényi/entanglement entropy growth in the $\epsilon \rightarrow 0$ limit is uniquely determined for the components in class 1 by demanding that the polynomial of the order of 5 is of the form (3.56). The power of the factor $(1 \pm r)$ is 3, which also coincides with the scaling dimension of curvature. In tables (1), (2) we list the behaviour of the Rényi/entanglement entropy of quenches created by components belonging to class 1 as well as scalars under $SO(2)_T \times SO(2)_L$ of the vector quench and the scalar. Figure (6) plots the behaviour of entanglement entropy.

Vectors under either $SO(2)_T \times SO(2)_L$, Class 2, 3

Consider the components in class 2, 3 for example R_{tytx}, R_{tytz} transform as a (pseudo) vector of $SO(2)_T$ and a vector $SO(2)_L$. Similarly components R_{yxxz}, R_{txxz} transform as (pseudo) vector of $SO(2)_L$ and a vector of $SO(2)_T$. There are 8 components in class 2 and 3 combined. The components of class 2 and class 3 each have the identical behaviour. The expressions for the Rényi entropy for quenches created by curvature components belonging to class 2 and class 3 are given in tables. The polynomials which determine the growth of Rényi entropy in both these classes are of the form

$$P_{\text{class 2,3}}(r) = \frac{1}{2}(1 + r)^2(1 + a_1r + a_2r + a_3r^2). \quad (3.60)$$

Now the condition

$$P(r) + P(-r) = 1. \quad (3.61)$$

determines the polynomial uniquely up to one coefficient, This is because there are 2 equations we obtain when we demand that the coefficients of even terms in r must vanish and there are 3 unknown coefficients in (3.60). Therefore say given a_∞ , the entire polynomial can be determined uniquely. Table (3) lists the Rényi entropies and its asymptotic behaviour at large times, table (4) lists the corresponding entanglement growth for quenches created by components in this class. These polynomials differ from that of the class 1 given in (3.56), in that the power of the factor $(1 \pm r)$ reduces by one. The figure 7 plots the growth of the entanglement entropy against t/y_0 for the vectors under $SO(2)_T \times SO(2)_L$ both from the $U(1)$ field as well as from spin-2 field.

Symmetric tensor of $SO(2)_T \times SO(2)_L$, Class 4, 5, 6, 7

All the components in these classes transform as a 2nd rank symmetric tensor in both $SO(2)_T$ as well as $SO(2)_L$, therefore there are 9 components in all. The expressions for the Rényi entropy for quenches created by curvature components belonging to class 4, 5, 6 are given in tables. For this class, the polynomial which determines the growth in Rényi entropy is of the form

$$P_{\text{class 4,5,6}}(r) = \frac{1}{2}(1+r)(1+a_1r+a_2r+a_3r^2+a_4r^4). \quad (3.62)$$

The equation $P(r) + P(-r) = 1$ results in 2 equations for the vanishing of the even powers of r . Therefore, these polynomials are uniquely determined once 2 coefficients are given. The power of the factor for $(1 \pm r)$ further reduces by 1 compared to the case of vectors in (3.60). The Rényi/entanglement entropies for quenches in these classes are listed in tables 5, 6 respectively. Figure 8 plots the growth of entanglement.

Field	$\Delta S_A^{(n)}$	$\lim_{t \rightarrow \infty} \Delta S_A^{(n)}$
ϕ	$\frac{1}{1-n} \log \left[\left(\frac{t+y_0}{2t} \right)^n + \left(\frac{t-y_0}{2t} \right)^n \right]$	$\log 2 - \frac{n}{2} \frac{y_0^2}{t^2}$
F_{ty}, F_{xz}	$\frac{1}{1-n} \log \left[\left(\frac{(2t-y_0)(t+y_0)^2}{4t^3} \right)^n + \left(\frac{(t-y_0)^2(2t+y_0)}{4t^3} \right)^n \right]$	$\log 2 - \frac{n}{2} \left(\frac{3y_0}{2t} \right)^2$
Class1	$\frac{1}{1-n} \log \left[\left(\frac{(t+y_0)^3(8t^2-9ty_0+3y_0^2)}{16t^5} \right)^n + \left(\frac{(t-y_0)^3(8t^2+9ty_0+3y_0^2)}{16t^5} \right)^n \right]$	$\log 2 - \frac{n}{2} \left(\frac{15y_0}{8t} \right)^2$

Table 1: Rényi entropy growth of scalars under $SO(2)_T \times SO(2)_L$. The last column contains the asymptotic behaviour of Rényi entropy after the quench enters the entangling region. We have combined the scalars under $SO(2)_T \times SO(2)_L$ created by quenches for fields ≤ 2 . Note that the order of the polynomial in $r = y_0/t$, which determines the Rényi entropy is $2s+1$ and the power of the factor $(1+r)$ is $s+1$ or the dimension of the operator creating the quench. Class 1 contains the curvature components $R_{tyty}, R_{zxzx}, R_{tyzx}$. This polynomial for the scalars $SO(2)_T \times SO(2)_L$ is completely determined by the spin of the field.

Summary:

From all our explicit computations we find that the Rényi/entanglement entropies for quenches created by components of a spin s field are determined by polynomials $P(r)$ of the degree $2s+1$ where $r = y_0/t$. For components which are scalars under $SO(2)_T \times SO(2)_L$, the polynomial is of the form

$$P(r) = \frac{1}{2}(1+r)^{s+1}(1+a_1r+a_2r^2+\dots+a_sr^s) \quad (3.63)$$

These polynomials have the property that $P(r) + P(-r) = 1$ which implies that the even powers of r apart from r^0 should vanish. This represents s conditions from which the polynomial can be completely determined. For components which below to vectors of

Field	ΔS_{EE}
Φ	$\frac{1}{2} \left(\log \left(\frac{4}{1-r^2} \right) - 2r \tanh^{-1}(r) \right)$
F_{ty}, F_{xz}	$\frac{1}{4} \left((r-2)(r+1)^2 \log(-r^3+3r+2) - (r^3-3r+2) \log(r^3-3r+2) + \log(256) \right)$
Class 1	$\frac{1}{16} \left[64 \log 2 - (r+1)^3(3(r-3)r+8) \log((r+1)^3(3(r-3)r+8)) + (r-1)^3(3r(r+3)+8) \log(-(r-1)^3(3r(r+3)+8)) \right]$,

Table 2: Growth of entanglement entropy for scalars under $SO(2)_T \times SO(2)_L$, here $r = y_0/t$.

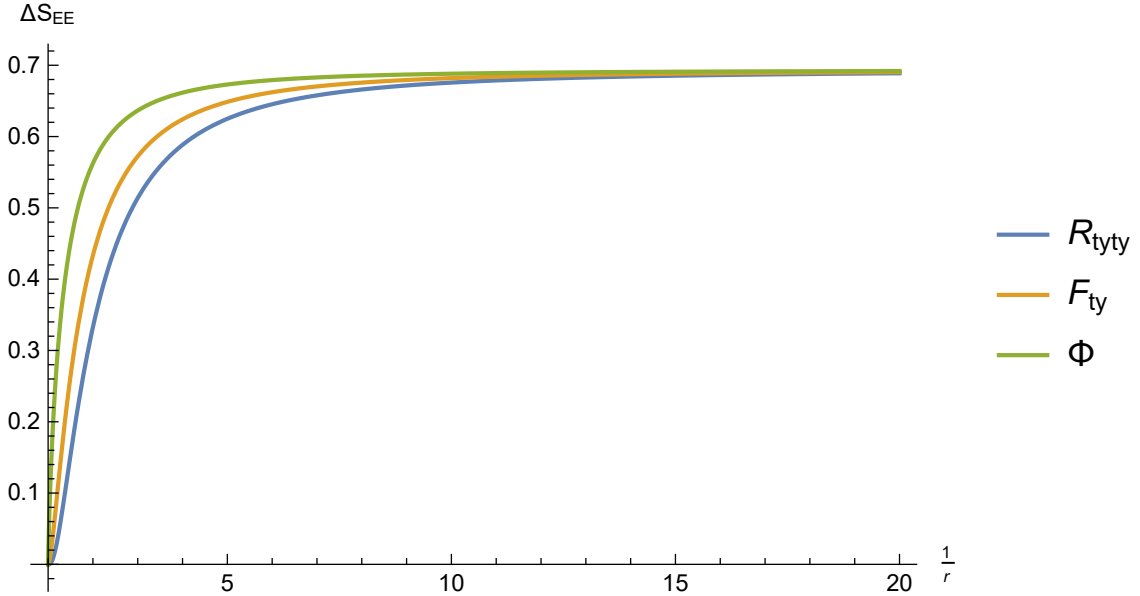


Figure 6: ΔS_{EE} as a function of $1/r = t/y_0$ in the zero width limit for scalars under $SO(2)_T \times SO(2)_L$. Note that the entanglement grows slower as the spin of the field creating the quench increases. the plot for R_{tyty} represents the growth for all components in class 1.

$SO(2)_T \times SO(2)_L$, the form of the polynomial is again of degree $2s + 1$, but the power of the prefactor $(1 + r)$ shifts from $s \rightarrow s - 1$. A similar shift occurs for tensors under $SO(2)_T \times SO(2)_L$. Given the fact that the even power r^2 does not occur in the polynomial, the long time behaviour of the Rényi entropies is given by

$$\lim_{t \rightarrow 0} \Delta S_A^{(n)} = \log(2) - \frac{n}{2} a_\infty^2 \frac{y_0^2}{t^2} + \dots \quad (3.64)$$

where a_∞ is the coefficient of the linear term in the polynomial $P(r)$.

Field	$\Delta S_A^{(n)}$	$\lim_{t \rightarrow \infty} \Delta S_A^{(n)}$
$F_{tx}, F_{tz}, F_{yx}, F_{yz}$	$\frac{1}{1-n} \log \left[\left(\frac{(t+y_0)(4t^2 - ty_0 + y_0^2)}{8t^3} \right)^n + \left(\frac{(t-y_0)(4t^2 + ty_0 + y_0^2)}{8t^3} \right)^n \right]$	$\log 2 - \frac{n}{2} \left(\frac{3y_0}{4t} \right)^2$
Class2	$\frac{1}{1-n} \log \left[\frac{\left(\frac{(t-y_0)^2(14t^3 + 13t^2 y_0 + 12t y_0^2 + 6y_0^3)}{128\pi^2 t^5 \epsilon^6} \right)^n + \left(\frac{(t+y_0)^2(14t^3 - 13t^2 y_0 + 12t y_0^2 - 6y_0^3)}{128\pi^2 t^5 \epsilon^6} \right)^n}{\left(\frac{7}{32\pi^2 \epsilon^6} \right)^n} \right]$	$\log 2 - \frac{n}{2} \left(\frac{15y_0}{14t} \right)^2$
Class3	$\frac{1}{1-n} \log \left[\frac{\left(\frac{(t-y_0)^2(22t^3 + 14t^2 y_0 + 6t y_0^2 + 3y_0^3)}{128\pi^2 t^5 \epsilon^6} \right)^n + \left(\frac{(t+y_0)^2(22t^3 - 14t^2 y_0 + 6t y_0^2 - 3y_0^3)}{128\pi^2 t^5 \epsilon^6} \right)^n}{\left(\frac{11}{32\pi^2 \epsilon^6} \right)^n} \right]$	$\log 2 - \frac{n}{2} \left(\frac{15y_0}{11t} \right)^2$

Table 3: Rényi entropy growth of vectors under $SO(2)_T \times SO(2)_L$. The order of the polynomial in $r = y_0/t$ is $2s + 1$. The power of the pre-factor $(1 + r)$ is one less than the scaling dimension of the field. Class 2, 3 together contain 8 curvature components which can be organised as vectors of $SO(2)_T \times SO(2)_L$.

Field	ΔS_{EE}
$F_{tx}, F_{tz}, F_{yx}, F_{yz}$	$\frac{1}{8} \left(- (r^3 + 3r + 4) \log (r^3 + 3r + 4) + (r^3 + 3r - 4) \log (4 - r(r^2 + 3)) + 8 \log(8) \right)$
Class 2	$\frac{1}{28} \left[(-6r^5 + 5r^3 + 15r - 14) \log (6r^5 - 5r^3 - 15r + 14) + (6r^5 - 5r^3 - 15r - 14) \log (-6r^5 + 5r^3 + 15r + 14) + 28 \log(28) \right]$
Class 3	$\frac{1}{44} \left[-(3r^5 + 5r^3 - 30r + 22) \log (3r^5 + 5r^3 - 30r + 22) + (3r^5 + 5r^3 - 30r - 22) \log (-3r^5 - 5r^3 + 30r + 22) + 44 \log(44) \right]$

Table 4: Entanglement growth of quenches due to vectors under $SO(2)_T \times SO(2)_L$.

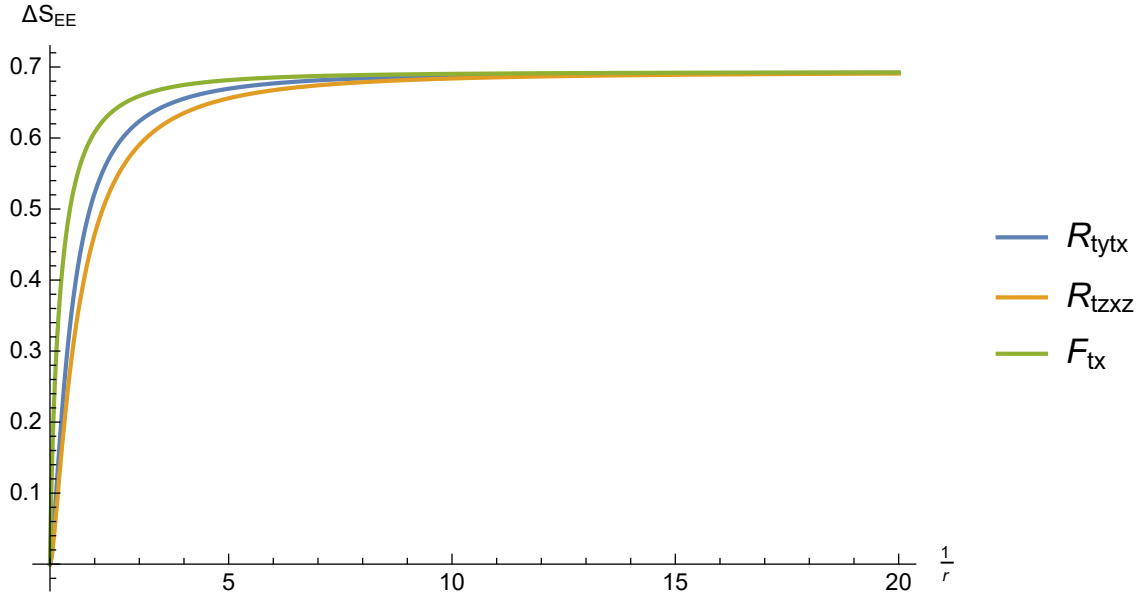


Figure 7: ΔS_{EE} as a function of $1/r = t/y_0$ in the zero width limit for vectors under $SO(2)_T \times SO(2)_L$. Class 2, 3 are represented by R_{tytx}, R_{tzxx} respectively. The growth due to the quench due to the vectors from the $U(1)$ field is higher than those due to the spin-2 fields.

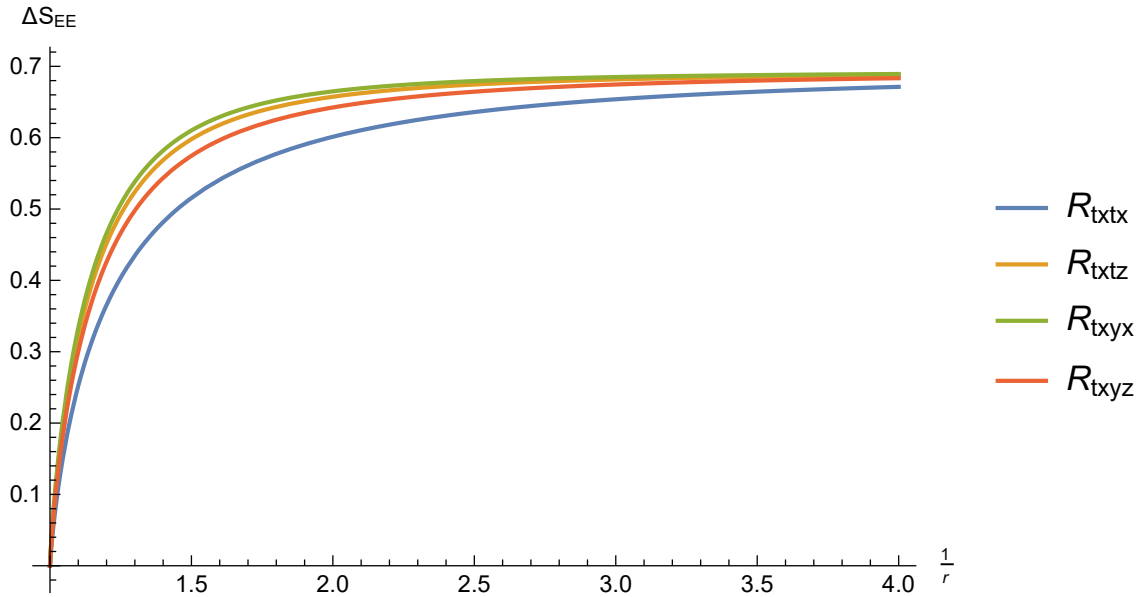


Figure 8: ΔS_{EE} as a function of $\frac{1}{r} = \frac{t}{y_0}$ in the zero width limit for the symmetric tensor under $SO(2)_T \times SO(2)_L$. Class 4, 5, 6, 7 contain all the 9 curvature components of these classes. We have plotted a representative from each of the classes

4 Conclusions

We have studied local quenches created by fields with integer spins $s \leq 2$. When the width of the quenches tends to zero, the growth of Rényi/entanglement entropies is determined

Field	$\Delta S_A^{(n)}$	$\lim_{t \rightarrow \infty} \Delta S_A^{(n)}$
Class4	$\frac{1}{1-n} \log \left[\frac{\left(\frac{9(t-y_0)(6t^4+t^3y_0+t^2y_0^2+ty_0^3+y_0^4)}{256\pi^2t^5\epsilon^6} \right)^n + \left(\frac{9(t+y_0)(6t^4-t^3y_0+t^2y_0^2-ty_0^3+y_0^4)}{256\pi^2t^5\epsilon^6} \right)^n}{\left(\frac{27}{64\pi^2\epsilon^6} \right)^n} \right]$	$\log 2 - \frac{n}{2} \left(\frac{5y_0}{6t} \right)^2$
Class5	$\frac{1}{1-n} \log \left[\frac{\left(\frac{(t-y_0)(38t^4+23t^3y_0+23t^2y_0^2+3ty_0^3+3y_0^4)}{1024\pi^2t^5\epsilon^6} \right)^n + \left(\frac{(t+y_0)(38t^4-23t^3y_0+23t^2y_0^2-3ty_0^3+3y_0^4)}{1024\pi^2t^5\epsilon^6} \right)^n}{\left(\frac{19}{256\pi^2\epsilon^6} \right)^n} \right]$	$\log 2 - \frac{n}{2} \left(\frac{15y_0}{38t} \right)^2$
Class6	$\frac{1}{1-n} \log \left[\frac{\left(\frac{3(t-y_0)(16t^4+11t^3y_0+11t^2y_0^2+ty_0^3+y_0^4)}{2048\pi^2t^5\epsilon^6} \right)^n + \left(\frac{3(t+y_0)(16t^4-11t^3y_0+11t^2y_0^2-ty_0^3+y_0^4)}{2048\pi^2t^5\epsilon^6} \right)^n}{\left(\frac{3}{16\pi^2\epsilon^6} \right)^n} \right]$	$\log 2 - \frac{n}{2} \left(\frac{5y_0}{16t} \right)^2$
Class7	$\frac{1}{1-n} \log \left[\frac{\left(\frac{3(t-y_0)(28t^4+13t^3y_0+13t^2y_0^2+3ty_0^3+3y_0^4)}{512\pi^2t^5\epsilon^6} \right)^n + \left(\frac{3(t+y_0)(28t^4-13t^3y_0+13t^2y_0^2-3ty_0^3+3y_0^4)}{512\pi^2t^5\epsilon^6} \right)^n}{\left(\frac{21}{64\pi^2\epsilon^6} \right)^n} \right]$	$\log 2 - \frac{n}{2} \left(\frac{15y_0}{28t} \right)^2$

Table 5: Rényi entropy growth for of symmetric tensors under both $SO(2)_T \times SO(2)_L$, Class 4, 5, 6, 7 together represent the 9 components of the symmetric tensors. The polynomial in r determining the Rényi entropy growth is a 5th order polynomial and the power of the $(1+r)$ is unity.

by a $2s+1$ order polynomial in $r = \frac{y_0}{t}$ where y_0 is the location the quench is initiated and t is the time elapsed. The behaviour of the quenches can be organised in terms of the $SO(2)_T \times SO(2)_L$ representation of the field creating the quench. The polynomial determining the Rényi entropy growth for $SO(2)_T \times SO(2)_L$ scalars is completely determined by the spin of the field creating the quench.

An obvious generalisation of this work is to study quenches created by fields with spins $1/2, 3/2$. Quenches created by Dirac fermions were studied in [25]. On examining the singularities of the propagator for $t > y_0$,⁴ we see that they are indeed proportional to polynomials of degree $2 = 2s+1, s = 1/2$ in the ratio r . It will interesting to revisit this work and also study the case of spin- $3/2$. One needs to choose a suitable gauge for studying

⁴See equations (48), (49) of [25]

Field	ΔS_{EE}
Class 4	$\frac{1}{12} (- (r^5 + 5r + 6) \log (r^5 + 5r + 6) + (r^5 + 5r - 6) \log (6 - r (r^4 + 5)) + 12 \log(12))$
Class 5	$\frac{1}{76} \left[- (3r^5 + 20r^3 + 15r + 38) \log (3r^5 + 20r^3 + 15r + 38) + (3r^5 + 20r^3 + 15r - 38) \log (-3r^5 - 20r^3 - 15r + 38) + 76 \log(76) \right]$,
Class 6	$\frac{1}{32} \left[- (r^5 + 10r^3 + 5r + 16) \log (r^5 + 10r^3 + 5r + 16) + (r^5 + 10r^3 + 5r - 16) \log (16 - r (r^4 + 10r^2 + 5)) + 32 \log(32) \right]$,
Class 7	$\frac{1}{56} \left[- (3r^5 + 10r^3 + 15r + 28) \log (3r^5 + 10r^3 + 15r + 28) + (3r^5 + 10r^3 + 15r - 28) \log (-3r^5 - 10r^3 - 15r + 28) + 56 \log(56) \right]$,

Table 6: Entanglement entropy of components transforming as tensors under $SO(2)_T \times SO(2)_L$.

quenches due to the gravitino.

One of the goals of our work is to explore the information theoretic properties of the graviton. This work has shown that the linearised graviton behaves just as a local field with gauge symmetry. It will be interesting to turn on the leading cubic interaction in Einstein’s theory and see how ory departs from local quantum field theories which have the ‘split property’ as argued in [31, 32]. The methods developed in this paper and [27–29] as well as the new approach to evaluating entanglement entropy in [35, 36] hopefully will help in providing a direct answer to this question.

A BCFT interpretation of scalar 2-point function on Σ_2 .

In this appendix we study the properties of the scalar correlator given in (2.12) on the replica surface. We see that it can be thought of as a correlator in a boundary conformal field theory with a co-dimension 2 defect. We demonstrate it explicitly for the case of $n = 2$. Let us begin with the two-point function on the replica surface for the replica parameter $n = 2$.

$$G(x, x')_{\Sigma_2} = \frac{\sinh \frac{\eta}{2}}{16\pi^2 r_1 r_2 \sinh \eta (\cosh \frac{\eta}{2} - \cos \frac{\theta}{2})}. \quad (\text{A.1})$$

It is convenient to use the cross ratio’s z, \bar{z} introduced in [37] to rewrite this correlator. These variables are related to η and θ by the following

$$\cosh \eta = \frac{1 + z\bar{z}}{2(z\bar{z})^{\frac{1}{2}}}, \quad \cos \theta = \frac{z + \bar{z}}{2(z\bar{z})^{\frac{1}{2}}}. \quad (\text{A.2})$$

The two-point function in (A.1) can be re-written as

$$G(z, \bar{z})_{\Sigma_2} = \frac{1}{16\pi^2 r_1 r_2} \frac{2\sqrt{z\bar{z}}}{(1 + \sqrt{z\bar{z}})(1 - \sqrt{z})(1 - \sqrt{\bar{z}})}. \quad (\text{A.3})$$

Now if this is a correlator of 2 scalar primaries in a BCFT with a codimension 2 defect it should admit an expansion of the form

$$\begin{aligned} G(z, \bar{z})_{\Sigma_2} &= \frac{g(z, \bar{z})}{r_1 r_2}, \\ &= \frac{1}{r_1 r_2} \sum_{\mathcal{O}} (b_{\phi\mathcal{O}})^2 \hat{f}_{\hat{\tau}, s}(z, \bar{z}). \end{aligned} \quad (\text{A.4})$$

$(b_{\phi\mathcal{O}})^2$ are positive coefficients due to the OPE of ϕ with the operators localized in the defect in the defect channel [34, 37].

$$\begin{aligned} \hat{f}_{\hat{\tau}, s}(z, \bar{z}) &= \left(\frac{\frac{q}{2} + s - 2}{\frac{q}{2} - 2} \right)^{-1} C_s^{\left(\frac{q}{2}-1\right)} \left(\frac{\bar{z} + z}{2\sqrt{z\bar{z}}} \right) {}_2F_1 \left(\frac{\Delta}{2} + \frac{1}{2}, \frac{\Delta}{2}; -\frac{p}{2} + \Delta + 1; \frac{4z\bar{z}}{(z\bar{z} + 1)^2} \right), \\ &= (z)^{\frac{\Delta-s}{2}} (\bar{z})^{\frac{\Delta+s}{2}} {}_2F_1 \left(-s, \frac{q}{2} - 1, 2 - \frac{q}{2} - s; \frac{z}{\bar{z}} \right) {}_2F_1 \left(\Delta, \frac{p}{2}, \Delta + 1 - \frac{p}{2}; z\bar{z} \right). \end{aligned} \quad (\text{A.5})$$

where $C_s^{\left(\frac{q}{2}-1\right)}$ refers to the Gegenbauer polynomial. For the co-dimension 2 defect in $d = 4$, these functions simplify drastically and we obtain

$$\hat{f}_{\hat{\tau}, s}(z, \bar{z})|_{p=2, d=4} = (z)^{\frac{\Delta-s}{2}} (\bar{z})^{\frac{\Delta+s}{2}} \frac{1}{1 - z\bar{z}}. \quad (\text{A.6})$$

Let us express the correlation function in (A.3) in the form (A.4) and obtain the positive coefficients $(b_{\phi\mathcal{O}})^2$.

$$\begin{aligned} G(z, \bar{z})_{\Sigma_2} &= \frac{1}{16\pi^2 r_1 r_2} \frac{2\sqrt{z\bar{z}}}{(1 + \sqrt{z\bar{z}})(1 - \sqrt{z})(1 - \sqrt{\bar{z}})}, \\ &= \frac{1}{16\pi^2 r_1 r_2} \frac{2\sqrt{z\bar{z}}(1 - \sqrt{z\bar{z}})}{(1 - z\bar{z})(1 - \sqrt{z})(1 - \sqrt{\bar{z}})}, \\ &= \frac{1}{16\pi^2 r_1 r_2} \sum_{m=0}^{\infty} \sum_{n=0}^{\infty} \frac{2\sqrt{z\bar{z}}(1 - \sqrt{z\bar{z}})}{(1 - z\bar{z})} z^{\frac{n}{2}} \bar{z}^{\frac{m}{2}}, \\ &= \frac{1}{16\pi^2 r_1 r_2} (2\sqrt{z\bar{z}}) \frac{(1 + \sum_{n=1}^{\infty} z^{\frac{n}{2}})(1 + \sum_{m=1}^{\infty} \bar{z}^{\frac{m}{2}}) - \sum_{m=1}^{\infty} \sum_{n=1}^{\infty} z^{\frac{n}{2}} \bar{z}^{\frac{m}{2}}}{1 - z\bar{z}}, \\ &= \frac{1}{16\pi^2 r_1 r_2} \frac{2}{1 - z\bar{z}} \left[(z\bar{z})^{\frac{1}{2}} + \sum_{n=1}^{\infty} z^{\frac{n+1}{2}} \bar{z}^{\frac{1}{2}} + \sum_{n=1}^{\infty} z^{\frac{1}{2}} \bar{z}^{\frac{n+1}{2}} \right]. \end{aligned} \quad (\text{A.7})$$

Now comparing (A.4), (A.6) and (A.7) we see that

$$b_{\phi\mathcal{O}}^2 = \frac{1}{8\pi^2}. \quad (\text{A.8})$$

for boundary operators \mathcal{O} with

$$\Delta = 1, s = 0, \quad \Delta = \frac{n}{2} + 1, s = \pm \frac{n}{2}, \quad n = 1, 2, \dots \quad (\text{A.9})$$

Therefore the scalar correlator on the cone can be expressed as a 2 point function of primaries of dimension 1 in the presence of a co-dimension 2 defect.

It is also interesting to track the behaviour of the cross ratios z, \bar{z} as we vary time given a particular y_0 . Inverting the relation in (A.2) we find

$$z = \left(\cosh(\eta) + \sqrt{\cosh^2(\eta) - 1} \right) \left(\cos(\theta) + \sqrt{\cos^2(\theta) - 1} \right), \quad (\text{A.10})$$

$$\bar{z} = \frac{\cosh(\eta) + \sqrt{\cosh^2(\eta) - 1}}{\cos(\theta) + \sqrt{\cos^2(\theta) - 1}}.$$

While performing the inversion of (A.2), there are 4 branches we can choose from. A pair of these occur because of the symmetry $z \rightarrow \bar{z}$ of the equations, while a second pair can be thought of as a time reversed version of the quench. As we will see, the above branch represents the physical situation in which the quench moves from $-y_0$ and the Rényi entropy increases as time increases. We can use the relation between $\cosh \eta, \cos \theta$ given in (2.13), to relate them to y, t by $r_1^2 = y_0^2 + (-\epsilon - it)^2, \tau_1 = -\epsilon - it$ and $r_2^2 = y_0^2 + (\epsilon - it)^2, \tau_2 = \epsilon - it$ with $x_1 = x_2, z_1 = z_2$. In figure (9) we have plotted the behaviour of z, \bar{z} as we begin with $y_0 = -5$ with $\epsilon = 0.5$ and t ranges from 0 to 10. We see that z moves on the unit circle from $z \sim 1$ to $e^{2\pi i} z$, while \bar{z} remains close to one below the real axis. This phenomenon is similar to that seen in 2d quenches, see for example in [19]⁵. Therefore when $t < y_0$, the singularity of the correlator (A.3) arises from the factors $(1 - \sqrt{z})(1 - \sqrt{\bar{z}})$ in the denominator. While for $t > y_0$, the singularity in the correlator arises from the factor $(1 + \sqrt{z\bar{z}})(1 - \sqrt{\bar{z}})$.

B Details for curvature correlators

We give the details of the derivations of two-point functions on the replica surface for curvature components belonging to class 1, 2, 3, 4, 5, 6, 7. We also show that the 2 point functions of curvature components belonging to the same class are identical. Therefore quenches due to these components will result in same time dependence of the Rényi/entanglement entropies.

Class 1: $R_{tyty}, R_{xzxz}, R_{tyxz}$

We have already demonstrated in the main text, that the two-point functions of the curvature components in class 1 are related. Let us consider R_{tyty} as the representative of this class. Here we present the complete expression for the two-point function of the curvature

⁵For the 2d quenches studied in [19] \bar{z} remained closed to unity above the real axis.

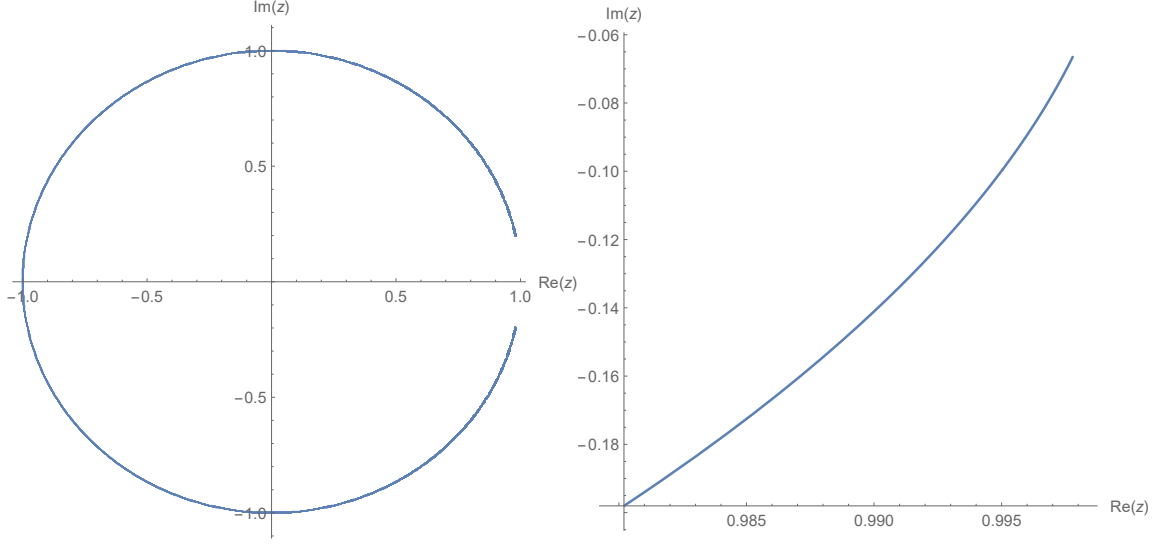


Figure 9: We plot z and \bar{z} as we increase t from 0 to 10 with $y_0 = 5, \epsilon = 0.5$. z moves on the unit circle from above the real axis to below the real axis counter clockwise, while \bar{z} always stays below the real axis close to unity.

component R_{tyty} in terms of the cross ratios θ and η .

$$\begin{aligned}
\langle R_{tyty} R_{tyty} \rangle &= \frac{1}{32\pi^2 n^3 r_1^3 r_2^3 (\cos(\frac{\theta}{n}) - \cosh(\frac{\eta}{n}))^3 (\sinh(\eta))^5} \\
&\times \left[2n^2 \sinh\left(\eta\left(2 - \frac{3}{n}\right)\right) + 6(n+3)n \sinh\left(\eta\left(2 - \frac{1}{n}\right)\right) - 12 \sinh\left(\frac{\eta}{n}\right) \right. \\
&+ 6 \sinh\left(\eta\left(\frac{1}{n} - 2\right)\right) + 6 \sinh\left(\eta\left(\frac{1}{n} + 2\right)\right) + 2n\left(3(-6 \cos\left(\frac{\theta}{n}\right) + \cosh\left(\frac{\eta + 2i\theta}{n}\right) \right. \\
&+ \cosh\left(\frac{\eta - 2i\theta}{n}\right)) \sinh(2\eta) + 4n \sinh\left(2\eta\left(\frac{1}{n} - 1\right)\right) \cos\left(\frac{\theta}{n}\right) - 3(n-3) \sinh\left(\eta\left(\frac{1}{n} + 2\right)\right) \\
&- 4n(\cosh(2\eta) + 2) \sinh\left(\frac{\eta}{n}\right) \cos\left(\frac{2\theta}{n}\right) - n\left(12 \sinh\left(\frac{\eta}{n}\right) + \sinh\left(\eta\left(\frac{3}{n} + 2\right)\right)\right) \\
&+ 16n \sinh\left(\frac{2\eta}{n}\right) \cos\left(\frac{\theta}{n}\right) - 3 \sinh\left(\frac{2\eta(n-1)}{n}\right) \cos\left(\frac{\theta}{n}\right) + (4n-3) \sinh\left(\frac{2\eta(n+1)}{n}\right) \cos\left(\frac{\theta}{n}\right) \\
&- 4n \sinh\left(\frac{3\eta}{n}\right) + 2 \sinh\left(\frac{2\eta + i\theta}{n}\right) + \sinh\left(\frac{2\eta(n-1) - i\theta}{n}\right) - \sinh\left(\frac{2\eta(n+1) - i\theta}{n}\right) \\
&+ \sinh\left(\frac{2\eta(n-1) + i\theta}{n}\right) - \sinh\left(\frac{2\eta(n+1) + i\theta}{n}\right) + 2\left(\sinh\left(\frac{2\eta - i\theta}{n}\right) + \sinh\left(\frac{\eta - 2i\theta}{n}\right)\right) \\
&2 \sinh\left(\frac{\eta + 2i\theta}{n}\right) - \sinh\left(\frac{\eta + 2i\theta + 2\eta n}{n}\right) + \sinh\left(\frac{\eta(2n-1) + 2i\theta}{n}\right) - \sinh\left(\frac{\eta + 2i\theta - 2\eta n}{n}\right) \\
&\left. - \sinh\left(\frac{\eta - 2i\theta + 2\eta n}{n}\right) \right]. \tag{B.1}
\end{aligned}$$

Class 2 : $\{R_{tytx}, R_{tytz}, R_{yzxz}, R_{yxzx}\}$

Let us begin with the curvature tensor R_{tytx} , from (3.3) we have

$$R_{tytx} = \frac{1}{2} \left[\partial_y \partial_t h_{tx} - \partial_t^2 h_{yx} + \partial_t \partial_x h_{yt} - \partial_y \partial_x h_{tt} \right]. \quad (\text{B.2})$$

Using the graviton propagator given in (3.11), the two-point function can be evaluated,

$$\begin{aligned} & \langle R_{tytx}(x) R_{tytx}(x') \rangle |_{x_1=x_2, z_1=z_2} = \\ & \frac{1}{4} \left[\partial_{y_1} \partial_{y_2} \partial_{t_1} \partial_{t_2} \langle h_{tx} h_{tx} \rangle - \partial_{y_1} \partial_{t_1} \partial_{t_2}^2 \langle h_{tx} h_{yx} \rangle + \partial_{t_1}^2 \partial_{t_2}^2 \langle h_{yx} h_{yx} \rangle \right. \\ & - \partial_{t_1}^2 \partial_{y_2} \partial_{t_2} \langle h_{yx} h_{tx} \rangle + \partial_{x_1} \partial_{x_2} \partial_{t_1} \partial_{t_2} \langle h_{yt} h_{yt} \rangle - \partial_{t_1} \partial_{x_1} \partial_{y_2} \partial_{x_2} \langle h_{yt} h_{tt} \rangle \\ & \left. + \partial_{y_1} \partial_{y_2} \partial_{x_1} \partial_{x_2} \langle h_{tt} h_{tt} \rangle - \partial_{y_1} \partial_{t_2} \partial_{x_1} \partial_{x_2} \langle h_{tt} h_{yt} \rangle \right] |_{x_1=x_2, z_1=z_2} \\ & = \frac{\partial_{x_1}^2 (-2\partial_{y_1} \partial_{y_2} + \partial_{t_1} \partial_{t_2}) (\partial_{t_1}^2 + \partial_{y_1}^2) (\partial_{t_2}^2 + \partial_{y_2}^2)}{\nabla^4} G(x, x') |_{x_1=x_2, z_1=z_2}, \\ & = \partial_{x_1}^2 (\partial_{t_1} \partial_{t_2} - 2\partial_{y_1} \partial_{y_2}) G(x, x') |_{x_1=x_2, z_1=z_2}. \end{aligned} \quad (\text{B.3})$$

To derive the last but one line we use isometry in x, z -plane derived in (D.4), (D.5)

$$\frac{\partial_{x_1}^2}{\nabla^2} G(x, x') |_{x_1=x_2, z_1=z_2} = \frac{\partial_{z_1}^2}{\nabla^2} G(x, x') |_{x_1=x_2, z_1=z_2} = \frac{1}{2} G(x, x') |_{x_1=x_2, z_1=z_2}. \quad (\text{B.4})$$

Let us compute $\langle R_{tytz}(x) R_{tytz}(x') \rangle$, the next element in this class. The expression for R_{tytz} from (3.3) is given by

$$R_{tytz} = \frac{1}{2} \left[\partial_y \partial_t h_{tz} - \partial_t^2 h_{yz} + \partial_t \partial_z h_{yt} - \partial_y \partial_z h_{tt} \right]. \quad (\text{B.5})$$

Using the graviton propagator in (3.11) we compute

$$\begin{aligned} & \langle R_{tytz}(x) R_{tytz}(x') \rangle |_{x_1=x_2, z_1=z_2} = \\ & \frac{1}{4} \left[\partial_{y_1} \partial_{y_2} \partial_{t_1} \partial_{t_2} \langle h_{tz} h_{tz} \rangle - \partial_{y_1} \partial_{t_1} \partial_{t_2}^2 \langle h_{tz} h_{yz} \rangle + \partial_{t_1}^2 \partial_{t_2}^2 \langle h_{yz} h_{yz} \rangle \right. \\ & - \partial_{t_1}^2 \partial_{y_2} \partial_{t_2} \langle h_{yz} h_{tz} \rangle + \partial_{x_1} \partial_{z_2} \partial_{t_1} \partial_{t_2} \langle h_{yt} h_{yt} \rangle - \partial_{t_1} \partial_{z_1} \partial_{y_2} \partial_{z_2} \langle h_{yt} h_{tt} \rangle \\ & \left. + \partial_{y_1} \partial_{y_2} \partial_{z_1} \partial_{z_2} \langle h_{tt} h_{tt} \rangle - \partial_{y_1} \partial_{t_2} \partial_{z_1} \partial_{z_2} \langle h_{tt} h_{yt} \rangle \right] |_{x_1=x_2, z_1=z_2} \\ & = \frac{\partial_{z_1}^2 (-2\partial_{y_1} \partial_{y_2} + \partial_{t_1} \partial_{t_2}) (\partial_{t_1}^2 + \partial_{y_1}^2) (\partial_{t_2}^2 + \partial_{y_2}^2)}{\nabla^4} G(x, x') |_{x_1=x_2, z_1=z_2}, \\ & = \partial_{z_1}^2 (\partial_{t_1} \partial_{t_2} - 2\partial_{y_1} \partial_{y_2}) G(x, x') |_{x_1=x_2, z_1=z_2}. \end{aligned} \quad (\text{B.6})$$

Again we have used the isotropy property of the x, z plane. Let us compute the two-point function of R_{yzxz} . The expression of R_{yzxz} is given by

$$R_{yzxz} = \frac{1}{2} \left[\partial_z \partial_x h_{yz} - \partial_y \partial_x h_{zz} + \partial_y \partial_z h_{zx} - \partial_z^2 h_{yx} \right] \quad (\text{B.7})$$

Using the graviton propagator we obtain

$$\begin{aligned}
& \langle R_{yzxz}(x)R_{yzxz}(x') \rangle|_{x_1=x_2, z_1=z_2} \\
&= \frac{1}{4} \left[\partial_{z_1} \partial_{z_2} \partial_{x_1} \partial_{x_2} \langle h_{yz} h_{yz} \rangle - \partial_{z_1} \partial_{x_1} \partial_{z_2}^2 \langle h_{yz} h_{yx} \rangle + \partial_{y_1} \partial_{x_1} \partial_{y_2} \partial_{x_2} \langle h_{zz} h_{zz} \rangle \right. \\
&\quad - \partial_{y_1} \partial_{x_1} \partial_{y_2} \partial_{z_2} \langle h_{zz} h_{zx} \rangle + \partial_{y_1} \partial_{z_1} \partial_{y_2} \partial_{z_2} \langle h_{zx} h_{zx} \rangle - \partial_{y_1} \partial_{z_1} \partial_{y_2} \partial_{x_2} \langle h_{zx} h_{zz} \rangle \\
&\quad \left. + \partial_{z_1}^2 \partial_{z_2}^2 \langle h_{yx} h_{yx} \rangle - \partial_{z_1}^2 \partial_{z_2} \partial_{x_2} \langle h_{yx} h_{yz} \rangle \right] |_{x_1=x_2, z_1=z_2}, \\
&= \frac{\partial_{z_1}^2 (\partial_{t_1} \partial_{t_2} - 2\partial_{y_1} \partial_{y_2}) (\partial_{z_1}^2 + \partial_{x_1}^2)^2}{\nabla^4} G(x, x')|_{x_1=x_2, z_1=z_2}, \\
&= \partial_{x_1}^2 (-2\partial_{y_1} \partial_{y_2} + \partial_{t_1} \partial_{t_2}) G(x, x')|_{x_1=x_2, z_1=z_2}. \tag{B.8}
\end{aligned}$$

Let us consider the last correlator in this class $\langle R_{yxxz}(x)R_{yxxz}(x') \rangle$. The expression of the curvature component R_{yxxz} is given by

$$R_{yxxz} = \frac{1}{2} \left[\partial_x^2 h_{yz} - \partial_y \partial_x h_{xz} + \partial_y \partial_z h_{xx} - \partial_x \partial_z h_{yx} \right]. \tag{B.9}$$

The two-point function is given by

$$\begin{aligned}
& \langle R_{yxxz}(x)R_{yxxz}(x') \rangle|_{x_1=x_2, z_1=z_2} \\
&= \frac{1}{4} \left[\partial_{x_1}^2 \partial_{x_2}^2 \langle h_{yz} h_{yz} \rangle - \partial_{z_2} \partial_{x_2} \partial_{x_1}^2 \langle h_{yz} h_{yx} \rangle + \partial_{y_1} \partial_{x_1} \partial_{y_2} \partial_{x_2} \langle h_{xz} h_{xz} \rangle \right. \\
&\quad - \partial_{y_1} \partial_{x_1} \partial_{y_2} \partial_{z_2} \langle h_{xz} h_{xx} \rangle + \partial_{y_1} \partial_{z_1} \partial_{y_2} \partial_{z_2} \langle h_{xx} h_{xx} \rangle - \partial_{y_1} \partial_{z_1} \partial_{y_2} \partial_{x_2} \langle h_{xx} h_{xz} \rangle \\
&\quad \left. + \partial_{z_1} \partial_{x_1} \partial_{x_2} \partial_{z_2} \langle h_{yx} h_{yx} \rangle - \partial_{z_2}^2 \partial_{z_1} \partial_{x_1} \langle h_{yx} h_{yz} \rangle \right] |_{x_1=x_2, z_1=z_2}, \\
&= \frac{\partial_{z_1}^2 (\partial_{t_1} \partial_{t_2} - 2\partial_{y_1} \partial_{y_2}) (\partial_{z_1}^2 + \partial_{x_1}^2)^2}{\nabla^4} G(x, x')|_{x_1=x_2, z_1=z_2}, \\
&= \partial_{x_1}^2 (-2\partial_{y_1} \partial_{y_2} + \partial_{t_1} \partial_{t_2}) G(x, x')|_{x_1=x_2, z_1=z_2}. \tag{B.10}
\end{aligned}$$

We have used the isotropy in the x, z directions.

Therefore, by explicit computation we have seen that

$$\begin{aligned}
\langle R_{tytx}(x)R_{tytx}(x') \rangle|_{x_1=x_2, z_1=z_2} &= \langle R_{tytz}(x)R_{tytz}(x') \rangle|_{x_1=x_2, z_1=z_2}, \\
&= \langle R_{yzxz}(x)R_{yzxz}(x') \rangle|_{x_1=x_2, z_1=z_2}, \\
&= \langle R_{yxxz}(x)R_{yxxz}(x') \rangle|_{x_1=x_2, z_1=z_2}. \tag{B.11}
\end{aligned}$$

The two-point function of all curvature components in the class are identical.

Class 3 : $\{R_{txxz}, R_{tzxz}, R_{tyyx}, R_{tyyz}\}$

Let us now compute the correlator of R_{txxz} .

$$R_{txxz} = \frac{1}{2} \left[\partial_x^2 h_{tz} - \partial_t \partial_x h_{xz} + \partial_t \partial_z h_{xx} - \partial_x \partial_z h_{tx} \right]. \tag{B.12}$$

Therefore, we evaluate the two-point function

$$\begin{aligned}\langle R_{txxz}(x)R_{txxz}(x') \rangle|_{x_1=x_2, z_1=z_2} &= (\partial_{y_1}\partial_{y_2} - 2\partial_{t_1}\partial_{t_2})\frac{\partial_{z_1}^2(\partial_{x_1}^2 + \partial_{z_1}^2)^2}{\nabla^4}G(x, x')|_{x_1=x_2, z_1=z_2}, \\ &= \partial_{x_1}^2(\partial_{y_1}\partial_{y_2} - 2\partial_{t_1}\partial_{t_2})G(x, x')|_{x_1=x_2, z_1=z_2}.\end{aligned}\quad (\text{B.13})$$

To derive the last line we use isometry in x, z -plane

$$\frac{\partial_{x_1}^2}{\nabla^2}G(x, x')|_{x_1=x_2, z_1=z_2} = \frac{\partial_{z_1}^2}{\nabla^2}G(x, x')|_{x_1=x_2, z_1=z_2}.\quad (\text{B.14})$$

Similarly we compute the two-point function of R_{tzxz} and observe that they are identical.

$$\begin{aligned}\langle R_{tzxz}(x)R_{tzxz}(x') \rangle|_{x_1=x_2, z_1=z_2} &= \partial_{x_1}^2(\partial_{y_1}\partial_{y_2} - 2\partial_{t_1}\partial_{t_2})G(x, x')|_{x_1=x_2, z_1=z_2} \\ &= \langle R_{tyyx}(x)R_{tyyx}(x') \rangle|_{x_1=x_2, z_1=z_2}.\end{aligned}\quad (\text{B.15})$$

To derive the last line we use the isometry of the scalar Green's function in the $x - z$ plane. Let us now compute the two-point functions of R_{tyyx}

$$\begin{aligned}\langle R_{tyyx}(x)R_{tyyx}(x') \rangle|_{x_1=x_2, z_1=z_2} &= \frac{1}{4}\left[\partial_{y_1}^2\partial_{y_2}^2\langle h_{tx}h_{tx} \rangle - \partial_{t_2}\partial_{y_2}\partial_{y_1}^2\langle h_{tx}h_{yx} \rangle + \partial_{y_1}\partial_{t_1}\partial_{y_2}\partial_{t_2}\langle h_{yx}h_{yx} \rangle \right. \\ &\quad + \partial_{t_1}\partial_{x_1}\partial_{t_2}\partial_{x_2}\langle h_{yy}h_{yy} \rangle - \partial_{t_1}\partial_{y_1}\partial_{y_2}^2\langle h_{yx}h_{tx} \rangle - \partial_{t_1}\partial_{x_1}\partial_{y_2}\partial_{x_2}\langle h_{yy}h_{ty} \rangle \\ &\quad \left. + \partial_{y_1}\partial_{x_1}\partial_{y_2}\partial_{x_2}\langle h_{ty}h_{ty} \rangle - \partial_{y_1}\partial_{x_1}\partial_{t_2}\partial_{x_2}\langle h_{ty}h_{yy} \rangle\right]G(x, x'), \\ &= \partial_{x_1}^2(\partial_{y_1}\partial_{y_2} - 2\partial_{t_1}\partial_{t_2})G(x, x')|_{x_1=x_2, z_1=z_2}.\end{aligned}\quad (\text{B.16})$$

Similarly we compute the two-point function of R_{tyyz} and obtain

$$\langle R_{tyyz}(x)R_{tyyz}(x') \rangle|_{x_1=x_2, z_1=z_2} = \partial_{z_1}^2(\partial_{y_1}\partial_{y_2} - 2\partial_{t_1}\partial_{t_2})G(x, x')|_{x_1=x_2, z_1=z_2}.\quad (\text{B.17})$$

From the isotropy of the scalar Green's function in the x, z plane, it is clear that

$$\begin{aligned}\langle R_{txxz}(x)R_{txxz}(x') \rangle|_{x_1=x_2, z_1=z_2} &= \langle R_{tzxz}(x)R_{tzxz}(x') \rangle|_{x_1=x_2, z_1=z_2}, \\ &= \langle R_{tyyx}(x)R_{tyyx}(x') \rangle|_{x_1=x_2, z_1=z_2}, \\ &= \langle R_{tyyz}(x)R_{tyyz}(x') \rangle|_{x_1=x_2, z_1=z_2}.\end{aligned}\quad (\text{B.18})$$

Class 4: $\{R_{txtx}, R_{yzyz}, R_{tztz}, R_{yxyx}\}$

We now compute the two-point function of R_{txtx} and show that this is identical to the two-point functions of three other curvature tensors which are R_{yzyz} , R_{tztz} and R_{yxyx} .

$$R_{txtx} = \frac{1}{2}\left[2\partial_x\partial_t h_{tx} - \partial_t^2 h_{xx} - \partial_x^2 h_{tt}\right]\quad (\text{B.19})$$

The two-point function is given by

$$\begin{aligned}
& \langle R_{txtx}(x)R_{txtx}(x') \rangle|_{x_1=x_2, z_1=z_2} \\
&= \frac{1}{4} \left[4\partial_{x_1}\partial_{x_2}\partial_{t_1}\partial_{t_2}\langle h_{tx}h_{tx} \rangle + \partial_{t_1}^2\partial_{t_2}^2\langle h_{xx}h_{xx} \rangle + \partial_{x_1}^2\partial_{x_2}^2\langle h_{tt}h_{tt} \rangle, \right. \\
&\quad \left. + \partial_{x_2}^2\partial_{t_1}^2\langle h_{xx}h_{tt} \rangle + \partial_{x_1}^2\partial_{t_2}^2\langle h_{tt}h_{xx} \rangle \right]|_{x_1=x_2, z_1=z_2} \\
&= \frac{1}{4\nabla^4} \left(-4\partial_{x_1}^2\partial_{z_1}^2\partial_{t_1}\partial_{t_2}\partial_{y_1}\partial_{y_2} + 2\partial_{z_1}^4\partial_{t_1}^2\partial_{t_2}^2 + 2\partial_{x_1}^4\partial_{y_1}^2\partial_{y_2}^2 \right. \\
&\quad \left. + 2\partial_{x_1}^2\partial_{z_1}^2(\partial_{t_1}^2\partial_{y_2}^2 + \partial_{y_1}^2\partial_{t_2}^2) \right) G(x, x')|_{x_1=x_2, z_1=z_2}, \\
&= \frac{1}{16} \left(3\partial_{t_1}^2\partial_{t_2}^2 + 3\partial_{y_1}^2\partial_{y_2}^2 + (\partial_{t_1}\partial_{y_2} - \partial_{y_1}\partial_{t_2})^2 \right) G(x, x')|_{x_1=x_2, z_1=z_2}. \tag{B.20}
\end{aligned}$$

Here we use the following identities to derive the last line. The proof of these identities are shown in (D.8) and (D.11).

$$\begin{aligned}
\frac{\partial_{x_1}^4}{\nabla^4} G(x, x')|_{x_1=x_2, z_1=z_2} &= \frac{\partial_{z_1}^4}{\nabla^4} G(x, x')|_{x_1=x_2, z_1=z_2}, \\
&= \frac{3}{8} G(x, x')|_{x_1=x_2, z_1=z_2}. \tag{B.21} \\
\frac{\partial_{x_1}^2\partial_{z_1}^2}{\nabla^4} G(x, x')|_{x_1=x_2, z_1=z_2} &= \frac{1}{8} G(x, x')|_{x_1=x_2, z_1=z_2}.
\end{aligned}$$

These identities arise because of the isotropy of the scalar Greens function. Therefore we expect that the two point function $\langle R_{tztz}(x)R_{tztz}(x') \rangle$ to be identical to $\langle R_{txtx}(x)R_{txtx}(x') \rangle$ in the coincident limit. The expression of R_{tztz} is given by

$$R_{tztz} = \frac{1}{2} \left[2\partial_z\partial_t h_{tz} - \partial_t^2 h_{zz} - \partial_z^2 h_{tt} \right]. \tag{B.22}$$

The two-point function is evaluated to

$$\begin{aligned}
& \langle R_{tztz}(x)R_{tztz}(x') \rangle|_{x_1=x_2, z_1=z_2} \\
&= \frac{1}{4\nabla^4} \left(-4\partial_{x_1}^2\partial_{z_1}^2\partial_{t_1}\partial_{t_2}\partial_{y_1}\partial_{y_2} + 2\partial_{z_1}^4\partial_{t_1}^2\partial_{t_2}^2 + 2\partial_{x_1}^4\partial_{y_1}^2\partial_{y_2}^2 \right. \\
&\quad \left. + 2\partial_{x_1}^2\partial_{z_1}^2(\partial_{t_1}^2\partial_{y_2}^2 + \partial_{y_1}^2\partial_{t_2}^2) \right) G(x, x')|_{x_1=x_2, z_1=z_2}, \\
&= \frac{1}{16} \left(3\partial_{t_1}^2\partial_{t_2}^2 + 3\partial_{y_1}^2\partial_{y_2}^2 + (\partial_{t_1}\partial_{y_2} - \partial_{y_1}\partial_{t_2})^2 \right) G(x, x')|_{x_1=x_2, z_1=z_2}. \tag{B.23}
\end{aligned}$$

Similarly we explicitly show that two-point function of R_{yzyz} and R_{yxyx} are identical to the two-point function of R_{txtx} or R_{tztz} .

$$R_{yzyz} = \frac{1}{2} \left[2\partial_z\partial_y h_{yz} - \partial_y^2 h_{zz} - \partial_z^2 h_{yy} \right]. \tag{B.24}$$

The two-point function is given by

$$\begin{aligned}
& \langle R_{yzyz}(x)R_{yzyz}(x') \rangle|_{x_1=x_2, z_1=z_2} & (B.25) \\
& = \frac{1}{4} \left[4\partial_{x_1}\partial_{x_2}\partial_{y_1}\partial_{y_2}\langle h_{yx}h_{yx} \rangle + \partial_{y_1}^2\partial_{y_2}^2\langle h_{xx}h_{xx} \rangle + \partial_{x_1}^2\partial_{x_2}^2\langle h_{yy}h_{yy} \rangle \right. \\
& \quad \left. + \partial_{x_2}^2\partial_{y_1}^2\langle h_{xx}h_{yy} \rangle + \partial_{x_1}^2\partial_{y_2}^2\langle h_{yy}h_{xx} \rangle \right]|_{x_1=x_2, z_1=z_2}, \\
& = \frac{1}{4\nabla^4} \left(-4\partial_{x_1}^2\partial_{z_1}^2\partial_{y_1}\partial_{y_2}\partial_{t_1}\partial_{t_2} + 2\partial_{z_1}^4\partial_{y_1}^2\partial_{y_2}^2 + 2\partial_{x_1}^4\partial_{t_1}^2\partial_{t_2}^2 \right. \\
& \quad \left. + 2\partial_{x_1}^2\partial_{z_1}^2(\partial_{y_1}^2\partial_{t_2}^2 + \partial_{t_1}^2\partial_{y_2}^2) \right) G(x, x')|_{x_1=x_2, z_1=z_2}, \\
& = \frac{1}{16} \left(3\partial_{t_1}^2\partial_{t_2}^2 + 3\partial_{y_1}^2\partial_{y_2}^2 + (\partial_{t_1}\partial_{y_2} - \partial_{y_1}\partial_{t_2})^2 \right) G(x, x')|_{x_1=x_2, z_1=z_2}, \\
& = \langle R_{yxxy}(x)R_{yxxy}(x') \rangle|_{x_1=x_2, z_1=z_2}. & (B.26)
\end{aligned}$$

In the last line, we use the identities (B.21). Therefore we find

$$\begin{aligned}
& \langle R_{txtx}(x)R_{txtx}(x') \rangle|_{x_1=x_2, z_1=z_2} = \langle R_{tztz}(x)R_{tztz}(x') \rangle|_{x_1=x_2, z_1=z_2} \\
& = \langle R_{yxxy}(x)R_{yxxy}(x') \rangle|_{x_1=x_2, z_1=z_2} = \langle R_{yzyz}(x)R_{yzyz}(x') \rangle|_{x_1=x_2, z_1=z_2}. & (B.27)
\end{aligned}$$

Class 5: $\{R_{txtz}, R_{yxyz}\}$

We now compute the two-point function of R_{txtz} and R_{yxyz} and show the equality between them. The curvature tensor R_{txtz} in terms of the field variable is given by

$$R_{txtz} = \frac{1}{2} \left[\partial_x\partial_t h_{tz} - \partial_t^2 h_{xz} + \partial_t\partial_z h_{xt} - \partial_z\partial_x h_{tt} \right]. \quad (B.28)$$

Therefore the two-point function is given by

$$\begin{aligned}
& \langle R_{txtz}(x)R_{txtz}(x') \rangle|_{x_1=x_2, z_1=z_2} & (B.29) \\
& = \frac{1}{4} \left[\partial_{x_1}\partial_{x_2}\partial_{t_1}\partial_{t_2}\langle h_{tz}h_{tz} \rangle + \partial_{x_1}\partial_{z_2}\partial_{t_1}\partial_{t_2}\langle h_{tz}h_{xt} \rangle + \partial_{t_1}^2\partial_{t_2}^2\langle h_{xz}h_{xz} \rangle \right. \\
& \quad + \partial_{z_1}\partial_{z_2}\partial_{t_1}\partial_{t_2}\langle h_{xt}h_{xt} \rangle + \partial_{t_1}\partial_{z_1}\partial_{t_2}\partial_{x_2}\langle h_{xt}h_{tz} \rangle + \partial_{x_1}^2\partial_{z_1}^2\langle h_{tz}h_{tz} \rangle \\
& \quad \left. + \partial_{t_1}^2\partial_{x_2}\partial_{z_2}\langle h_{xz}h_{tt} \rangle + \partial_{x_1}\partial_{z_1}\partial_{t_2}^2\langle h_{tt}h_{xz} \rangle \right]|_{x_1=x_2, z_1=z_2}, \\
& = \frac{1}{16} \left(2\partial_{y_1}\partial_{y_2}\partial_{t_1}\partial_{t_2} + (\partial_{t_1}\partial_{t_2} - \partial_{y_1}\partial_{y_2})^2 - (\partial_{t_1}\partial_{y_2} - \partial_{y_1}\partial_{t_2})^2 \right) G(x, x')|_{x_1=x_2, z_1=z_2}.
\end{aligned}$$

To derive the second line, we use the identity given in (B.21). Similarly we evaluate the correlator of R_{yxyz} . The curvature component R_{yxyz} is given by

$$R_{yxyz} = \frac{1}{2} \left[\partial_x\partial_y h_{yz} - \partial_y^2 h_{xz} + \partial_z\partial_y h_{xy} - \partial_x\partial_z h_{yy} \right]. \quad (B.30)$$

The correlator is given by

$$\begin{aligned}
& \langle R_{yxyz}(x)R_{yxyz}(x') \rangle|_{x_1=x_2, z_1=z_2} \tag{B.31} \\
&= \frac{1}{4} \left[\partial_{x_1} \partial_{x_2} \partial_{y_1} \partial_{y_2} \langle h_{yz} h_{yz} \rangle + \partial_{x_1} \partial_{z_2} \partial_{y_1} \partial_{y_2} \langle h_{yz} h_{xy} \rangle + \partial_{y_1}^2 \partial_{y_2}^2 \langle h_{xz} h_{xz} \rangle \right. \\
&\quad + \partial_{z_1} \partial_{z_2} \partial_{y_1} \partial_{y_2} \langle h_{xy} h_{xy} \rangle + \partial_{y_1} \partial_{z_1} \partial_{y_2} \partial_{x_2} \langle h_{xy} h_{yz} \rangle + \partial_{x_1}^2 \partial_{z_1}^2 \langle h_{yz} h_{yz} \rangle \\
&\quad \left. + \partial_{y_1}^2 \partial_{x_2} \partial_{z_2} \langle h_{xz} h_{yy} \rangle + \partial_{x_1} \partial_{z_1} \partial_{y_2}^2 \langle h_{yy} h_{xz} \rangle \right] |_{x_1=x_2, z_1=z_2}, \\
&= \frac{1}{16} \left(2\partial_{y_1} \partial_{y_2} \partial_{t_1} \partial_{t_2} + (\partial_{t_1} \partial_{t_2} - \partial_{y_1} \partial_{y_2})^2 - (\partial_{t_1} \partial_{y_2} - \partial_{y_1} \partial_{t_2})^2 \right) G(x, x')|_{x_1=x_2, z_1=z_2}.
\end{aligned}$$

In the last line we use the isotropy of the Green's function along the x, z direction. Therefore by explicit computation we have seen that

$$\langle R_{txtz}(x)R_{txtz}(x') \rangle|_{x_1=x_2, z_1=z_2} = \langle R_{yxyz}(x)R_{yxyz}(x') \rangle|_{x_1=x_2, z_1=z_2}. \tag{B.32}$$

Class 6: $\{R_{txyx}, R_{tzyz}\}$

Similarly we find two more curvature tensors R_{txyx} and R_{tzyz} having same two-point functions. We compute two-point function of R_{tzyz} . The expression of R_{txyx} in terms of field variables is given by

$$R_{txyx} = \frac{1}{2} \left[\partial_x \partial_y h_{tx} - \partial_t \partial_y h_{xx} + \partial_x \partial_t h_{xy} - \partial_x^2 h_{ty} \right]. \tag{B.33}$$

The two-point function is evaluated as

$$\begin{aligned}
& \langle R_{txyx}(x)R_{txyx}(x') \rangle|_{x_1=x_2, z_1=z_2} \tag{B.34} \\
&= \frac{1}{4} \left[\partial_{x_1} \partial_{x_2} \partial_{y_1} \partial_{y_2} \langle h_{tx} h_{tx} \rangle + \partial_{x_1} \partial_{x_2} \partial_{y_1} \partial_{t_2} \langle h_{tx} h_{xy} \rangle + \partial_{t_1} \partial_{t_2} \partial_{y_1} \partial_{y_2} \langle h_{xx} h_{xx} \rangle \right. \\
&\quad + \partial_{x_1} \partial_{x_2} \partial_{t_1} \partial_{t_2} \langle h_{xy} h_{xy} \rangle + \partial_{t_1} \partial_{x_1} \partial_{y_2} \partial_{x_2} \langle h_{xy} h_{tx} \rangle + \partial_{x_1}^2 \partial_{x_2}^2 \langle h_{ty} h_{ty} \rangle \\
&\quad \left. + \partial_{t_1} \partial_{y_1} \partial_{x_2}^2 \langle h_{xx} h_{ty} \rangle + \partial_{x_1}^2 \partial_{t_2} \partial_{y_2} \langle h_{ty} h_{xx} \rangle \right] |_{x_1=x_2, z_1=z_2}, \\
&= \frac{1}{4} \left[2 \frac{\partial_{x_1}^4}{\nabla^4} \partial_{t_1} \partial_{t_2} \partial_{y_1} \partial_{y_2} + 2 \frac{\partial_{z_1}^4}{\nabla^4} \partial_{t_1} \partial_{t_2} \partial_{y_1} \partial_{y_2} + 2 \frac{\partial_{x_1}^2 \partial_{z_1}^2}{\nabla^4} (\partial_{t_1}^2 \partial_{y_2}^2 \partial_{y_1}^2 \partial_{t_2}^2 \right. \\
&\quad \left. - \partial_{t_1}^2 \partial_{t_2}^2 - \partial_{y_1}^2 \partial_{y_2}^2 - 4\partial_{t_1} \partial_{t_2} \partial_{y_1} \partial_{y_2}) \right] G(x, x')|_{x_1=x_2, z_1=z_2}, \\
&= \left[\frac{1}{32} (\partial_{t_1} \partial_{y_2} + \partial_{y_1} \partial_{t_2})^2 - \frac{1}{32} (\partial_{t_1} \partial_{t_2} - \partial_{y_1} \partial_{y_2})^2 \right] G(x, x')|_{x_1=x_2, z_1=z_2}.
\end{aligned}$$

Note that, the second line of equation (B.34) is symmetric under the exchange of variable $x_1 \rightarrow z_1$. Therefore the two-point function of R_{tzyz} is also the same as R_{txyx} .

$$\langle R_{txyx}(x)R_{txyx}(x') \rangle|_{x_1=x_2, z_1=z_2} = \langle R_{tzyz}(x)R_{tzyz}(x') \rangle|_{x_1=x_2, z_1=z_2}. \tag{B.35}$$

Class 7: $\{R_{txyz}\}$

Now we are left with only one independent curvature component which is R_{txyz} . The curvature tensor R_{txyz} in terms of field variables is given by

$$R_{txyz} = \frac{1}{2} \left[\partial_x \partial_y h_{tz} - \partial_t \partial_y h_{xz} + \partial_z \partial_t h_{xy} - \partial_x \partial_z h_{ty} \right]. \quad (\text{B.36})$$

From the two-point function of the field variables, we compute

$$\begin{aligned} & \langle R_{txyz}(x) R_{txyz}(x') \rangle |_{x_1=x_2, z_1=z_2} \quad (\text{B.37}) \\ &= \frac{1}{4} \left[\partial_{x_1} \partial_{x_2} \partial_{y_1} \partial_{y_2} \langle h_{tz} h_{tz} \rangle + \partial_{x_1} \partial_{z_2} \partial_{y_1} \partial_{t_2} \langle h_{tz} h_{xy} \rangle + \partial_{t_1} \partial_{t_2} \partial_{y_1} \partial_{y_2} \langle h_{xz} h_{xz} \rangle \right. \\ & \quad + \partial_{z_1} \partial_{z_2} \partial_{t_1} \partial_{t_2} \langle h_{xy} h_{xy} \rangle + \partial_{t_1} \partial_{z_1} \partial_{y_2} \partial_{x_2} \langle h_{xy} h_{tz} \rangle + \partial_{x_1} \partial_{x_2} \partial_{z_1} \partial_{z_2} \langle h_{ty} h_{ty} \rangle \\ & \quad \left. + \partial_{t_1} \partial_{y_1} \partial_{x_2} \partial_{z_2} \langle h_{xz} h_{ty} \rangle + \partial_{x_1} \partial_{z_1} \partial_{t_2} \partial_{y_2} \langle h_{ty} h_{xz} \rangle \right] |_{x_1=x_2, z_1=z_2}, \\ &= - \left(\frac{3}{32} (\partial_{t_1} \partial_{t_2} - \partial_{y_1} \partial_{y_2})^2 + \frac{1}{32} (\partial_{y_1} \partial_{t_2} - \partial_{t_1} \partial_{y_2})^2 \right) G(x, x') |_{x_1=x_2, z_1=z_2}. \end{aligned} \quad (\text{B.38})$$

C Expectation value of the Kretschmann scalar

Since there is no local stress tensor in gravity, we use Kretschmann scalar to probe the quench created by curvature components. Let us consider the curvature component R_{tyty} . We wish to evaluate the 3 point function

$$\begin{aligned} \text{Tr}[K(0, 0)\rho(t, -y_0)] &= \text{Tr}[K(0, y_0)\rho(t, 0)], \quad (\text{C.1}) \\ &= \frac{\langle R_{tyty}(-\epsilon - it, 0) K(0, y_0) R_{tyty}(\epsilon - it, 0) \rangle}{\langle R_{tyty}(-\epsilon - it, 0) R_{tyty}(\epsilon - it, 0) \rangle}, \end{aligned}$$

where

$$K = R_{\mu\nu\rho\sigma} R^{\mu\nu\rho\sigma}. \quad (\text{C.2})$$

We have not explicitly mentioned the coordinates in the x, z plane since the Kretschman scalar is located at the same point in the x, z plane at which the quench is created. This makes the computation easier. Opening up the sum in the Kretschman scalar, we see that we see that by Wick contractions the 3-point function in the numerator breaks up into product of 2 point functions. The 2 point functions involve the component of R_{tyty} with every other component of the Riemann tensors. Since we have already grouped the components of the Riemann tensors into classes, we will evaluate these 2 point functions by considering one class at a time.

Consider components in class 1.

$$\langle R_{tyty} R_{tyty} \rangle |_{x_1=x_2, z_1=z_2} = \frac{1}{2} (\partial_{t_1}^2 + \partial_{y_1}^2)^2 G(x, x') |_{x_1=x_2, z_1=z_2}. \quad (\text{C.3})$$

Similarly, one obtains

$$\langle R_{tyty}R_{zxzx} \rangle|_{x_1=x_2, z_1=z_2} = \frac{1}{2} (\partial_{t_1}^2 + \partial_{y_1}^2)^2 G(x, x')|_{x_1=x_2, z_1=z_2}. \quad (\text{C.4})$$

From (3.11) we see $\langle h_{ai}h_{c'd'} \rangle = 0$, this implies

$$\langle R_{tyty}R_{tyxz} \rangle|_{x_1=x_2, z_1=z_2} = 0. \quad (\text{C.5})$$

We now evaluate the two-point function of R_{tyty} with the field operators belonging to class 2 and class 3. Components in this class can be organised as vectors of $SO(2)_T \times SO(2)_L$.

$$\begin{aligned} & \langle R_{tyty}R_{tytx} \rangle|_{x_1=x_2, z_1=z_2} \\ &= \frac{1}{4} \left[2\partial_{y_1}\partial_{t_1}\partial_{t_2}\partial_{x_2} \langle h_{ty}h_{yt} \rangle - 2\partial_{y_1}\partial_{t_1}\partial_{y_2}\partial_{x_2} \langle h_{ty}h_{tt} \rangle - \partial_{t_1}^2\partial_{t_2}\partial_{x_2} \langle h_{yy}h_{yt} \rangle \right. \\ & \quad \left. + \partial_{t_2}^2\partial_{x_2}\partial_{y_2} \langle h_{yy}h_{tt} \rangle - \partial_{y_1}^2\partial_{t_2}\partial_{x_2} \langle h_{tt}h_{yt} \rangle + \partial_{y_1}^2\partial_{x_2}\partial_{y_2} \langle h_{tt}h_{tt} \rangle \right]|_{x_1=x_2, z_1=z_2}, \\ &= 0. \end{aligned} \quad (\text{C.6})$$

The last line follows from the fact that

$$\partial_{x_2}G(x, x')|_{x_1=x_2, z_1=z_2} = 0.$$

Similarly it is easy to show in the coincident limit, any odd number of derivative with respect to the coordinate along the direction of the defect acting on the scalar two-point function on the flat space will also vanish. We demonstrate one more correlator

$$\begin{aligned} \langle R_{tyty}R_{txxz} \rangle|_{x_1=x_2, z_1=z_2} &= -\frac{1}{2}\partial_{t_2}\partial_{z_2}(\partial_{x_2}^2 + \partial_{z_2}^2)G(x, x')|_{x_1=x_2, z_1=z_2}, \\ &= 0. \end{aligned} \quad (\text{C.7})$$

Therefore, all the two-point functions of R_{tyty} with components in class 2 and class 3 vanishes when we take the positions along x, z directions to coincide.

We evaluate the correlators with components in class 4

$$\begin{aligned} \langle R_{tyty}R_{txtx} \rangle|_{x_1=x_2, z_1=z_2} &= \langle R_{tyty}R_{tztz} \rangle|_{x_1=x_2, z_1=z_2}, \\ &= \langle R_{tyty}R_{yxyx} \rangle|_{x_1=x_2, z_1=z_2} \\ &= \langle R_{tyty}R_{yzyz} \rangle|_{x_1=x_2, z_1=z_2}, \\ &= \frac{1}{2}\partial_{x_1}^2(\partial_{t_2}^2 + \partial_{y_2}^2)G(x, x')|_{x_1=x_2, z_1=z_2}, \\ &= -\frac{1}{4}(\partial_{t_1}^2 + \partial_{y_1}^2)^2G(x, x')|_{x_1=x_2, z_1=z_2}. \end{aligned} \quad (\text{C.8})$$

To obtain the last line we have used (D.4) and the on-shell condition of the scalar Greens function.

We evaluate the two-point functions of R_{tyty} with curvature components in class 5.

But note that, these components R_{txtz} and R_{yxyz} , have two indices in the x, z directions, which are parallel direction to the defect. Therefore all terms in the two-point functions will involve two derivatives with respect to x and z . But in the coincident limit

$$\partial_{x_2} \partial_{z_2} G(x, x')|_{x_1=x_2, z_1=z_2} = 0. \quad (\text{C.9})$$

Therefore, all the two-point functions R_{tytty} with curvature components in class 5 vanish in the coincident limit.

Consider two-point functions of R_{tyty} with components in class 6.

$$\begin{aligned} \langle R_{tyty} R_{txyx} \rangle|_{x_1=x_2, z_1=z_2} &= \langle R_{tyty} R_{tzyz} \rangle|_{x_1=x_2, z_1=z_2}, \\ &= \frac{1}{2} \partial_{t_2} \partial_{y_2} (\partial_{x_1}^2 - \partial_{z_1}^2) G_f(x, x')|_{x_1=x_2, z_1=z_2}|_{x_1=x_2, z_1=z_2}, \\ &= 0. \end{aligned} \quad (\text{C.10})$$

The last line follows from the isotropy relations (D.4) and (D.5). Therefore components in class 6 do not contribute to the expectation value of the Kretschman scalar.

We are left with one more correlator from class 7, which is $\langle R_{tyty} R_{tyxz} \rangle$. But, note that all terms in this two-point function have a single derivative each in both x and z directions. Therefore in the coincident limit this too will vanish.

$$\langle R_{tyty} R_{txyz} \rangle|_{x_1=x_2, z_1=z_2} = 0. \quad (\text{C.11})$$

Using all these two-point functions, we evaluate (C.1) in the coincident limit in the x, z direction

$$\frac{\langle R_{tyty}(-\epsilon - it, 0) K(0, y_0) R_{tyty}(\epsilon - it, 0) \rangle}{\langle R_{tyty}(-\epsilon - it, 0) R_{tyty}(\epsilon - it, 0) \rangle} = \frac{6144\epsilon^6}{\left(t^4 + 2t^2(\epsilon^2 - y_0^2) + (y_0^2 + \epsilon^2)^2\right)^3}. \quad (\text{C.12})$$

D Relations due to isotropy

In this appendix we prove a few relations which relate derivatives on the Green's function along the x and z directions at the coincident limit along the directions parallel to the defect. The first relation we prove is the isotropy relation in (2.50). For this it is useful to consider the Green's function (2.12) in Fourier space along the x, z direction which is defined by

$$\tilde{G}(r_1, r_2, \theta_1, \theta_2, k_x, k_z) = \int_{-\infty}^{\infty} dx dz G(r_1, r_2, \theta_1, \theta_2, x, z) e^{-i(k_x x + k_z z)}. \quad (\text{D.1})$$

There is translation invariance in x, z directions, so we have replaced $x_1 - x_2, z_1 - z_2$ by x, z respectively. It is easy to show that due to rotational invariance in the directions x, z , the Fourier transform $\tilde{G}(r_1, r_2, \theta_1, \theta_2, k_x, k_z)$ is only a function of the form $\tilde{G}(r_1, r_2, \theta_1, \theta_2, k_x^2 +$

k_z^2) or $\tilde{G}(r_1, r_2, \theta_1, \theta_2, k)$, where $k = \sqrt{k_x^2 + k_z^2}$. Now let us consider

$$\begin{aligned}\partial_x^2 G(r_1, r_2, \theta_1, \theta_2, x, z)|_{x=z=0} &= \frac{1}{(2\pi)^2} \int_0^\infty k dk \int_0^{2\pi} d\phi k_x^2 \tilde{G}(r_1, r_2, \theta_1, \theta_2, k), \quad (\text{D.2}) \\ &= \frac{2\pi}{2} \frac{1}{(2\pi)^2} \int_0^\infty k dk k^2 \tilde{G}(r_1, r_2, \theta_1, \theta_2, k)\end{aligned}$$

To obtain the last line we have substituted $k_x = k \cos \phi$ and performed the angular integral. Compare this to action of the Laplacian along the longitudinal directions

$$\begin{aligned}\nabla^2 G(r_1, r_2, \theta_1, \theta_2, x, z)|_{x=z=0} &= \frac{1}{(2\pi)^2} \int_0^\infty k dk \int_0^{2\pi} d\phi (k_x^2 + k_z^2) \tilde{G}(r_1, r_2, \theta_1, \theta_2, k), \\ &= (2\pi) \frac{1}{(2\pi)^2} \int_0^\infty k dk k^2 \tilde{G}(r_1, r_2, \theta_1, \theta_2, k)\end{aligned} \quad (\text{D.3})$$

Comparing (D.2) and (D.3), we obtain

$$\partial_x^2 G(r_1, r_2, \theta_1, \theta_2, x, z)|_{x=z=0} = \frac{1}{2} \nabla^2 G(r_1, r_2, \theta_1, \theta_2, x, z)|_{x=z=0} \quad (\text{D.4})$$

A very similar analysis shows

$$\partial_z^2 G(r_1, r_2, \theta_1, \theta_2, x, z)|_{x=z=0} = \frac{1}{2} \nabla^2 G(r_1, r_2, \theta_1, \theta_2, x, z)|_{x=z=0} \quad (\text{D.5})$$

Now consider

$$\begin{aligned}\partial_x^4 G(r_1, r_2, \theta_1, \theta_2, x, z)|_{x=z=0} &= \frac{1}{(2\pi)^2} \int_0^\infty k dk \int_0^{2\pi} d\phi k_x^4 \tilde{G}(r_1, r_2, \theta_1, \theta_2, k), \\ &= \frac{3}{8} \times 2\pi \frac{1}{(2\pi)^2} \int_0^\infty k dk k^4 \tilde{G}(r_1, r_2, \theta_1, \theta_2, k)\end{aligned} \quad (\text{D.6})$$

To obtain the last line we have replaced $k_x^4 = k^4 \cos^4 \phi$ and performed the integral over ϕ . We can compare this to the action of the square of the Laplacian

$$\begin{aligned}\nabla^4 G(r_1, r_2, \theta_1, \theta_2, x, z)|_{x=z=0} &= \frac{1}{(2\pi)^2} \int_0^\infty k dk \int_0^{2\pi} d\phi (k_x^2 + k_z^2)^2 \tilde{G}(r_1, r_2, \theta_1, \theta_2, k), \\ &= 2\pi \frac{1}{(2\pi)^2} \int_0^\infty k dk k^4 \tilde{G}(r_1, r_2, \theta_1, \theta_2, k)\end{aligned} \quad (\text{D.7})$$

Comparing (D.6) and (D.7), we see that

$$\partial_x^4 G(r_1, r_2, \theta_1, \theta_2, x, z)|_{x=z=0} = \frac{3}{8} \nabla^4 G(r_1, r_2, \theta_1, \theta_2, x, z)|_{x=z=0}. \quad (\text{D.8})$$

Again similarly we obtain

$$\partial_z^4 G(r_1, r_2, \theta_1, \theta_2, x, z)|_{x=z=0} = \frac{3}{8} \nabla^4 G(r_1, r_2, \theta_1, \theta_2, x, z)|_{x=z=0}. \quad (\text{D.9})$$

Finally consider

$$\begin{aligned}\partial_x^2 \partial_z^2 G(r_1, r_2, \theta_1, \theta_2, x, z)|_{x=z=0} &= \frac{1}{(2\pi)^2} \int_0^\infty k dk \int_0^{2\pi} d\phi k_x^2 k_z^2 \tilde{G}(r_1, r_2, \theta_1, \theta_2, k), \\ &= \frac{1}{8} \times 2\pi \frac{1}{(2\pi)^2} \int_0^\infty k dk k^4 \tilde{G}(r_1, r_2, \theta_1, \theta_2, k).\end{aligned}\quad (\text{D.10})$$

where we obtain the last line by replacing $k_x^2 k_z^2 = k^4 \cos^2 \phi \sin^2 \phi$ and performing the integral over ϕ . Thus comparing (D.10) and (D.7) we obtain

$$\partial_x^2 \partial_z^2 G(r_1, r_2, \theta_1, \theta_2, x, z)|_{x=z=0} = \frac{1}{8} \nabla^4 G(r_1, r_2, \theta_1, \theta_2, x, z)|_{x=z=0}.\quad (\text{D.11})$$

References

- [1] H. Liu and J. Sonner, *Holographic systems far from equilibrium: a review*, [arXiv:1810.02367](#).
- [2] P. Calabrese and J. L. Cardy, *Evolution of entanglement entropy in one-dimensional systems*, *J. Stat. Mech.* **0504** (2005) P04010, [[cond-mat/0503393](#)].
- [3] P. Calabrese and J. Cardy, *Quantum Quenches in Extended Systems*, *J. Stat. Mech.* **0706** (2007) P06008, [[arXiv:0704.1880](#)].
- [4] P. Calabrese and J. Cardy, *Entanglement and correlation functions following a local quench: a conformal field theory approach*, *J. Stat. Mech.* **0710** (2007), no. 10 P10004, [[arXiv:0708.3750](#)].
- [5] V. Eisler and I. Peschel, *Evolution of entanglement after a local quench*, *Journal of Statistical Mechanics: Theory and Experiment* **2007** (jun, 2007) P06005–P06005.
- [6] J.-M. Stéphan and J. Dubail, *Local quantum quenches in critical one-dimensional systems: entanglement, the loschmidt echo, and light-cone effects*, *Journal of Statistical Mechanics: Theory and Experiment* **2011** (aug, 2011) P08019.
- [7] C. T. Asplund and A. Bernamonti, *Mutual information after a local quench in conformal field theory*, *Phys. Rev. D* **89** (2014), no. 6 066015, [[arXiv:1311.4173](#)].
- [8] P. Calabrese and J. Cardy, *Quantum quenches in 1 + 1 dimensional conformal field theories*, *J. Stat. Mech.* **1606** (2016), no. 6 064003, [[arXiv:1603.02889](#)].
- [9] D. S. Ageev, A. I. Belokon, and V. V. Pushkarev, *From locality to irregularity: Introducing local quenches in massive scalar field theory*, [arXiv:2205.12290](#).
- [10] C. T. Asplund and S. G. Avery, *Evolution of Entanglement Entropy in the D1-D5 Brane System*, *Phys. Rev. D* **84** (2011) 124053, [[arXiv:1108.2510](#)].
- [11] M. Nozaki, T. Numasawa, and T. Takayanagi, *Holographic Local Quenches and Entanglement Density*, *JHEP* **05** (2013) 080, [[arXiv:1302.5703](#)].
- [12] M. Nozaki, T. Numasawa, and T. Takayanagi, *Quantum Entanglement of Local Operators in Conformal Field Theories*, *Phys. Rev. Lett.* **112** (2014) 111602, [[arXiv:1401.0539](#)].
- [13] P. Caputa, M. Nozaki, and T. Takayanagi, *Entanglement of local operators in large- N conformal field theories*, *PTEP* **2014** (2014) 093B06, [[arXiv:1405.5946](#)].

- [14] M. Nozaki, *Notes on Quantum Entanglement of Local Operators*, *JHEP* **10** (2014) 147, [[arXiv:1405.5875](#)].
- [15] S. He, T. Numasawa, T. Takayanagi, and K. Watanabe, *Quantum dimension as entanglement entropy in two dimensional conformal field theories*, *Phys. Rev. D* **90** (2014), no. 4 041701, [[arXiv:1403.0702](#)].
- [16] P. Caputa and A. Veliz-Orsorio, *Entanglement constant for conformal families*, *Phys. Rev. D* **92** (2015), no. 6 065010, [[arXiv:1507.00582](#)].
- [17] C. T. Asplund, A. Bernamonti, F. Galli, and T. Hartman, *Holographic Entanglement Entropy from 2d CFT: Heavy States and Local Quenches*, *JHEP* **02** (2015) 171, [[arXiv:1410.1392](#)].
- [18] P. Caputa, J. Simón, A. Štikonas, and T. Takayanagi, *Quantum Entanglement of Localized Excited States at Finite Temperature*, *JHEP* **01** (2015) 102, [[arXiv:1410.2287](#)].
- [19] J. R. David, S. Khetrapal, and S. P. Kumar, *Universal corrections to entanglement entropy of local quantum quenches*, *JHEP* **08** (2016) 127, [[arXiv:1605.05987](#)].
- [20] J. R. David, S. Khetrapal, and S. P. Kumar, *Local quenches and quantum chaos from higher spin perturbations*, *JHEP* **10** (2017) 156, [[arXiv:1707.07166](#)].
- [21] Y. Kusuki and T. Takayanagi, *Renyi entropy for local quenches in 2D CFT from numerical conformal blocks*, *JHEP* **01** (2018) 115, [[arXiv:1711.09913](#)].
- [22] J. Zhang and P. Calabrese, *Subsystem distance after a local operator quench*, *JHEP* **02** (2020) 056, [[arXiv:1911.04797](#)].
- [23] Y. Kusuki and K. Tamaoka, *Entanglement Wedge Cross Section from CFT: Dynamics of Local Operator Quench*, *JHEP* **02** (2020) 017, [[arXiv:1909.06790](#)].
- [24] C. A. Agón, S. F. Lokhande, and J. F. Pedraza, *Local quenches, bulk entanglement entropy and a unitary Page curve*, *JHEP* **08** (2020) 152, [[arXiv:2004.15010](#)].
- [25] M. Nozaki, T. Numasawa, and S. Matsuura, *Quantum Entanglement of Fermionic Local Operators*, *JHEP* **02** (2016) 150, [[arXiv:1507.04352](#)].
- [26] M. Nozaki and N. Watamura, *Quantum Entanglement of Locally Excited States in Maxwell Theory*, *JHEP* **12** (2016) 069, [[arXiv:1606.07076](#)].
- [27] V. Benedetti and H. Casini, *Entanglement entropy of linearized gravitons in a sphere*, *Phys. Rev. D* **101** (2020), no. 4 045004, [[arXiv:1908.01800](#)].
- [28] J. R. David and J. Mukherjee, *Hyperbolic cylinders and entanglement entropy: gravitons, higher spins, p-forms*, *JHEP* **01** (2021) 202, [[arXiv:2005.08402](#)].
- [29] J. R. David and J. Mukherjee, *Entanglement entropy of gravitational edge modes*, [[arXiv:2201.06043](#)].
- [30] P. Candelas and D. Deutsch, *On the vacuum stress induced by uniform acceleration or supporting the ether*, *Proc. Roy. Soc. Lond. A* **A354** (1977) 79–99.
- [31] A. Laddha, S. G. Prabhu, S. Raju, and P. Shrivastava, *The Holographic Nature of Null Infinity*, *SciPost Phys.* **10** (2021), no. 2 041, [[arXiv:2002.02448](#)].
- [32] S. Raju, *Failure of the split property in gravity and the information paradox*, *Class. Quant. Grav.* **39** (2022), no. 6 064002, [[arXiv:2110.05470](#)].
- [33] H. Osborn and A. C. Petkou, *Implications of conformal invariance in field theories for general dimensions*, *Annals Phys.* **231** (1994) 311–362, [[hep-th/9307010](#)].

- [34] M. Billò, V. Gonçalves, E. Lauria, and M. Meineri, *Defects in conformal field theory*, *JHEP* **04** (2016) 091, [[arXiv:1601.02883](#)].
- [35] T. Anegawa, N. Iizuka, and D. Kabat, *Defining entanglement without tensor factoring: A Euclidean hourglass prescription*, *Phys. Rev. D* **105** (2022), no. 8 085003, [[arXiv:2111.03886](#)].
- [36] T. Anegawa, N. Iizuka, and D. Kabat, *Extractable entanglement from a Euclidean hourglass*, [arXiv:2205.01137](#).
- [37] M. Lemos, P. Liendo, M. Meineri, and S. Sarkar, *Universality at large transverse spin in defect CFT*, *JHEP* **09** (2018) 091, [[arXiv:1712.08185](#)].